MONASH University

Synthesis of Inorganic-Biodegradable Polymer Composite Microspheres for Controlled Delivery of a DNA Prime-Protein Boost Vaccine

A thesis submitted in fulfilment of the requirement for the degree of

Doctor of Philosophy

by

Jenny Ho

Bachelor of Engineering (Chemical)

Department of Chemical Engineering

Monash University, Clayton.

Australia

June 2008

General Declaration

Monash University

Monash Research Graduate School

Declaration for thesis based or partially based on conjointly published or unpublished work

In accordance with Monash University Doctorate Regulation 17 / Doctor of Philosophy and Master of Philosophy (MPhil) regulations the following declarations are made:

I hereby declare that this thesis contains no material which has been accepted for the award of any other degree or diploma at any university or equivalent institution and that, to the best of my knowledge and belief, this thesis contains no material previously published or written by another person, except where due reference is made in the text of the thesis.

This thesis includes 4 original papers published in and submitted to international peer-reviewed journals and 3 peer-reviewed conference papers. The core theme of the thesis is “synthesis of inorganic-biodegradable polymer composite microspheres for controlled delivery of a DNA prime–protein boost vaccine”. The ideas, development and writing up of all the papers in the thesis were the principal responsibility of myself, the candidate, working within the Department of Chemical Engineering under the supervision of Dr. Gareth Michael Forde and Dr. Huanting Wang. The inclusion of co-authors reflects the fact that the work came from active collaboration between researchers and acknowledges input into team-based research.

The following international peer-reviewed academic journal articles are presented in this thesis:

Item No.	Thesis chapter	Publication title	Publication status	Nature and extent of candidate's contribution
1	**2**	Mesoporous silica spheres from colloids	Journal of Colloid and Interface Science, 308 (2007) 374 - 380	Initiation, Key ideas, Experimental, Development, Results interpretations, Writing up [85%]
2	**3**	Protein loaded mesoporous silica spheres as a controlled delivery platform	Journal of Chemical Technology and Biotechnology, 83 (2007) 351 - 358	Initiation, Key ideas, Experimental, Development, Results interpretations, Writing up [85%]
3	**4**	Process considerations related to the microencapsulation of plasmid DNA via ultrasonic atomization	Biotechnology and Bioengineering, 101(1)(2008) 172 – 181	Initiation, Key ideas, Experimental, Development, Results interpretations, Writing up [90%]
4	**5**	Biodegradable polymer-mesoporous silica composite microspheres for DNA prime-protein boost vaccination	Journal of Controlled Release, Under review (May 2008) Manuscript number: JCR-D-08-00460	Initiation, Key ideas, Experimental, Development, Results interpretations, Writing up [90%]

The following peer–reviewed conference papers are presented in this thesis:

Item No.	Thesis chapter	Publication title	Publication status	Nature and extent of candidate's contribution
5	**A1**	Synthesis of mesoporous silica for controlled biomolecule delivery	CHEMECA 2007 proceeding, pp. 160 – 167	Initiation, Key ideas, Experimental, Development, Results interpretations, Writing up [90%]
6	**A2**	Inorganic-organic composite particle as a staged delivery platform for plasmid DNA-based biopharmaceuticals	AIChE Annual Meeting 2007 proceeding, P84273	Initiation, Key ideas, Experimental, Development, Results interpretations, Writing up [90%]
7	**A3**	Production of nano and micro particles via ultrasonication for biopharmaceutical delivery	CHEMECA 2007 proceeding, pp. 11 – 21	Key ideas, Experimental, Results interpretations [25%]

Signed: ……..

(JENNY HO)

Date: ……..

TABLE OF CONTENTS

To my family and love one

ACKNOWLEDGMENTS

I wish to express my deepest gratitude to all who have contributed toward my understanding and thoughts, and to those who have provided technical, intellectual and moral support throughout the development, production and writing of this research.

My humble thanks go to Almighty God for what He hath promised: strength for the day, light for the way, grace for the trials, help from above and love which is undying.

My thanks and appreciation go to Dr. Gareth M. Forde for his guidance and encouragement. His constructive criticism and advice have greatly improved the quality of my work. His teaching will greatly help me in my future endeavours.

My thanks and appreciation also go to Dr. Huanting Wang for his guidance, advice and insightful suggestions, which enabled me to complete my research. I wish to thank him for allowing me to carry out some experimental work in his laboratory.

Many thanks go to the Monash Research Graduate School (MRGS), Monash Faculty of Engineering and Monash Department of Chemical Engineering for funding this work. Thanks also to the Victorian Endowment for Science, Knowledge and Innovation (VESKI) for the collaborative work in the establishment of the Bio-Engineering Laboratory (BEL) where most of the experimental stages of this work were undertaken. I acknowledge with gratitude the editorial assistance given by Mrs. Jane Moodie from Language and Learning Centre (CALT) of the Faculty of Engineering.

My sincere appreciation also extends to my friends from both near and far; the general staff of the Monash Department of Chemical Engineering; and others who have provided assistance at various occasions: Michael K. Danquah, Wei Zhu, Seefei Yeo, Huan-Ming Chen, Yi Huang, Nipen Shah, Zhuozhi Liu. Their views and advice were useful indeed. Unfortunately, it is not possible to list all of them in this limited space.

Finally yet importantly, my sincere gratitude also goes to my beloved father, mother, boyfriend, two younger brothers and all my family members, for their support and love.

SUMMARY

The demand for an efficient delivery system for plasmid DNA-based vaccines has increased vastly in response to the rapidly growing use of plasmid DNA (pDNA) as a non-viral vector for vaccination. However, several limitations such as ineffective cellular uptake and intracellular delivery, and degradation of pDNA need to be overcome. Intranasal vaccination has been an area of interest for the pharmaceutical industries in recent years to overcome the alarming pattern of unsafe injection practices, and the poor availability of injectable and orally administered vaccines. The advent of particulate delivery systems for the administration of pDNA through intranasal inhalation is relatively new. In this study, a novel and scalable technique has been developed to create an inorganic-biodegradable polymer composite system, which enables controlled delivery of a heterologous prime-boost vaccine via intranasal vaccination. This delivery system offers to increase the potency of pDNA vaccines because the prime-boost vaccine is administrated in a single dose. Therefore, this delivery system makes vaccines more accessible to a larger population and brings great benefit to remote areas that have minimal access to medical services.

In the present work, a novel synthesis method was first developed to synthesise mesoporous silica spheres with pore sizes tailored to match specific molecules or applications. This new method offers greater control of pore size by using inexpensive commercial silica colloids and a simple electrolyte in the presence of a temporary polymer hydrogel network. Silica colloids were used as a feedstock for the mesoporous silica because the resultant pore size of the mesoporous silica is not limited by the molecular size of the organic template. Using this method, mesoporous silica spheres at the sub-micrometer and micrometer scale (0.50 to 1.60 μm) with a tailored pore size

(14.1 to 28.8 nm) were obtained. In order to investigate the potential application of these mesoporous silica spheres to provide a delivery platform for biomolecules, adsorption studies of a model protein (bovine serum albumin, BSA) onto the mesoporous silica spheres were performed by employing real time *in situ* measurements. The adsorption isotherm obtained fitted the Langmuir model and high adsorption capacities (up to 71.43 mg BSA/ml adsorbent) were observed. It was found that the conformation of the BSA molecules remained intact after the *in vitro* release kinetics studies.

In the current study, a new and improved microencapsulation method, which shields the pDNA molecules from deleterious conditions and enables a narrow microsphere size distribution, was developed. In this method, the pUC19 plasmids are condensed with polyethylenimine (PEI), and then embedded into poly(lactide-co-lactide) (PLGA) using a 40 kHz ultrasonic atomization system. Biodegradable polymer microspheres with volume weighted mean diameters (D[4,3]) of 6.0 – 15.0 μm were obtained and 95 – 99% of the encapsulated pUC19 plasmids exhibited zero order release kinetics over the 30 day *in vitro* delivery studies. The use of ultrasonic atomization for the production of biodegradable polymer microspheres containing pDNA molecules is a new application. This method has several distinct advantages including the ability to control particle size; the ability to self clean; and it does not require elevated temperatures and phase separation inducing agents.

In order to study the feasibility of ultrasonic atomization system in microencapsulating the prime-boost vaccines, the system was then extended to encapsulate both pEGFP-N1 plasmids and mesoporous silica spheres loaded with BSA into PLGA. The feeding system was modified by feeding the feedstocks into the nozzle

of the atomizer through the dual-concentric-feeding needles. This fabrication technique produced composite microspheres with D[4,3] ranging from 6.0 to 34.0 μm, depending on the conditions during the microsphere preparation, such as polymer concentration and volumetric ratio. The *in vitro* release profiles obtained over 40 days showed that pDNA and protein have different release kinetics. Protein appeared to follow quasi-zero order release kinetics with a minimal initial burst rate. These release profiles showed an effective method to enhance immune responses by facilitating different delivery regimes between the pDNA prime and protein boost through advanced particle design. This technique has the potential for aseptic manufacturing and easy scaling-up for industrial applications. The development of enhanced vaccine delivery system is particularly important to combat a host of current and emerging infectious diseases in areas with limited medical services.

DETAILS OF PUBLICATIONS

Details of the findings in this thesis are described in four published/submitted international peer-reviewed academic journal papers and three peer-reviewed conference papers. In addition to the four articles and three conference papers presented in this thesis, listed below are a further five articles, and eight conference papers and posters that have been contributed to throughout the course of the doctoral studies program as part of the wider research program of the Bio Engineering Laboratory (BEL), Department of Chemical Engineering, Monash University. This constitutes the requirements based on Monash University guidelines for PhD thesis by publications.

Peer-reviewed Journal Papers

- **Jenny Ho**, Wei Zhu, Huanting Wang, Gareth M. Forde, 'Mesoporous silica spheres from colloids', *Journal of Colloid and Interface Science*, 308 (2007) 374 – 380.
- **Jenny Ho**, Michael K. Danquah, Huanting Wang, Gareth M. Forde, 'Protein loaded mesoporous silica as a controlled delivery platform', *Journal of Chemical Technology and Biotechnology*, 83 (2008) 351 – 358.
- **Jenny Ho**, Huanting Wang, Gareth M. Forde, 'Process considerations related to the microencapsulation of plasmid DNA via ultrasonic atomization', *Biotechnology and Bioengineering*, 101(1) (2008) 172 – 181. (This article has been selected by editors as the Spotlight featured article.)
- **Jenny Ho**, Huanting Wang, Gareth M. Forde, 'Biodegradable polymer-mesoporous silica composite microspheres for DNA prime-protein boost vaccination', *Journal of Controlled Release*, under review, May 2008.

Peer-reviewed Conference Papers

- **Jenny Ho**, Gareth M. Forde, Huanting Wang, 'Synthesis of mesoporous silica for controlled biomolecule delivery', *CHEMECA 2007*, Melbourne, Victoria – Australia, 24 – 26 September 2007, pp. 160 – 167.
- **Jenny Ho**, Gareth M. Forde, Huanting Wang, 'Inorganic-organic composite particle as a staged delivery platform for plasmid DNA-based biopharmaceuticals', *AIChE Annual Meeting 2007*, Salt Lake City, Utah – United States, 4 – 9 November 2007, P84273.
- Gareth M. Forde, **Jenny Ho**, Wen Li, Judin Sahayanathan, Nyomi Uduman, Chamithri Wimalajeewa, 'Production of nano and micro particles via ultrasonication for biopharmaceutical delivery', *CHEMECA 2007*, Melbourne, Victoria – Australia, 24 – 26 September 2007, pp. 11 – 21.
- **Jenny Ho**, Gareth M Forde, Huanting Wang, 'Inorganic-organic composite microspheres for prime-boost genetic therapies via nasal cavity', *CHEMECA 2008*, Newcastle, New South Wales – Australia, 28 September – 1 October 2008, pp. 241 – 250.

Other Relevant Publications

- Michael K. Danquah, **Jenny Ho**, Gareth M.Forde, 'Performance of R-N(R')-R" functionalised poly(glycidyl methacrylate-co-ethylene glycol dimethacrylate) monolithic sorbent for plasmid DNA adsorption', *Journal of Separation Science* 30 (2007) 2843 - 2850.
- Michael K. Danquah, **Jenny Ho**, Gareth M.Forde, 'A thermal expulsion approach to homogeneous large-volume methacrylate monolith preparation; enabling large-scale rapid purification of biomolecules', *Journal of Applied Polymer Science*, 109 (2008) 2426 – 2433.

- Michael K. Danquah, Shan Liu, **Jenny Ho**, Lina Wang, Ross L. Coppel, Gareth M. Forde, 'Rapid production of a plasmid DNA encoding a malaria vaccine candidate via amino-functionalised poly(GMA-*co*-EDMA) monolith', *AIChE Journal*, accepted, June 2008.
- Shan Liu, **Jenny Ho**, Michael K. Danquah, Gareth M. Forde, 'Using DNA as a drug – Bioprocessing and delivery strategies', *Chemical Engineering Research and Design*, accepted, 2008.
- Shan Liu, Michael K. Danquah, **Jenny Ho**, Charles Ma, Lina Wang, Gareth M. Forde and Ross Coppel, 'Synthesis and delivery of DNA molecules encoding a malaria vaccine candidate via poly(lactic-*co*-glycolic acid) carrier systems', *Journal of Chemical Technology and Biotechnology*, accepted, 2008.
- Li Han, Jianfeng Yao, Dan Li, **Jenny Ho**, Xinyi Zhang, , Chun-Hua (Charlie) Kong, Zhi-Min Zong, Xian-Yong Wei and Huanting Wang, 'Hollow Zeolite Structures Formed by Crystallization in Crosslinked Polyacrylamide Hydrogels', *Journal of Materials Chemistry*, 18(28) (2008) 3337 – 3341.
- **Jenny Ho**, Gareth M. Forde, Huanting Wang, 'Inorganic-Biodegradable Polymer Composite Spheres as a Controlled Vaccine Delivery Platform', *SBE's 3rd International Conference on Bioengineering and Nanotechnology*, Singapore, 12 – 15 August 2007.
- **Jenny Ho**, Gareth M. Forde, Huanting Wang, 'Nasal Delivery Platform for Plasmid DNA Based Vaccines', *Monash University Engineering Research Month Poster Competition,* Monash University, August 2007.
- **Jenny Ho**, Gareth M. Forde, Huanting Wang, 'Mesoporous Silica and Polymer Hybrid Structure for Controlled Biopharmaceutical Delivery', *Monash Infection and Immunity Network Symposium*, Monash University, 28 June 2007.

- **Jenny Ho**, Gareth M. Forde, Huanting Wang, 'Inorganic-biodegradable polymer composite particles for staged vaccine delivery', *Tri-University Advanced Research Workshop 2007*, Monash University, 6 – 7 December 2007.
- **Jenny Ho**, Gareth M. Forde, Huanting Wang, 'Nanoparticles-Biodegradable Polymer Particle for Staged Delivery of a Prime-Boost Vaccine', *Bioengineering Symposium*, Monash University, December 2005.
- Gareth M. Forde, **Jenny Ho**, 'Inorganic-polymer composite particles for staged vaccine delivery via nasal inhalation', *MC8: Advancing Materials by Chemical Design (Materials Chemistry Forum of the Royal Society of Chemistry)*, University College London, United Kingdom, 2 – 5 July 2007.
- Gareth M. Forde, James R. Friend, **Jenny Ho**, Michael K. Danquah, 'Creation of micro and nanoparticles via ultrasonic atomization for enhanced biopharmaceutical delivery', *Nanomed Conference 2006*, Newcastle upon Tyne, United Kingdom, 27 – 28 June 2006.

NOMENCLATURE

A	Adenine
ANOVA	Analysis of variance
AM	Monomer acrylamide
APC	Antigen presenting cells
BET	Brumauer-Emmett-Teller
BJH	Barrett-Joyner-Halenda
BSA	Bovine serum albumin
C	Cytosine
ccc	Covalently closed circle
CD	Cluster of differentiation
$CD8^+$	Cytotoxic T cell
$CD4^+$	Helper T cell
CpG	Cytidine-phosphate-guanosine
CTL	Cytotoxic T lymphocyte
Da	Dalton
DNA	Deoxyribonucleic acid
D[4,3]	Volume weighted mode mean diameter
dsDNA	Double stranded deoxyribonucleic acid
***E. coli* DH5α**	Recombinant *Escherichia coli*
EDMA	Ethylene glycol dimethacrylate
EDS	Energy dispersive X-ray spectroscopy
EDTA	Ethylene diamine tetraacetic acid
EtBr-AGE	Ethidium bromide agarose gel electrophoresis
FDA	Food and Drug Administration
G	Guanine

gDNA	Genomic deoxyribonucleic acid
GI	Gastrointestinal
GMA	Glycidyl methacrylate
HIV	Human immunodeficiency virus
H5N1	Subtype of the influenza A virus
IgA	Immunoglobulin A
IUPAC	International Union of Pure and Applied Chemistry
kbp	Kilobase pairs
K_D	Dissociation constant
LD 50	Lethal dose which causes the death of 50%
MBAM	N, N'-methylenebisacrylamide
MHC	Major histocompatibility
MPS	Mesoporous silica spheres
NaCl	Sodium Chloride
NALT	Nasal-associated lymphoid tissue
NH_4NO_3	Ammonium nitrate
N/P	Nitrogen to phosphorous ratio
OC	Open circular
PBS	Phosphate Buffered Saline
PDMR	Plasmid DNA medium with optimised carbon to nitrogen ratio
pDNA	Plasmid deoxyribonucleic acid
PEI	Polyethylenimine
pEGFP-N1	Recombinant plasmid DNA
PLGA	Poly(lactide-co-glycolide)
PVA	Poly(vinyl alcohol)
pUC 19	Recombinant plasmid DNA

q_{max}	Maximum monolayer adsorption capacity
RNA	Ribonucleic acid
sc pDNA	Supercoiled plasmid deoxyribonucleic acid
SDS-PAGE	Sodium dodecyl sulphate polyacrylamide gel eletrophoresis
SEM	Scanning electron microscopy
SiO_2	Silica dioxide
T	Thymine
TEOS	Tetraethylorthosilicate
T_g	Glass transition tempertature
v	Volume
w	Weight
WHO	World Health Organization

Greek symbols

μ	Micron
n	Nano
σ	Surface tension
η	Viscosity
υ	Velocity

CHAPTER 1

INTRODUCTION AND BACKGROUND

1.1 DNA vaccines

Vaccination or immunisation is regarded as the key intervention for emerging diseases such as influenza and bird flu. However, only about 25 infectious diseases are controlled by vaccines, leaving a large number of bacterial, fungal, parasitic and viral diseases ungoverned [1, 2]. This preventive bottleneck is primarily due to the lack of facilities to create and deliver suitable vaccines. For example, the measles virus still causes over 30 million infections and 600,000 deaths annually [3]. Currently, most effective vaccines are made of live attenuated viral vaccines or inactivated viruses. Life-long protection against infectious diseases is induced by the development of effective immune responses. However, with these vaccines, the tendency of attenuated viruses to revert to their virulent forms has generated some safety concerns; hence, making their use contraindicated in immunodeficiency diseases [4]. As a result, the control of life threatening infectious diseases, such as malaria, tuberculosis, and human immunodeficiency virus (HIV) is hampered by conventional viral vaccines. The unique pathophysiological characteristics of these diseases have also contributed to the difficulty of using existing technologies to generate efficient vaccines for their treatment [2]. Therefore, researchers have been prompted to institute viable replacements that would be safer and more effective to use.

Currently, because of their highly evolved and specialised components, viral systems are the most effective means for both DNA/gene deliveries and expressions, associated with high efficiencies (generally >90%) [5]. As yet, viral-mediated deliveries have several limitations, including toxicity; limited DNA carrying capacity; restricted target to specific cell types; production and packing problems; and high cost [5]. Thus,

non-viral systems, particularly a synthetic DNA delivery system such as DNA plasmids, are highly desirable in both research and clinical applications as gene delivery vehicles.

In the early 1990s, Wolff *et al.* [6] reported that *in vivo* expressions of the encoded protein were induced after the intramuscular inoculation of unformulated plasmid DNA (pDNA) that encoded a reporter gene. This work laid the foundation for the first observation by Ulmer *et al.* in 1993 – the generation of nucleoprotein-specific cytotoxic T lymphocytes (CTLs) after the injection of pDNA that encoded a viral protein. This immune response protected animals from the influenza A virus [7]. In 2003, the first use of pDNA as a vaccine outside of an experimental setting was for the immunisation of Californian Condors against the West Nile Virus [8]; and in June 2006, positive results in humans for a bird flu pDNA vaccine were announced [9]. Several features of pDNA vaccines make them more attractive than conventional and recombinant subunit vaccines; thus, pDNA vaccines have gained global interest for a variety of applications. The ease of construction and manufacture for pDNA vectors encoding antigens from pathogens has shortened the time to create a working vaccine against a new disease from 4 – 9 months to 1 month [10]. These exciting features have propelled interest in the development of plasmid-based products, both as prophylactic vaccines and as immunotherapies [11].

1.1.1 Plasmid DNA

Plasmid DNA (pDNA) vaccines are generally composed of double stranded plasmids, which have an inner helical structure. The strands in plasmids are made of chemically linked chains of nucleotides, and each chain consists of a sugar, a phosphate

and one of the four kinds of nitrogen bases, *i.e.* adenine (A), thymine (T), cytosine (C) and guanine (G). Plasmids isolated from bacteria are covalently closed circles (ccc) and compact "supercoiled" structures, formed by the DNA segment joining the two ends under twist strain and enables the structure to move freely. These supercoiled structures are considered the most physiologically active form of pDNA when presented as vectors for gene therapy or vaccination. The breaking of one strand via enzymatic processes (e.g. nucleases) or mechanical action results in the formation of the open circular (OC) form; and the breakage of both strands at the same position by endonuclease cleavage forms linear pDNA molecules [12].

Plasmid DNA contains a gene encoding the target antigen under the transcriptional directory and a promoter to make the gene express in mammalian cells [2]. The expressed antigen protein mimics intracellular pathogenic infection, and induces both humoral and cellular immune responses [4]. pDNA vaccines offer a greater degree of flexibility in vaccine design, which includes the choice of antigens and co-stimulants to be used; the place to elicit the response; and the cytokines to be co-expressed. When required, several antigens can be encoded simultaneously [13]. Hence, pDNA has been termed the 'reverse engineered' therapeutic vector. In addition, it may be possible to ameliorate the adjuvant effects of pDNA vaccination by the addition of multiple immunostimulatory sequences into the pDNA belt [10]. The production cost and stability of pDNA vaccines are also anticipated to be more favourable than traditional vaccines [11]. These features could facilitate worldwide availability and distribution of pDNA vaccines.

A schematic representation of a pDNA vaccine structure is shown in Figure 1.1 [2]. The bacterially derived plasmids used for vaccination purposes share the basic attributes

of vectors. These basic attributes include (1) a gene encoding the desired antigen; (2) a promoter that actively drives expression in mammalian cells; (3) a transcription terminator; (4) an antibiotic resistance gene to confer antibiotic-selected growth during production in bacteria. In addition, sites for increasing the potency of pDNA vaccines could be incorporated – additional genes encoding cytokines or co-stimulatory molecules; and an origin of replication (ori) suitable to provide high yields of pDNA [2].

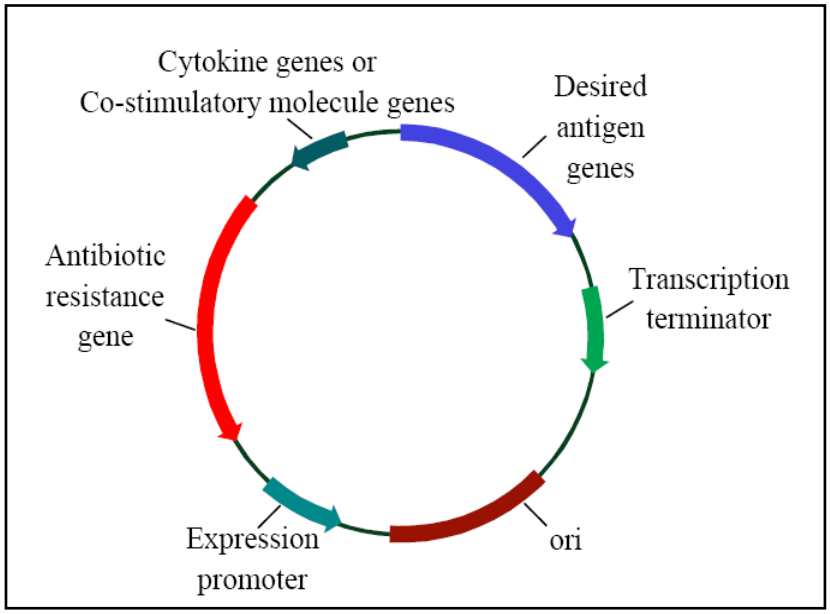

Figure 1.1 Schematic representation of a plasmid DNA vaccine [2].

After administration of pDNA vaccines, epitope peptides are presented on major histocompatibility (MHC I) molecules, and stimulate $CD8^+$ T cells [14]. Alternatively, a cross-priming mechanism has also been demonstrated, wherein the gene products expressed by transfected muscle cells are transferred to antigen presenting cells (APC), and the antigens are either cross-presented on MHC I or MHC II molecules; thus, inducing $CD4^+$ T cell responses [15]. In addition, the cytidine-phosphate-guanosine (CpG) motifs of vaccine plasmids also helped to induce the expression of co-stimulatory molecules on APC. The combination of co-stimulation with MHC I and II presentation

of antigen leads to the initiation of improved responses [15]. The ability of genetic pDNA vaccines to generate T-cell responses has been identified as a promising technique to prevent intracellular bacteria and viral infections, and cancer.

1.1.2 Plasmid DNA vaccine delivery strategies

The transfection efficiency of pDNA is relatively low when compared to other vectors such as viruses, viral-like particles and cellular vectors. This is because, after administration, naked pDNA is susceptible to degradation by serum enzymes such as endonucleases, thereby reducing the amount of pDNA that is available in hosts to express antigen gene. Upon entry into a host cell, the transport of pDNA across cell membranes is limited by its net negative surface charge and large hydrodynamic diameter [16]. In addition, one possible mechanism of pDNA uptake is endocytosis, after which the pDNA travels through the endosome-lysosome compartment, where it may be degraded. The acidic condition in endosome promotes acidic hydrolysis and activates the lysosomal enzymes that can rapidly degrade plasmids [17, 18]. Thus, improved pDNA delivery strategies are needed. At present, pDNA-based vaccine deliveries in preclinical and clinical animal studies are achieved by using physical (e.g. injection, gene gun, electroporation or aerosol delivery), chemical (e.g. cationic lipid or polymer condensing agents) and biological (e.g. use of the cellular transport mechanism) approaches [10, 13, 19].

The direct injection of naked pDNA is feasible, but relatively few cells take up the pDNA (1-3 %) [20] and this is due to the high molecular weight and the polyanionic nature of the nucleic acids. This leads to reduced expression of the encoded protein [21].

Intramuscular injection of naked pDNA resulted in low *in situ* transfection of cells, and several limitations such as distribution of the vaccine solution within the injected tissue, cellular uptake, and intracellular delivery to the nucleus need to be improved [22]. Also, unsafe injection practice is a serious issue on a global scale. The World Health Organization (WHO) [3] estimates that over 12 billion injections are administered annually [23], and up to 30% of these injections are unsafe [24]. The transmission of blood-borne pathogens from patient to patient because of using unsterilised needles has been recorded for over half a century [25]. These unsafe injection practices, which are prevalent in poorer and developing countries, have caused numerous hepatitis B, hepatitis C and human immunodeficiency virus (HIV) infections, and have contributed to substantial mortality rates [25-27].

Plasmid DNA vaccines are also commonly delivered by gene-gun technology. This delivery method has gained popularity because of its delivery efficiency. However, only a limited amount of gold beads coated with plasmid DNA can be discharged directly into the cellular cytoplasm of skin cells by using the gene-gun [15]. Another delivery method is electroporation – previous studies have shown that intradermal or intramuscular injections, followed by electroporation of the injection sites, resulted in higher transfection efficiency and immune responses in mice and pigs [28]. However, severe tissue damage and toxicity could accompany electroporation and this is due to the release of heat during the transfer of electric pulses of high strength into the tissues [28].

Oral administration is another popular route for vaccine delivery [29, 30]. However, oral vaccine delivery is hampered by the low mucosal permeability of vaccines; restricted vaccines absorption in the gastrointestinal (GI) tract; and the lack of stability

of vaccines in the GI environment, thus results in the degradation of vaccines components prior to its absorption [31]. The lack of efficiency associated with these pDNA vaccines delivery mechanisms is compromised by administering larger doses; however, this causes unwanted side effects such as toxicity and multi-drug resistance, as well as an increase in the cost per dose [32].

The immune response associated with pDNA vaccination is influenced by the site and mode of immunisation. Various routes of administration and different types of carriers have been evaluated based on their ability to improve the efficiency of pDNA vaccines [33]. New methods such as subcutaneous, intraperitoneal, intravenous and mucosal (vaginal, intranasal or intratracheal) deliveries of pDNA carry a number of potential advantages over conventional methods. Such advantages include increased safety, acceptability and treatment compliance; increased efficacy linked to a broader tissue distribution of the antigen; ease of use leading to self-administration; and administration of smaller doses of the antigen.

1.1.3 Prime-boost immunisation strategies

Strong antibody and T-cell responses against antigens induced by pDNA vaccines have been demonstrated in animal models. However, the levels of antibodies induced are often low or moderate, and this is particularly true in humans [34]. Therefore, there is an urgent need to develop potent and efficient pDNA vaccines before they can be used effectively in humans. A number of strategies have been proposed as possible means to improve the potency of pDNA vaccines. These include delivery systems, administration of adjuvants, targeting strategies, boosting strategies, and immunising by

different routes [35]. Several researches have proven that prime-boost strategies can successfully generate impressive cell-mediated immunity against a variety of encoded antigens [36-39].

Homologous and heterologous prime-boost immunisation strategies are the mechanisms being used to enhance the immune responses. However, repeated immunisation with the same vaccine (homologous) has been shown to be ineffective at boosting the level of specific T-cell responses [40]. In contrast, heterologous prime-boost immunisation strategy has been shown to induce very high levels of protection and specific $CD8^+$ T-cell [41, 42]. A recent study demonstrated that potent cellular immunity was induced against a highly pathogenic strain of avian H5N1 influenza virus by using a heterologous prime-boost approach [43]. pDNA immunisation alone is usually not potent enough to stimulate immune responses. In many studies, boosting with an antigen is required to elicit measurable immune responses, such antigen includes peptides or protein-based antigen [44, 45]; or with viral vectors [46]; or with inactivated virus [47].

1.2 Nasal vaccine delivery

In the last decade, nasal vaccination has been recognised as a very promising route, because it offers a faster and more effective therapeutic effect. The nasal route is an important arm of local mucosal and systemic immune system, since it is often the first point of contact for inhaled antigens and both humoral and cellular immune responses can be induced [48]. In addition, the loss of drug by first-pass metabolism in the liver can be avoided because the venous blood from the nose passes directly into the systemic

circulation. The mucosal surface in the nasal cavity is highly vascularised and interspersed with immunologically active tissues, which are responsible for the induction and mediation of immune responses against the potential pathogenic organisms [49]. After the intranasal immunisation, the antigen is sampled and passed on to underlying lymphoid cells in the submucosa, where the antigen is being processed and the presentation takes place. This resulted in the activation of T-cells that help B-cells to develop into immunoglobulin A (IgA) plasma cells [50]. Figure 1.2 shows the scheme of pathway in the nasal mucosa and nasal-associated lymphoid tissue (NALT), and this scheme can elicit a local immune response.

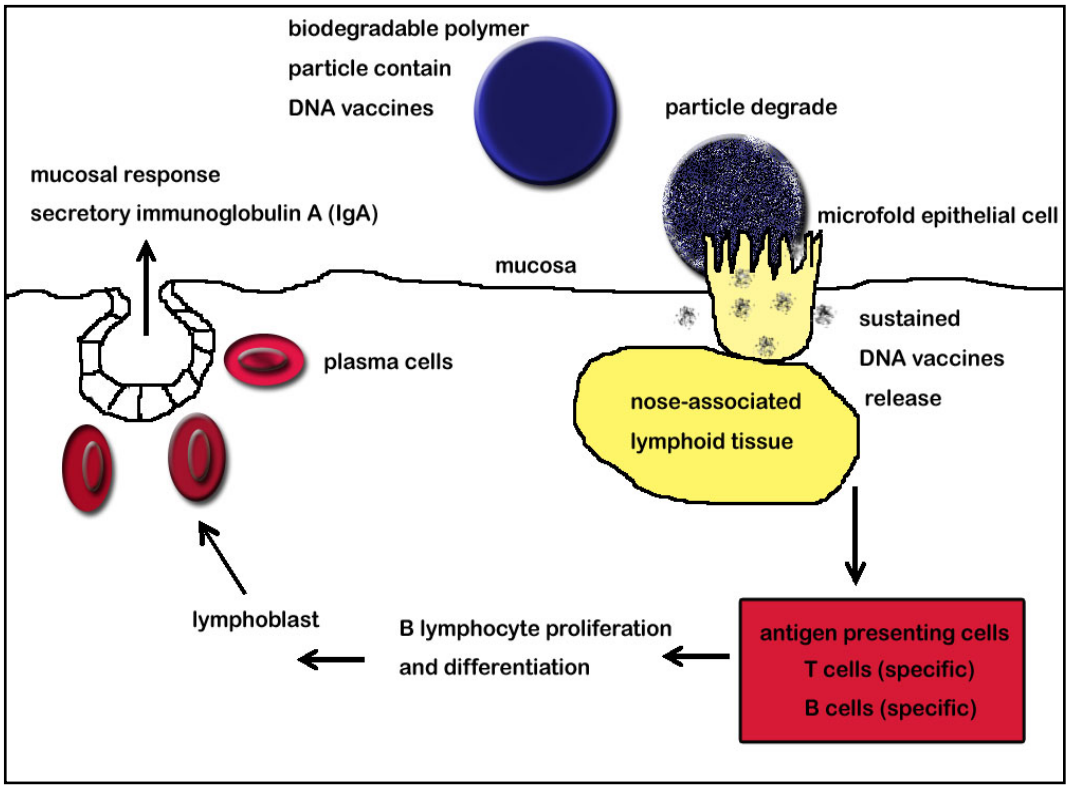

Figure 1.2 Hypothetical scheme of pathway eliciting local mucosal response via NALT after administration of DNA vaccines encapsulated in biodegradable polymer particle (adapted from [51] with permission from Elsevier).

The major limitation of nasal delivery is the inadequate absorption of vaccines. The main factors such as physiochemical properties of vaccine, nasal mucociliary clearance, and nasal absorption enhancers greatly affect absorption of the vaccines through the nasal mucosa. Vaccine molecular weight, perfusion rate, perfusate volume, concentration, and solution pH also contribute to the rate and extent of absorption [52]. As a result, several enhancers have been utilised to improve the nasal absorption and these include enhancers that can alter the physiochemical properties of vaccines (*i.e.* solubility, partition coefficient and ionic interaction) and enhancers that can affect the mucosa surface. Examples of such enhancers include microspheres, liposomes and gels [52]. Deposition of particles in the nasal cavity region is most common for larger particles, and it takes place via inertial impaction. Both theoretical and experimental studies have indicated that particles of 10 – 20 μm in diameter favour deposition in the upper airways and minimise deposition in the lungs and gastro-intestinal tract during nasal inhalation [53-55].

1.3 Biomaterials and synthesis strategies for plasmid DNA vaccine delivery systems

The demand for an efficient delivery system for pDNA-based vaccines has increased vastly in response to rapid advances in the use of pDNA molecules as a non-viral vector for vaccination. Mesoporous silica and biodegradable polymers are among the biomaterials being investigated intensively for their potential applications in vaccine delivery systems.

1.3.1 Mesoporous silica

Inorganic host materials, such as silica, have attracted increasing attention for biomolecule encapsulation and non-viral drug delivery. Silica is a relatively benign material in terms of biocompatibility; less toxic compared to polycations; and versatile in terms of the variety of chemical and physical modifications that are available [56, 57]. Ongoing research is investigating the usability of nanoporous materials in a variety of bio-related applications due to their high specific surface areas, high specific pore volumes, and tailorable pore structures to selectively store different molecules of interests. Of the many nanoporous materials available, those in the mesoscale range (2 – 50 nm) are of particular interest in biotechnology, because a large proportion of biomolecules are within this size range [58]. Hence, mesoporous silica materials have been successfully utilised as a non-viral gene delivery vector [56, 59, 60], gene transfection reagents [61], carriers of molecules [62], catalyst support [63], as well as adsorbents [64, 65]. Mesoporous silica exhibits its diversity and potential applications in many facets of biological science.

Methods such as solution growth [66, 67] and aerosol self assembly [68] have been developed to synthesise mesoporous silica spheres. Organosilicates such as tetraethylorthosilicate (TEOS) are used in these syntheses. In addition, organic templates are also required in the syntheses because they are essential for generating the mesoporous structures of silica spheres. However, organosilicates are expensive; and the pore sizes for mesoporous silica materials are limited by the molecular size of organic templates. These drawbacks have hindered the use of mesoporous silica in large-scale application. In addition, different biomolecules possess different

hydrodynamic sizes and surface chemistries in different environments; therefore, the ease and flexibility of tailoring the pore sizes of the mesoporous materials is very vital.

1.3.2 Biodegradable polymer microspheres

Polymers are the most versatile class of biomaterials that can be engineered to meet specific end-use requirements. Specific biodegradability of polymers can be achieved by incorporating a variety of labile groups such as ester, orthoester, anhydride, carbonate, amide, urea and urethane in their backbone [69]. This characteristic of biodegradable polymer has greatly assisted the development of controlled delivery technology, which aims at systematic release of a pharmaceutical agent to maintain a therapeutic level of the drug in the body for a sustained period of time (Figure 1.3). Therapeutic agent will be released continuously as the polymer matrix erodes and the characteristics of the erosion predominantly depends on the polymer chemistry, molecular weight, hydrophilicity, crystallinity; and the matrix size, shape and porosity [70]. Biodegradable polymers will biodegrade into non-harmful products such as natural metabolites, or materials that can be readily excreted from the body [70]. Polyester-based polymers such as poly(lactide-co-glycolide) (PLGA) are the most widely investigated and approved by Food and Drug Administration (FDA) for drug/vaccine delivery applications. The popularity of PLGA is ascribed to its versatility, biocompatibility, and hydrolytic degradation into resorbable products. The hydrophilicity of PLGA increases with increasing number of glycolide, and crystallinity decreases with an increase in the content of either co-monomer [70].

The encapsulation of biomolecules into polymer microspheres presents an effortful problem because of the delicacy of the biomolecules. Therefore, much efforts have been spent in evaluating the PLGA delivery systems; especially microspheres preparation, biomolecule stability, bioactivity, and release kinetics [70]. Currently, the most commonly used method to embed biomolecules into polymer microspheres is emulsion-solvent extraction/evaporation [71, 72]. However, this method is inherently seen as a batch operation; thereby, making large-scale production difficult and costly. In addition, bioactivity of biomolecules can be eliminated due to the presence of organic solvents, because these solvents are difficult to remove completely [72]. Spray drying is frequently being employed to prepare microspheres on a large-scale [73, 74]. However, this method is not feasible for temperature sensitive compounds, and has considerable product lost due to inefficient separation in the collecting process [74]. Several methods have been proposed to circumvent the deleterious effects of encapsulation. These include complexation of biomolecules with cationic polymers [75]; cryopreparation [76]; and the addition of buffering excipients [77]. Yet, after several decades of intensive and ever increasing research and development of PLGA for drug/vaccine delivery applications, the number of commercially available products on the market is relatively low, and this is mainly due to the economics and the productivity of the development process. Purity, reproducibility, safety, performance and stringent regulatory requirements must be considered throughout the development of vaccine delivery systems.

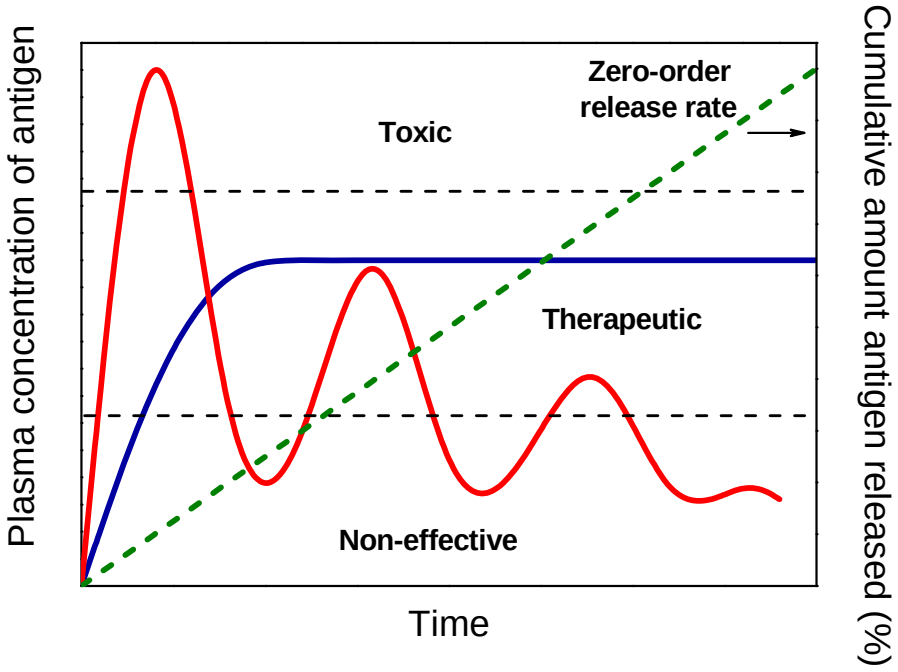

Figure 1.3 Controlled delivery system provides sustained release of antigen (zero-order release rate) and maintains concentration of antigen at therapeutic level over a period of time after administration, compared with traditional system which diminishes with time and requires repetitive administration [70].

1.4 Objectives of this study

The use of particulate delivery systems for administrating pDNA vaccines through the nasal cavity is a novel strategy due to the advent of pDNA-based vaccines being relatively new [48]. The development of an effective carrier system is currently the key element to improve the potency of pDNA vaccines. The main objective of this study is to develop a particulate system for the controlled delivery of a pDNA prime and protein boost vaccine, which can be administered via the nasal cavity. This particulate delivery system aims to encapsulate pDNA and protein in different segments (see Figure 1.4, page 17), and thus allow a controlled vaccine release profile over a period of time. Experimental investigations have been designed and performed to develop a scalable

synthesis technique for the production of an enhanced vaccine delivery system that is suitable for intranasal delivery (10 – 20 μm).

The specific objectives of this study are as follows:

- To develop and optimise a novel and cost effective method for *in situ* controlled formation of mesoporous silica spheres from silica colloids in the presence of a polymer hydrogel network. This method offers flexibility in the synthesisation of mesoporous materials with controllable structure and pore size.

- To examine the adsorption potential of the mesoporous silica spheres using a model protein, and to investigate the controlled release profile of the protein. Both the mesoporous silica spheres and the protein will be characterised to investigate the optimum conditions for protein adsorption. Through process innovation and optimisation, high adsorption capacity of protein can be obtained.

- To establish a microencapsulation method that synthesises polymeric microspheres containing pDNA by utilizing the 40 kHz ultrasonic atomization system. Through this method, microspheres with sizes within the range required (10 – 20μm) will be obtained. These sizes of microspheres are required to facilitate the deposition of microspheres on the mucosa of nasal cavity during intranasal inhalation. The impact of different procedures and formulation conditions on the structure, size, morphology and encapsulation efficiency of polymeric microspheres will also be considered.

- To develop a scaleable and commercially viable technique that fabricates inorganic-biodegradable polymer composite microspheres containing pDNA and protein in different segments. This technique reduces the contacting time between biomolecule and organic solvents, and makes the process of tailoring the contents of the composite microspheres much easier – this is achieved by using a modified apparatus comprised of dual-concentric-feeding needles attached to the 40 kHz ultrasonic atomization system. This delivery system will potentially achieve different delivery regimes between the pDNA prime and protein boost through the advanced particle design.

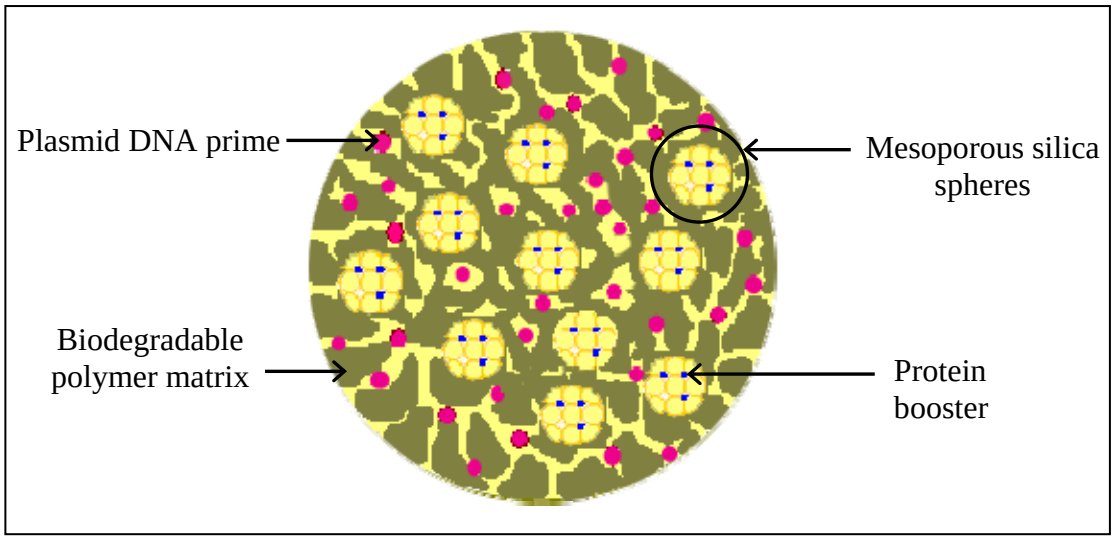

Figure 1.4 Schematic illustration of an inorganic-biodegradable polymer composite microsphere for controlled delivery of a pDNA prime and protein boost vaccine.

1.5 Layout of the thesis

The research conducted to achieve the specific objectives as outlined above are reported in the publications, which form the main chapters of this thesis. This thesis contains six chapters. There are two framing chapters: *Introduction and Background*, and *Conclusions and Recommendations for Future Work*. Chapters 2 – 5 present the laboratory research via three published and one submitted internationally peer-reviewed academic journal papers. Three peer-reviewed conference papers are also presented in the appendices. The contextual layout of this thesis is as follows:

- **Chapter 1** forms the thesis introduction and background of the study. The objectives of this study are also stated.

- **Chapter 2** presents the development and optimisation of a method to synthesise mesoporous silica spheres for biomolecule delivery. In this work, the tailoring of the pore sizes via a series of different silica colloids and electrolytes is reported. The influences of synthesis conditions including solution composition and calcination temperature on the formation and characteristics of the mesoporous silica spheres are discussed.

- **Chapter 3** presents the application of the mesoporous silica spheres as a biomaterial for the adsorption of a model protein. This chapter also discusses the adsorption capacity and *in vitro* delivery (desorption) profiles of protein to be an indicator for the development of a new biomaterial for biopharmaceutical. In order to probe the interactions between the model protein and the mesoporous silica spheres, this work investigates the stabilities, hydrodynamic diameters and

zeta potentials of both materials. The adsorption study, employing real time *in situ* measurements, is described. This is seen as a vital method towards the establishment of a scaleable scheme for protein adsorption, and this method has minimises the errors associated with the batch mode method.

- **Chapter 4** reports the establishment of a microencapsulation method, which uses a 40 kHz ultrasonic atomizer to enable large-scale production of polymeric microspheres containing pDNA. The process synthesis parameters that are important to the scale-up in microencapsulating pDNA via ultrasonic atomization are discussed. This work also discusses the role of cationic polymer in condensing pDNA to protect the pDNA from shear-induced degradation during the myriad of processing steps. The characteristics and *in vitro* performance of the resultant polymeric microspheres are also described.

- **Chapter 5** presents the development of a technique to synthesise a composite microsphere delivery system comprised of pDNA and mesoporous silica spheres loaded with protein entrapped in a polymeric particulate matrix. This work reports a technique to prepare a single formulation consisting of both pDNA prime and protein boost vaccines. In an extension of the reported method in chapter 4, feedstocks are fed into the nozzle of the atomizer through the dual-concentric-feeding needles. This chapter also discusses the effect of process synthesis parameters and the characteristics of composite microspheres. The *in vitro* release profiles of pDNA prime-protein boost from the resulting composite microspheres are presented to investigate the different delivery regimes.

- **Chapter 6** presents the major conclusions of the research work, highlighting the achievements of study objectives. It also makes some recommendations for future work.

CHAPTER TWO

SYNTHESIS AND CHARACTERISATION OF MESOPOROUS SILICA SPHERES

Mesoporous silica spheres from colloids

Jenny Ho, Wei Zhu, Huanting Wang, Gareth M. Forde

Journal of Colloid and Interface Science

308 (2007) 374 – 380

Monash University

Declaration for Thesis Chapter Two

Declaration by candidate

In the case of Chapter 2, the nature and extent of my contribution to the work was the following:

Nature of contribution	**Extent of contribution (%)**
Initiation, Key ideas, Experimental works, Development, Data analysis, Writing up	85

The following co-authors contributed to the work. Co-authors who are students at Monash University must also indicate the extent of their contribution in percentage terms:

Name	**Nature of contribution**
Dr Gareth M. Forde	Initiation, Development, Review
Dr. Huanting Wang	Initiation, Key ideas, Development, Review
Dr. Wei Zhu	Results Interpretations

Candidate's signature		**Date**

Declaration by co-authors

The undersigned hereby certify that:

(1) the above declaration correctly reflects the nature and extent of the candidate's contribution to this work, and the nature of the contribution of each of the co-authors.
(2) they meet the criteria for authorship in that they have participated in the conception, execution, or interpretation, of at least that part of the publication in their field of expertise;
(3) they take public responsibility for their part of the publication, except for the responsible author who accepts overall responsibility for the publication;
(4) there are no other authors of the publication according to these criteria;
(5) potential conflicts of interest have been disclosed to (a) granting bodies, (b) the editor or publisher of journals or other publications, and (c) the head of the responsible academic unit; and
(6) the original data are stored at the following location(s) and will be held for at least five years from the date indicated below:

Location	Department of Chemical Engineering, Monash University – Clayton campus, Australia.

Signature		**Date**
Signature		**Date**
Signature		**Date**

Available online at www.sciencedirect.com
ScienceDirect
Journal of Colloid and Interface Science 308 (2007) 374–380
JOURNAL OF Colloid and Interface Science
www.elsevier.com/locate/jcis

Mesoporous silica spheres from colloids

Jenny Ho, Wei Zhu, Huanting Wang *, Gareth M. Forde *

Department of Chemical Engineering, Monash University, Clayton, VIC 3800, Australia

Received 6 October 2006; accepted 5 January 2007
Available online 10 January 2007

Abstract

A novel method has been developed to synthesize mesoporous silica spheres using commercial silica colloids (SNOWTEX) as precursors and electrolytes (ammonium nitrate and sodium chloride) as destabilizers. Crosslinked polyacrylamide hydrogel was used as a temporary barrier to obtain dispersible spherical mesoporous silica particles. The influences of synthesis conditions including solution composition and calcination temperature on the formation of the mesoporous silica particles were systematically investigated. The structure and morphology of the mesoporous silica particles were characterized via scanning electron microscopy (SEM) and N_2 sorption technique. Mesoporous silica particles with particle diameters ranging from 0.5 to 1.6 μm were produced whilst the BET surface area was in the range of 31–123 $m^2\,g^{-1}$. Their pore size could be adjusted from 14.1 to 28.8 nm by increasing the starting particle diameter from 20–30 nm up to 70–100 nm. A simple and cost effective method is reported that should open up new opportunities for the synthesis of scalable host materials with controllable structures.

Keywords: Mesoporous silica; Colloidal silica; Electrolyte; Sphere; Polyacrylamide hydrogel

1. Introduction

Over the past few years, inorganic silica has become attractive as a biomaterial because of its biocompatibility and excellent ability for functionalization through a broad range of chemical and physical methods [1–9]. In particular, spherical mesoporous silica spheres have been studied as hosts for encapsulation and immobilization of enzymes and other biomolecules, as vehicles for gene and drug delivery, as templates for the fabrication of mesoporous proteins and biopolymers, and as packing for high performance liquid chromatography [10–15]. Methods such as solution growth [10–16] and aerosol self assembly [17–19] have been developed to synthesize mesoporous silica spheres. Organosilicates such as tetraethylorthosilicate (TEOS) are used in these syntheses, and particularly organic templates are essential for generating the mesoporous structures of silica spheres.

Present in this paper is a novel, and alternative method for preparing mesoporous silica spheres. Commercial silica colloids (SNOWTEX) are used as starting materials, and the spherical agglomerates of silica nanoparticles are formed by adding inorganic salts (electrolytes) into the colloids. In order to retrieve these spherical agglomerates from the destabilized colloids, a polymer temporary barrier technique [20] is used to prevent their further agglomeration. This technique of using highly crosslinked polyacrylamide hydrogel was developed to effectively retrieve zeolite nanocrystals from colloidal suspension through drying and calcination without agglomeration [20]. High temperature treatment is adopted to improve the bonding strength of starting silica nanoparticles, and therefore the resulting mesoporous silica spheres are mechanically strong. The packing pore sizes (in the mesopore range) of the silica spheres obtained in this study are readily adjusted by using silica colloids with different particle diameters. The preparation and characterization of mesoporous silica spheres will be described in detail in this paper.

2. Experimental

2.1. Materials

All the solutions were prepared using analytical grade reagents. Deionized water was prepared with a Milli-Q Aca-

* Corresponding authors. Fax: +61 3 9905 5686.
E-mail addresses: huanting.wang@eng.monash.edu.au (H. Wang), gareth.forde@eng.monash.edu.au (G.M. Forde).

0021-9797/$ – see front matter
doi:10.1016/j.jcis.2007.01.009

demic A10 system. Three SNOWTEX silica colloids (ST-50: 20–30 nm, ST-20L: 40–50 nm, and ST-ZL: 70–100 nm) were provided by Nissan Chemical Industries (Tokyo, Japan), and were diluted into 10 wt% aqueous silica solution for later use. Ammonium nitrate (NH_4NO_3, 99%, Ajax Chemicals) and sodium chloride (NaCl, >99.5%, Aldrich) were used as electrolytes to destabilize the silica colloids. Monomer acrylamide, (CH_2=CHCONH$_2$, AM, 99%, Sigma–Aldrich), N,N'-methylenebisacrylamide, ((CH_2=CHCONH$_2$)$_2$CH$_2$, MBAM, 99%, Sigma–Aldrich), and initiator ammonium persulfate, ((NH_4)$_2$S$_2$O$_8$, >98%, Sigma–Aldrich) were used to produce the polymer temporary barrier.

2.2. Synthesis of mesoporous silica spheres

5 ml of 10 wt% colloidal silica solution was added dropwise into 5 ml of a given concentration of NH_4NO_3 or NaCl under magnetic stirring (500 rpm) and then stirred for 1 h at room temperature. To the resulting suspension, water-soluble monomer acrylamide, crosslinker N,N'-methylenebisacrylamide, and initiator ammonium persulfate (2 AM:0.02 MBAM:0.01 (NH_4)$_2$S$_2$O$_8$:1 SiO_2 by weight) were added under stirring. After the monomer, crosslinker, and initiator were dissolved, the whole suspension was further stirred for 10 min and ultrasonicated in an ultrasonic bath (Branson, Model 1510E-MT) for 5 min. The suspension obtained was heated at 90 °C for 30 min to form polymer hydrogel, followed by drying overnight at 90 °C. The resulting solids were heated at a heating rate of 2 °C min^{-1} up to 500 or 700 °C, and kept at this temperature for 2 h under nitrogen (99.999%, Linde) to sinter silica nanoparticles. The carbonized polymer hydrogel was finally removed by calcination under oxygen (99.5%, Linde) at 500 °C for 5 h to yield mesoporous silica spheres. As a comparison, a number of samples were also prepared without using polyacrylamide hydrogel. For those mesoporous silica spheres prepared with NaCl, the samples were washed with deionized water to remove residual NaCl and collected via centrifugation (Beckman Coulter, Allegra X-22 Centrifuge).

2.3. Characterization

Samples were characterized with a JEOL JSM-6300F field emission scanning electron microscope (FESEM) operated at an accelerating voltage of 15 kV. Nitrogen sorption measurements were performed at −196 °C on a Micromeritics ASAP 2020MC analyzer. Samples were degassed at 300 °C for 3 h prior to analysis. The surface areas were calculated by the BET (Brumauer–Emmett–Teller) method and the pore-size distribution curves were obtained from the desorption branch by using the BJH (Barrett–Joyner–Halenda) method. The pore volumes were estimated from the desorption branch of the isotherm at $P/P_0 = 0.98$ assuming complete pore saturation. The porosity of mesoporous silica particles was calculated from their pore volume and the density of dense silica (2.20 g cm^{-3}).

3. Results and discussion

3.1. Formation of mesoporous silica spheres

The formation of mesoporous silica spheres is schematically illustrated in Fig. 1. First, mesoporous silica agglomerates were formed in water by agglomerations of colloidal silica. The electrolyte dissolved in the water interferes with the surface charge of the colloids resulting in a charge imbalance that disrupts the stability of the colloids [21]. When retrieving silica agglomerates from the solution, drying or centrifugation would result in further agglomerations, hence a temporary barrier was introduced in order to separate the silica spherical agglomerates and prevent further agglomerations. This enabled dispersible spheres to form as compared to the bulky agglomerates obtained in the absence of a barrier. Silica spheres were then calcined at 500 °C under nitrogen with associated silanol group (Si–OH) condensation between the surfaces of the silica nanoparticles (show below) which resulting in high binding strength.

$$\cdots \underset{\vdots}{\overset{\vdots}{\text{Si}}} \cdots \text{OH} + \text{HO} \cdots \underset{\vdots}{\overset{\vdots}{\text{Si}}} \cdots \rightarrow \cdots \underset{\vdots}{\overset{\vdots}{\text{Si}}} \cdots \text{O} \cdots \underset{\vdots}{\overset{\vdots}{\text{Si}}} \cdots + \text{H}_2\text{O}.$$

Meanwhile, the polymer hydrogel was converted to carbon which acted as the barrier. Individual mesoporous silica spheres

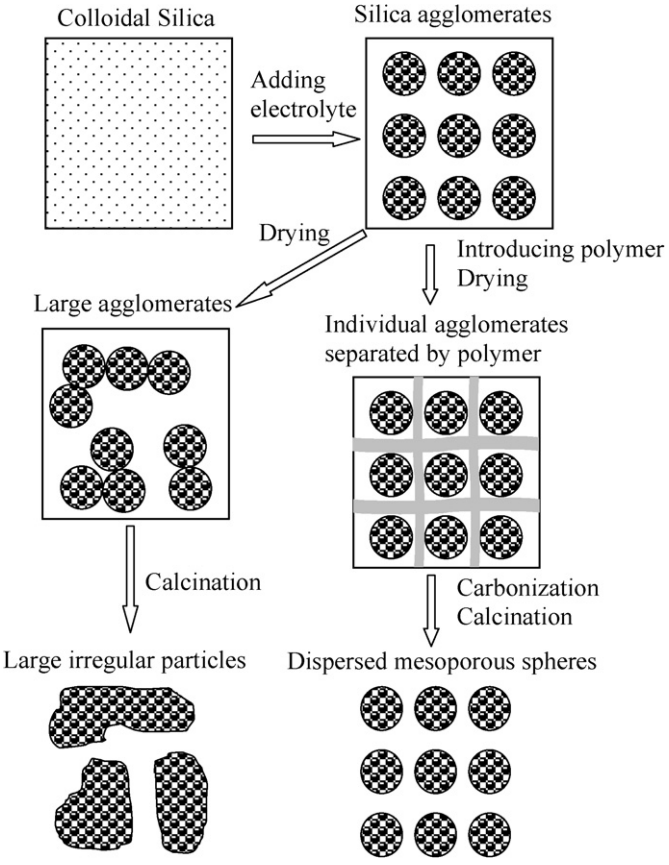

Fig. 1. Schematic illustration of the formation of mesoporous silica spheres with a temporary barrier.

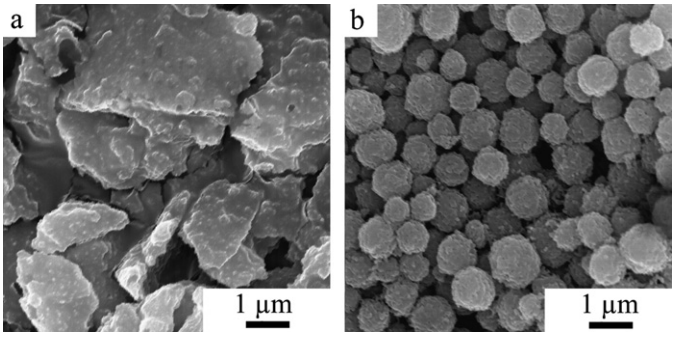

Fig. 2. SEM images of mesoporous silica particles prepared from SNOWTEX ST-50 (20–30 nm) and NaCl (0.5 mol L^{-1}). (a) Without polyacrylamide hydrogel, calcined at 500 °C and (b) with polyacrylamide hydrogel, calcined at 500 °C.

were obtained after the removal of the carbon barrier by combustion. The SEM images of mesoporous silica particles prepared with and without using polyacrylamide hydrogel are shown in Fig. 2. As expected, large mesoporous silica particles were formed without using polyacrylamide hydrogel (Fig. 2a) whereas mesoporous silica spheres with a narrow particle size distribution were obtained from polyacrylamide hydrogel (Fig. 2b). Thus, the three dimensional microsized pores of the highly crosslinked polyacrylamide hydrogel accommodating the silica agglomerates, assisted in the formation of mesoporous silica spheres. The hydrogel further served as a temporary barrier to prevent agglomeration of the resulting mesoporous silica spheres during drying and calcination.

3.2. *Effect of electrolyte concentration*

The concentration of NH_4NO_3 solution was varied from 0.13 to 0.50 mol L^{-1} in order to destabilize the colloid silicas. The SEM images of the silica agglomerates obtained at various NH_4NO_3 concentrations are shown in Fig. 3. Bulky and irregular silica agglomerates were formed by using a lower concentration of electrolyte (Fig. 3a) with a wide pore size distribution as shown in Fig. 4. More regular agglomerates (Figs. 3b–3d) with a narrow pore size distribution were obtained by increasing the electrolyte concentration. Moreover, the agglomerates obtained from the low concentration electrolyte have higher porosity and a larger average pore size (Table 1), suggesting that the precursors were loosely packed. Since the shape and pore structure of the silica agglomerates almost remained unchanged during calcination, it is suggested that the starting silica particle colloids were not coagulated uniformly when a low concentration electrolyte was used as the destabilizer. The colloid stability is generally determined by the sum of the attractive (van der Waals) and repulsive (electrical double layers) forces, which are a function of the distance of separation of the particles. The thickness of electrical double layers of particles is dependent on the concentration of counterions in solution, and decreases as the electrolyte concentration increases and therefore the energy barrier for stabilizing is reduced. At a critical concentration, the energy barrier disappears and the colloid particles then rapidly agglomerate [22]. As the energy barrier exists at the lower electrolyte concentration, a

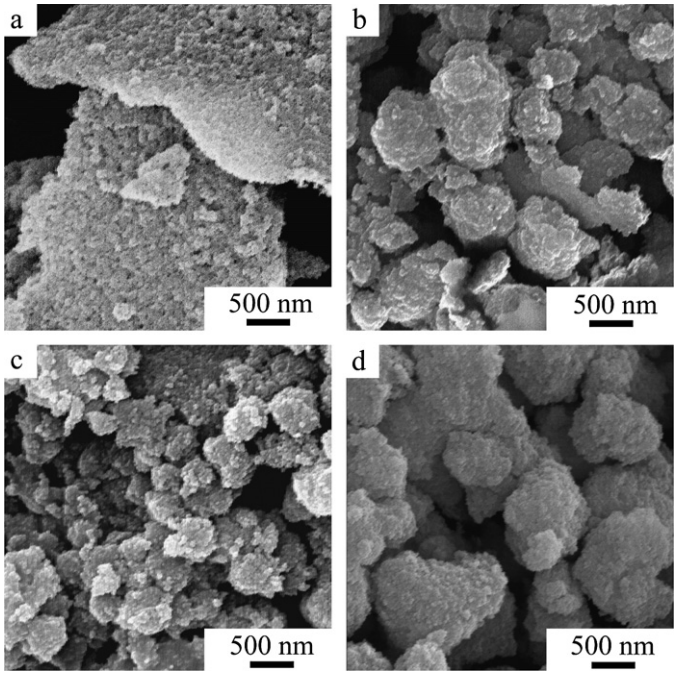

Fig. 3. SEM images of mesoporous silica prepared using SNOWTEX ST-50 (20–30 nm) and different concentrations of NH_4NO_3 (mol L^{-1}). (a) 0.13, (b) 0.25, (c) 0.30, and (d) 0.50 mol L^{-1}.

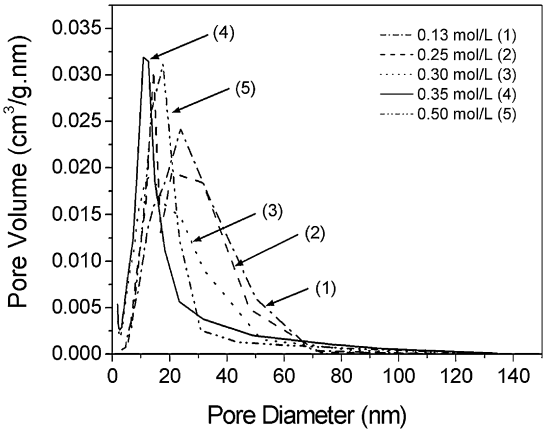

Fig. 4. Pore size distributions of mesoporous silica prepared using SNOWTEX ST-50 (20–30 nm) as precursor and several concentrations of NH_4NO_3 (mol L^{-1}).

slow coagulation process occurs resulting in incomplete agglomerations within a certain time. At low electrolyte concentrations, the starting silica particles might agglomerate loosely to form irregular particles with various sizes. When the electrolyte concentration increased, agglomerations of the colloid were complete when the electrolyte concentration increased; hence agglomerates with a narrow size distribution and regular shape were obtained. However, highly concentrated electrolyte caused rapid coagulation of precursors to form irregular particles (Fig. 3d). Therefore, the concentration of electrolyte is a crucial factor in determining agglomeration of the silica precursor into mesoporous particles. In our experiment, we found that the critical concentration was 0.35 mol L^{-1} NH_4NO_3 for the SNOWTEX ST-50 (20–30 nm), 0.25 mol L^{-1} NH_4NO_3 for the

Table 1
Nitrogen sorption results for mesoporous silica particles prepared using SNOWTEX ST-50 (20–30 nm) and different concentrations of NH_4NO_3 as electrolyte and calcined at 500 °C

NH_4NO_3 concentration (mol L^{-1})	BET surface area (m^2 g^{-1})	Pore volume (cm^3 g^{-1})	Mean pore size (nm)	Porosity (%)
0.13	117.0	0.77	23.4	63.1
0.25	112.9	0.75	22.0	62.5
0.30	124.1	0.57	16.7	55.9
0.35	123.0	0.49	14.1	52.1
0.50	117.9	0.49	18.1	52.1

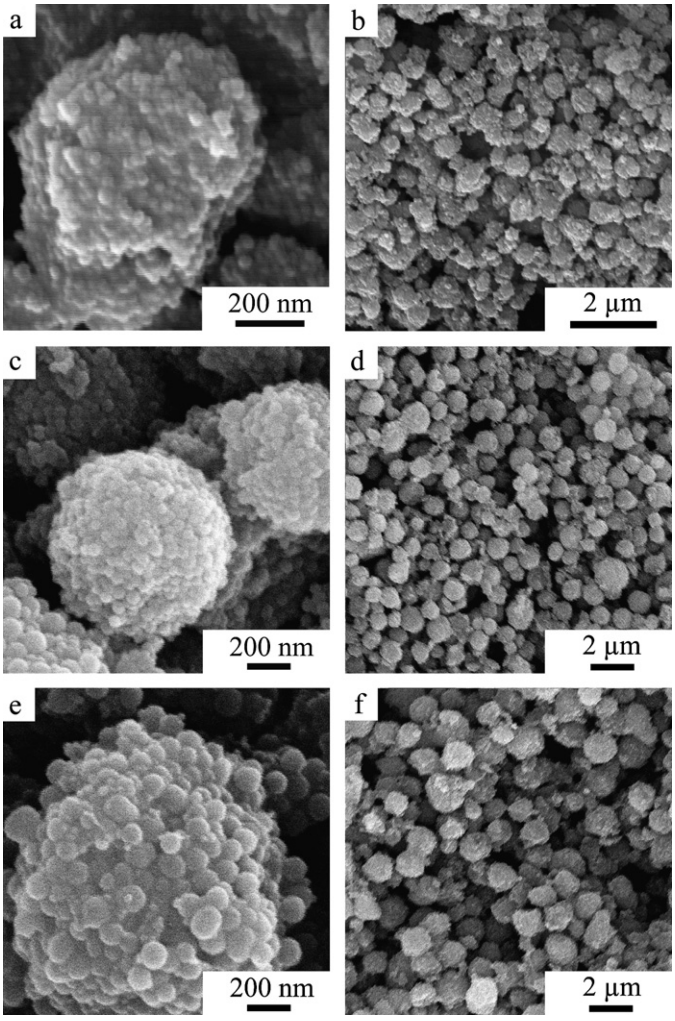

Fig. 5. SEM images of spherical mesoporous silica spheres prepared using NH_4NO_3 as electrolyte and different silica colloids. (a) and (b) 0.35 mol L^{-1} NH_4NO_3 and SNOWTEX ST-50 (20–30 nm), (c) and (d) 0.25 mol L^{-1} NH_4NO_3 and SNOWTEX ST-20L (40–50 nm), (d) and (e) 0.25 mol L^{-1} NH_4NO_3 and SNOWTEX ST-ZL (70–100 nm). All these spheres were obtained at 500 °C carbonization and calcination.

SNOWTEX ST-20L (40–50 nm), and 0.25 mol L^{-1} NH_4NO_3 for the SNOWTEX ST-ZL (70–100 nm), respectively.

3.3. Ammonium nitrate as a destabilizer

Typical SEM images of mesoporous silica spheres obtained from three different silica colloids are shown in Fig. 5. The

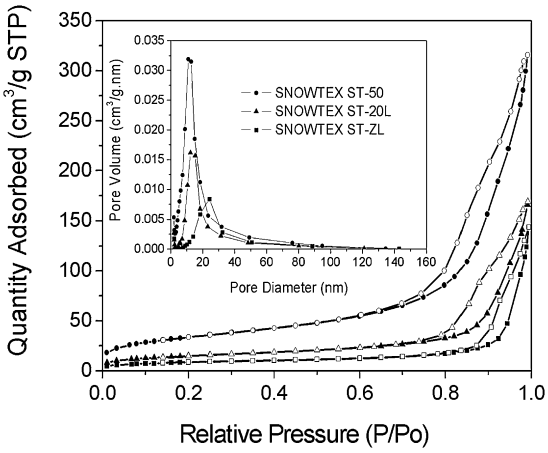

Fig. 6. Nitrogen adsorption (solid) and desorption (open) isotherms and pore size distributions (insets) of mesoporous silica spheres prepared with NH_4NO_3 and different silica colloids.

Table 2
Nitrogen sorption results for mesoporous silica spheres prepared using NH_4NO_3 as electrolyte and calcined at 500 °C

Silica colloids	BET surface area (m^2 g^{-1})	Pore volume (cm^3 g^{-1})	Mean pore size (nm)	Porosity (%)
SNOWTEX ST-50	123.0	0.49	14.1	52.1
SNOWTEX ST-20L	54.7	0.26	17.5	36.6
SNOWTEX ST-ZL	31.2	0.22	28.8	32.8

particles are well-defined spheres and have particle diameters ranging from 0.5 to 0.8 μm for the SNOWTEX ST-50 (20–30 nm), 0.6 to 1.3 μm for the SNOWTEX ST-20L (40–50 nm), and 0.8 to 1.6 μm for the SNOWTEX ST-ZL (70–100 nm). The diameters of the silica spheres (or the agglomerate size) may be determined by several factors such as (1) the number of precursor colloidal particles in each sphere (or agglomerate). The smaller the colloidal particles are, the greater the number of colloidal particles in each agglomerate to effectively minimize the surface energy; (2) the sizes of colloidal particles; (3) the packing density of precursor colloidal particles. Under the present experimental conditions, the diameters of mesoporous silica spheres increase with increasing the particle size of the precursor colloids. Obviously the sizes of colloidal particles play a major role in determining the diameters of mesoporous silica spheres. The SEM images at high magnification indicate that the starting silica nanoparticles were sintered together.

The nitrogen sorption isotherms of mesoporous silica spheres are shown in Fig. 6. The hysteresis loops clearly imply a mesoporous structure in the silica spheres [23]. The silica spheres derived from the SNOWTEX ST-50 (20–30 nm) have a BET surface area of 123.0 m^2 g^{-1}, a pore volume of 0.49 cm^3 g^{-1}, and a narrow pore distribution centered at 14.1 nm. The silica spheres derived from the SNOWTEX ST-20L (40–50 nm) and the SNOWTEX ST-ZL (70–100 nm) have a narrow pore distribution centered at 17.5 and 28.8 nm, respectively. The nitrogen sorption results and porosities of the mesoporous silica particles are summarized in Table 2. It can be seen that the pore size of silica spheres increases as the precursor particle diameter increases as the pore structure is the interstice of loosely packed

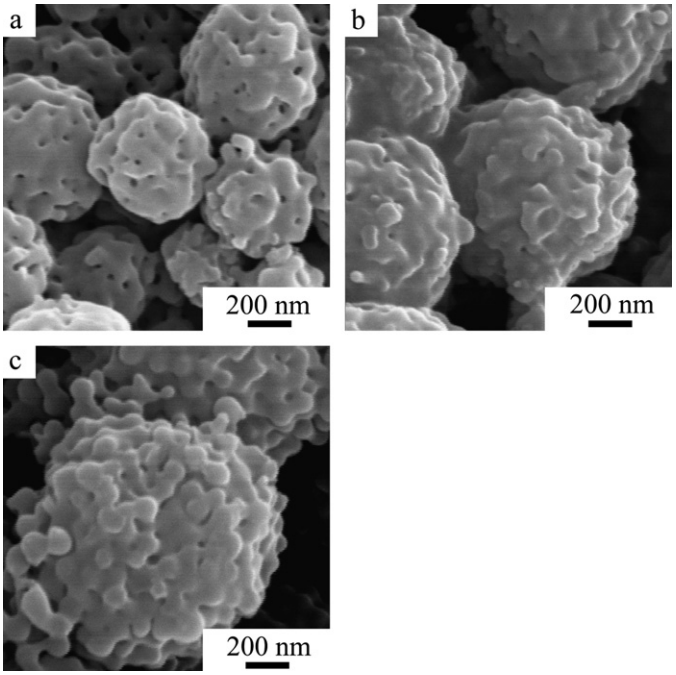

Fig. 7. SEM images of spherical mesoporous silica particles prepared using NaCl as electrolyte and different silica colloids. (a) 0.50 mol L^{-1} NaCl and SNOWTEX ST-50 (20–30 nm), (b) 0.25 mol L^{-1} NaCl and SNOWTEX ST-20L (40–50 nm), and (c) 0.25 mol L^{-1} NaCl and SNOWTEX ST-ZL (70–100 nm). All these particles were obtained at 500 °C carbonization and calcination.

precursor particles. Therefore, it is clear that the pore size of the mesoporous silica particles can be readily adjusted by changing the precursor particle diameter. It is noted that the BET surface areas of mesoporous silica spheres obtained are lower as compared with those templated mesoporous silicas [24,25], and they are limited by their precursor silica colloids. For instance, the BET surface area of 123.0 $m^2 g^{-1}$ of the silica spheres derived from SNOWTEX ST-50 is quite close to 128 $m^2 g^{-1}$ of the sample directly dried from SNOWTEX ST-50. Based on the BET surface area of 128 $m^2 g^{-1}$ and silica density of 2.2 g cm^{-3}, the average diameter of SNOWTEX ST-50 is calculated to be 21.3 nm, which is within the range of 20–30 nm.

3.4. Sodium chloride as a destabilizer

Sodium chloride (NaCl) was also used as the destabilizer to synthesize mesoporous silica spheres. The SEM images (Fig. 7) show coalescence of precursor nanoparticles occurred in the resultant spherical mesoporous silica particles. The nitrogen sorption results shows that the BET surface area and pore volume of mesoporous silica particles are small, while pore size distributions are fairly wide as compared with those prepared with NH_3NO_3 (Fig. 8 and Table 3). The precursor silicas were sintered in the presence of sodium chloride since the sodium silicate might form when silica reacts with sodium chloride at high temperatures [26]. This is supported by the fact that sodium was detected by energy dispersive X-ray spectroscopy (EDS). By contrast, NH_4NO_3 decomposed at a low temperature (approximately 210 °C), and could be completely removed from the mesoporous spheres.

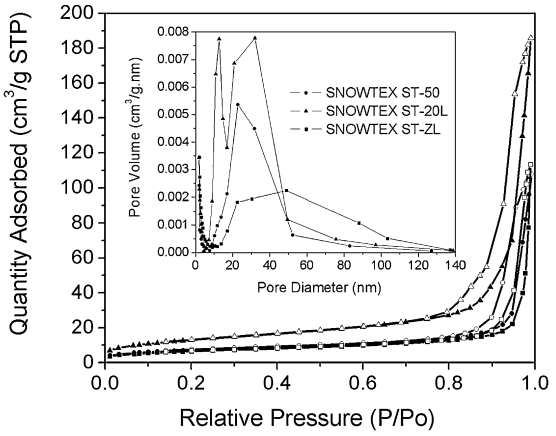

Fig. 8. Nitrogen adsorption (solid) and desorption (open) isotherms and pore size distributions (insets) of mesoporous silica particles prepared with NaCl and different silica colloids.

Table 3
Nitrogen sorption results for mesoporous silica particles prepared using NaCl as electrolyte and calcined at 500 °C

Silica colloids	BET surface area ($m^2 g^{-1}$)	Pore volume ($cm^3 g^{-1}$)	Mean pore size (nm)	Porosity (%)
SNOWTEX ST-50	26.1	0.17	25.9	27.4
SNOWTEX ST-20L	47.6	0.23	22.1	33.8
SNOWTEX ST-ZL	23.6	0.18	30.2	28.6

3.5. Effect of calcination temperature

The SEM images of the mesoporous silica particles obtained at 700 °C from different silica colloids are shown in Figs. 9 and 10 (as compared to Figs. 5 and 7).

These images show the extensive coalescence between the precursor silica nanoparticles. The role of heat treatment (carbonization and calcination) is to allow strained siloxane bonds to form between precursor silica particles and hence improve the mechanical strength of each individual mesoporous silica particle. These particles change from soft agglomerate to hard agglomerate after the heat treatment. In our experiment, mesoporous silica particles with well-defined pore size distribution were obtained by calcination at 500 °C. However, high temperature treatment (700 °C) leads to the coalescence of precursor silica nanoparticles (Figs. 9 and 10). Thus, the intensive sintering causes loss of BET surface area. The BET surface areas of mesoporous silica spheres obtained by using NH_4NO_3 are 41.5 $m^2 g^{-1}$ for SNOWTEX ST-50, 19.6 $m^2 g^{-1}$ for SNOWTEX ST-20L, and 16.7 $m^2 g^{-1}$ for SNOWTEX ST-ZL, respectively. In addition, their pore size distributions became wider and their average pore size increased: 32.1 nm for SNOWTEX ST-50, 30.3 nm for SNOWTEX ST-20L, and 38.9 nm for SNOWTEX ST-ZL, respectively. The results were attributed to the coalescence of precursor silica nanoparticles. Dehydration of the silanol groups occurred at 500 °C and the particles remain unchanged at this temperature. But at approximately 700 °C, surface fusion between the precursor silica particles occurred and subsequently caused the irregular distribution and reduction of the pore size. The same trends were observed in the synthesis of mesoporous spheres by using NaCl.

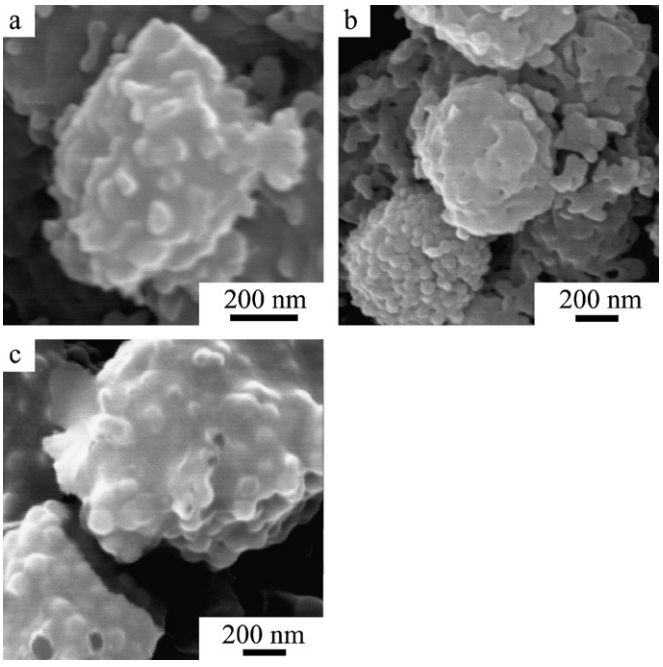

Fig. 9. SEM images of spherical mesoporous silicas prepared using NH_4NO_3 as electrolyte and different silica colloids. (a) 0.35 mol L^{-1} NH_4NO_3 and SNOWTEX ST-50 (20–30 nm), (b) 0.25 mol L^{-1} NH_4NO_3 and SNOWTEX ST-20L (40–50 nm), and (c) 0.25 mol L^{-1} NH_4NO_3 and SNOWTEX ST-ZL (70–100 nm). All these particles were obtained by calcination at 700 °C.

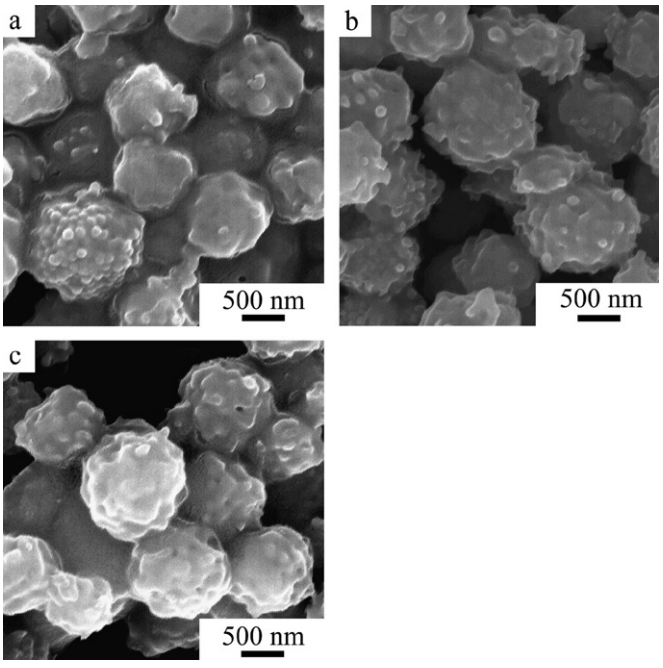

Fig. 10. SEM images of spherical mesoporous silicas prepared using NaCl as electrolyte and different silica colloids. (a) 0.50 mol L^{-1} NaCl and SNOWTEX ST-50 (20–30 nm), (b) 0.25 mol L^{-1} NaCl and SNOWTEX ST-20L (40–50 nm), and (c) 0.25 mol L^{-1} NaCl and SNOWTEX ST-ZL (70–100 nm). All these particles were obtained by calcination at 700 °C.

4. Conclusions

Novel synthesis of mesoporous silica particles at the micrometer scale with tailored pore size has been developed by using a simple electrolyte (ammonium nitrate or sodium chloride) and inexpensive commercial inorganic silica. Mesopore size can be easily adjusted by changing the precursor particle diameter. It is anticipated that our new method will offer great flexibility in tuning the pore size of the silica spheres since the pore size of templated silicas is limited by the organic template's molecular size. Also, other parameters such as the type of electrolyte, concentration of electrolyte and heat treatment temperature were shown to affect the morphology and structure of the final particles. Polyacrylamide hydrogel is essential as a temporary barrier to prevent further agglomerations during synthesis in order to achieve monodisperse particle distributions. This novel method is easily scalable to produce large quantities of mesoporous silica spheres for potential use in bio-nanotechnology, drug delivery and inorganic adsorbent applications.

Acknowledgments

This work was supported by the Australian Research Council and Monash University. The facilities and technical assistance from staff at the Electron Microscopy and Microanalysis Facility, Monash University, are gratefully appreciated. H.W. thanks the Australian Research Council for the QEII Fellowship. G.M.F. thanks the Victorian Endowment for Science, Knowledge and Innovation (VESKI) for the Innovation Fellowship and support of this research. J.H. gratefully acknowledges the financial support from Monash Departmental Scholarship. We thank SNOWTEX, Nissan Chemical Industries, Tokyo, Japan, for providing silica colloids.

References

[1] C. Kneuer, M. Sameti, E.G. Haltner, T. Schiestel, H. Schirra, H. Schmidt, C.M. Lehr, Int. J. Pharm. 196 (2000) 257–261.
[2] D. Luo, W.M. Saltzman, Gene Ther. 13 (2006) 585–586.
[3] D. Luo, W.M. Saltzman, Nat. Biotechnol. 18 (2000) 893–895.
[4] D. Luo, E. Han, N. Belcheva, W.M. Saltzman, J. Control. Rel. 95 (2004) 333–341.
[5] L. Ji, A. Katiyar, N.G. Pinto, M. Jaroniec, P.G. Smirniotis, Micropor. Mesopor. Mater. 75 (2004) 221–229.
[6] H.H.P. Yiu, C.H. Botting, N.P. Botting, P.A. Wright, Phys. Chem. Chem. Phys. 3 (2001) 2983–2985.
[7] J. Lei, J. Fan, C.Z. Yu, L.Y. Zhang, S.Y. Jiang, B. Tu, D.Y. Zhao, Micropor. Mesopor. Mater. 73 (2004) 121–128.
[8] M. Fujiwara, F. Yamamoto, K. Okamoto, K. Shiokawa, R. Nomura, Anal. Chem. 77 (2005) 8138–8145.
[9] D.R. Radu, C.Y. Lai, K. Jeftinija, E.W. Rowe, S. Jeftinija, V.S.Y. Lin, J. Am. Chem. Soc. 126 (2004) 13216–13217.
[10] A.M. Yu, Y.J. Wang, E. Barlow, F. Caruso, Adv. Mater. 17 (2005) 1737–1741.
[11] Y.J. Wang, F. Caruso, Chem. Mater. 17 (2005) 953–961.
[12] Y.J. Wang, F. Caruso, Adv. Mater. 18 (2006) 795–800.
[13] D. Luo, MRS Bull. 30 (2005) 654–658.
[14] K.K. Unger, D. Kumar, M. Grun, G. Buchel, S. Ludtke, T. Adam, K. Schumacher, S. Renker, J. Chromatogr. A 892 (2000) 47–55.
[15] Y.R. Ma, L.M. Qi, J.M. Ma, Y.Q. Wu, O. Liu, H.M. Cheng, Colloids Surf. A Physicochem. Eng. Aspects 229 (2003) 1–8.
[16] K. Do Kim, G.B. Kim, H.T. Kim, J. Chem. Eng. Jpn. 38 (2005) 547–552.
[17] J.E. Hampsey, S. Arsenault, Q.Y. Hu, Y.F. Lu, Chem. Mater. 17 (2005) 2475–2480.

[18] N. Baccile, D. Grosso, C. Sanchez, J. Mater. Chem. 13 (2003) 3011–3016.
[19] W. Liang, M. Liu, G. Guo, Microemulsions, in: Z.L. Wang, Y. Liu, Z. Zhang (Eds.), Handbook of Nanophase and Nanostructured Materials, Kluwer Academic/Plenum, New York, 2003, pp. 1–25.
[20] H. Wang, Z. Wang, Y. Yan, Chem. Commun. (2000) 2333–2334.
[21] L.H. Allen, E. Matijević, J. Colloid Interface Sci. 31 (1969) 287–296.
[22] M. Drew, Colloids and Colloidal Stability, in: Surfaces, Interfaces, and Colloids, second ed., Wiley–VCH, Weinheim, 2002, pp. 214–252.
[23] K.S.W. Sing, D.H. Everett, R.A.W. Haul, L. Moscou, R.A. Pierotti, J. Rouquerol, T. Siemieniewska, Pure Appl. Chem. 57 (1985) 603–619.
[24] D.Y. Zhao, J.L. Feng, Q.S. Huo, N. Melosh, G.H. Fredrickson, B.F. Chmelka, G.D. Stucky, Science 279 (1998) 548–552.
[25] J.S. Beck, J.C. Vartuli, W.J. Roth, M.E. Leonowicz, C.T. Kresge, K.D. Schmitt, C.T.W. Chu, D.H. Olson, E.W. Sheppard, S.B. McCullen, J.B. Higgins, J.L. Schlenker, J. Am. Chem. Soc. 114 (1992) 10834–10843.
[26] F.H. Clews, H.V. Thompson, J. Chem. Soc. 121 (1922) 1442–1448.

CHAPTER THREE

APPLICATION AND PERFORMANCE OF MESOPOROUS SILICA SPHERES FOR PROTEIN ADSORPTION

Protein loaded mesoporous silica spheres as a controlled delivery platform

Jenny Ho, Michael K. Danquah, Huanting Wang, Gareth M. Forde

Journal of Chemical Technology and Biotechnology

83 (2008) 351 – 358

Monash University

Declaration for Thesis Chapter Three

Declaration by candidate

In the case of Chapter 3, the nature and extent of my contribution to the work was the following:

Nature of contribution	Extent of contribution (%)
Initiation, Key ideas, Experimental works, Development, Data analysis, Writing up	85

The following co-authors contributed to the work. Co-authors who are students at Monash University must also indicate the extent of their contribution in percentage terms:

Name	Nature of contribution
Dr Gareth M. Forde	Key ideas, Development, Review
Dr. Huanting Wang	Key ideas, Development, Review
Dr. Michael K. Danquah	Experimental works, Review

Candidate's signature		**Date**

Declaration by co-authors

The undersigned hereby certify that:

(1) the above declaration correctly reflects the nature and extent of the candidate's contribution to this work, and the nature of the contribution of each of the co-authors.
(2) they meet the criteria for authorship in that they have participated in the conception, execution, or interpretation, of at least that part of the publication in their field of expertise;
(3) they take public responsibility for their part of the publication, except for the responsible author who accepts overall responsibility for the publication;
(4) there are no other authors of the publication according to these criteria;
(5) potential conflicts of interest have been disclosed to (a) granting bodies, (b) the editor or publisher of journals or other publications, and (c) the head of the responsible academic unit; and
(6) the original data are stored at the following location(s) and will be held for at least five years from the date indicated below:

Location	Department of Chemical Engineering, Monash University – Clayton campus, Australia.

Signature		**Date**
Signature		**Date**
Signature		**Date**

Journal of Chemical Technology and Biotechnology J Chem Technol Biotechnol 83:351–358 (2008)

Protein loaded mesoporous silica spheres as a controlled delivery platform

Jenny Ho,* Michael K Danquah, Huanting Wang and Gareth M Forde*
Department of Chemical Engineering, Monash University, Clayton, 3800, VIC, Australia

Abstract

BACKGROUND: The adsorption of bovine serum albumin (BSA) onto mesoporous silica spheres (MPS) synthesized from silica colloids was studied employing real time *in situ* measurements. The stabilities of the BSA at different pH values, their isoelectric points and zeta potentials were determined in order to probe the interactions between the protein and the mesoporous silica.

RESULTS: The pore size of MPS was designed for protein, and this, coupled with an in depth understanding of the physico-chemical characteristics of the protein and MPS has yielded a better binding capacity and delivery profile. The adsorption isotherm at pH 4.2 fitted the Langmuir model and displayed the highest adsorption capacity (71.43 mg mL^{-1} MPS). Furthermore, the delivery rates of BSA from the MPS under physiological conditions were shown to be dependent on the ionic strength of the buffer and protein loading concentration.

CONCLUSION: Economics and scale-up considerations of mesoporous material synthesized via destabilization of colloids by electrolyte indicate the scaleability and commercial viability of this technology as a delivery platform for biopharmaceutical applications.

Keywords: mesoporous silica sphere; protein delivery platform; protein adsorption; colloidal silica; *in vitro* delivery studies

INTRODUCTION

Biopharmaceuticals represent a new generation of therapeutics that will account for a market worth billions of dollars in the near future: biogenerics in the USA and Europe alone are predicted to generate sales of $16.39 billion by 2011 at an average annual growth rate of 69.8%.[1] As a result, improved delivery systems for biomolecules that provide sustained release over time while simultaneously protecting the biopharmaceuticals from degradation are increasing in importance. Inorganic silica has become attractive as a biomaterial because of its good biocompatibility, low cytotoxicity, tailorable surface charge and excellent ability for functionalization through a broad range of chemical and physical methods, thus enabling a tailored interaction with the biomolecule of interest. In particular, silica spheres have been studied as vehicles for gene and drug delivery, specifically employed as hosts for encapsulation and immobilization of enzymes and other biomolecules.[2–7] There have been a number of reports describing the immobilization of protein onto mesoporous silica surface and the favorable conditions for this reaction to happen.[8–11] Balkus *et al*.[12,13] and Han *et al*.[14] have shown that the adsorption of protein is strongly dependent on the pore size of the materials, while other researchers[9–11,15,16] have established that many factors, such as surface area, pore size distribution, ionic strength, isoelectric point, and surface characteristics of both the support and adsorbate, have a strong influence on the loading of the protein. However, most of this research has focused on the immobilization of enzymes onto two mesoporous materials, SBA-15 and MCM-41, which are made by the use of self-assembled surfactants as templates and organosilicates as silica source, to retain the activity and stability of the enzymes. Adsorption and controlled release of drugs/biopharmaceuticals from mesoporous materials as a delivery platform have not been studied in detail. In previous studies dealing with the synthesis of mesoporous silica,[17,18] organosilicates such as tetraethylorthosilicate (TEOS) and organic templates have been shown to be essential for generating conventional mesoporous silica materials. Very recently, a novel, cost-effective method has been developed for synthesis of mesoporous silica spheres (MPS) from commercial silica colloids.[19]

This paper reports on the binding of bovine serum albumin (BSA), which was chosen as a model protein due to its good antigenic properties and strong cellular immunity via T lymphocytes as well as humoral immunity via B-lymphocytes,[20] to MPS that were synthesized from commercial silica

* Correspondence to: Jenny Ho and Gareth M Forde , Department of Chemical Engineering, Monash University, Clayton, 3800, VIC, Australia
E-mail: jenny.ho@eng.monash.edu.au; gareth.forde@monash.edu.au
(*Received 3 September 2007; revised version received 28 September 2007; accepted 28 September 2007*)
Published online 27 December 2007; DOI: 10.1002/jctb.1818

 J Chem Technol Biotechnol 0268–2575/2007/$30.00

colloids. The kinetics of the adsorption of BSA onto MPS was studied as well as the influence of surface potential, isoelectric point and pH. In order to study the potential of these MPS for use as a drug delivery system, the *in vitro* release profiles of BSA under physiological and different ionic conditions were investigated. A great advantage of the inorganic MPS particles as delivery carriers is their good biocompatibility and low cytotoxicity. They have a high LD 50 ($>1\,mg\,mL^{-1}$)[2,21] and do not cause tissue damage or immunological side effects. Almost all inorganic biomaterials are chemically stable and their physiochemical properties can be kept unchanged during the whole delivery process. These biomaterials will be accumulated in cells, circulated in plasma or metabolized away.[7,22] This paper can guide future studies in tailoring the MPS to match with different properties of relevant proteins.

EXPERIMENTAL

Materials

All solutions were prepared using analytical grade reagents. Deionized water was prepared with a Milli-Q Gradient A10 system and filtered through a 0.22 μm sterile filter. SNOWTEX® silica colloid (ST-20L: 40–50 nm) was provided by Nissan Chemical Industries (Tokyo, Japan) and was diluted into a 10 wt % aqueous silica before use. Ammonium nitrate (NH_4NO_3, 99%, Ajax Chemicals) was used as an electrolyte to destabilize the silica colloids. Monomer acrylamide (AM, $CH_2{=}CHCONH_2$, 99%, Sigma-Aldrich), *N*,*N*′- methylenebisacrylamide (MBAM, $(CH_2{=}CHCONH_2)_2CH_2$, 99%, Sigma-Aldrich) and initiator ammonium persulfate ($(NH_4)_2S_2O_8$, >98%, Sigma-Aldrich) were used to produce the polymer temporary barrier. Bovine serum albumin (BSA, 98%, MW ~66 kDa, Sigma-Aldrich) stock solutions were prepared by dissolving in sodium acetate buffer (10 mmol L^{-1} CH_3COONa, ~ pH 4.2).

Methods

Synthesis and characterization of MPS

MPS were produced using the method previously reported.[19] Briefly, MPS were synthesized from commercially available silica colloids (SNOWTEX®ST-20L, Tokyo, Japan) with simple electrolyte. 5.0 mL of 10 wt % colloidal silica solution was added dropwise into 5.0 mL of a given concentration of NH_4NO_3 under magnetic stirring (500 rpm) and then stirred for 1 h at room temperature. To the resulting suspension, water-soluble monomer acrylamide, crosslinker *N*,*N*′-methylenebisacrylamide, and initiator ammonium persulfate (2 AM : 0.02 MBAM : 0.01 $(NH_4)_2S_2O_8$: 1 SiO_2 by weight) were added under stirring. After the monomer, crosslinker, and initiator were dissolved, the whole suspension was further stirred for 10 min and ultrasonicated in an ultrasonic bath (Branson, Model 1510E-MT; Danbury, CT, USA) for 5 min. The suspension obtained was heated at 90 °C for 30 min to form polymer hydrogel, followed by drying overnight at 90 °C. The resulting solids were heated at a rate of 2 °C min^{-1} to 500 °C, and kept at this temperature for 2 h under N_2 (99.999%, Linde, Murray Hill, NJ, USA) to sinter the silica nanoparticles. The carbonized polymer hydrogel was finally removed by calcination under oxygen (99.999%, Linde) at 500 °C for 5 h to yield MPS. Nitrogen sorption measurements were performed at −196 °C using a Micromeritics (Norcross, GA, USA) ASAP 2020MC analyser for the MPS and MPS with adsorbed BSA (MPS-BSA). The MPS and MPS-BSA samples were weighed and degassed at room temperature and 5.0 mbar for 3 h prior to analysis. Degassing was performed at room temperature to prevent protein denaturation. Surface areas were calculated by the BET (Brumauer–Emmett–Teller) method and pore-size distribution curves were obtained from the desorption branch using the BJH (Barrett–Joyner–Halenda) method. The pore volumes were estimated from the desorption branch of the isotherm at $P/P_0 = 0.98$ assuming complete pore saturation. The MPS and MPS-BSA samples were also characterized using a JEOL (Tokyo, Japan) JSM-6300F field emission scanning electron microscope (FESEM) operated at an accelerating voltage of 15 kV.

Zeta potential measurements

Isoelectric points and size distributions of BSA and MPS were determined using a Malvern Instruments (Malvern, UK) Zetasizer Nano ZS series (ZEN 3600) equipped with an autotitration system (Malvern multipurpose titrator MPT2). Sample of BSA was dissolved and MPS was suspended (20.0 mg per 100.0 mL) in deionized water and 10.0 mL aliquots of these solutions were then titrated with 0.25 mol L^{-1} and 0.025 mol L^{-1} CH_3COOH from ~ pH 5.0 to 2.0 in 0.5 steps. Zeta measurements were determined in triplicate at each pH point, and the isoelectric points were calculated using Dispersion Technology Software, version 4.20 (Malvern Instruments Ltd.).

BSA adsorption

BSA adsorption isotherms were generated by loading BSA solution (5.0–50.0 mg mL^{-1}) in a continuous flow fashion at a flowrate of 0.2 mL min^{-1} onto 1.0 mL (~400 mg) of MPS packed in an Econo-Pac column (ID 1.5 cm, BIO-RAD, Hercules, CA, USA) at 25 °C. The outlet concentrations of BSA were measured with a UV spectrophotometer at 280 nm. The resulting MPS loaded with BSA were then washed continuously with deionized water (1.0 mL min^{-1}) for 20 min in order to leach out loosely bound BSA from the silica surface. The outlet deionized water was collected and the concentrations of BSA were measured at 280 nm using a UV-visible spectrophotometer (UV-2450, Shimadzu, Japan). The total amount of bound BSA was calculated by performing a mass balance of the BSA using data from the breakthrough curve and leaching stage.

BSA delivery

A study was undertaken to determine whether the MPS-BSA particles were capable of delivering the adsorbed BSA under physiological conditions *in vitro* (phosphate buffered saline (PBS), 37 °C, 200 rpm). 100.0 mg of MPS-BSA particles were suspended in 2.0 mL of PBS buffer (0.01 mol L^{-1}). At predetermined times (every 10 min for the initial burst period (4 h) and every 10 h in the subsequent period), the samples were subjected to centrifugation (14 000 *g* for 1 min in a Heraeus Multifuge® 3 S-R centrifuge) to pellet the MPS. The supernatant was removed and the concentration of released BSA was determined using a Bradford Reagent (Sigma-Aldrich, St Louis, MO, USA) assay: 0.9 mL of Bradford Reagent was added to a 0.1 mL aliquot of sample. The solution was mixed by inversion and allowed to sit for 5 min. The optical density of the solution was measured at 595 nm using a UV-visible spectrophotometer (UV-2450, Shimadzu, Tokyo, Japan). The volume of supernatant removed was replaced with fresh PBS. Blank MPS was subjected to the *in vitro* study condition in parallel with the BSA loaded MPS in order to study the contribution of MPS to the absorption at 595 nm. Blank MPS were harvested as described above, the absorption at 595 nm determined, and subtracted from those obtained from the BSA- loaded MPS system. Release experiments were performed in triplicate ($n = 3$), and the results averaged. The influence of buffer ionic strength on protein delivery was also studied by introducing known concentrations of NaCl.

Electrophoresis studies

The molecular weight and conformation of BSA before adsorption and after delivery were observed using an Experion Automated Electrophoresis System (BIO-RAD) used according to manufacturer's instructions.

RESULTS AND DISCUSSION

Characterization of BSA and MPS

Both the BSA and MPS were carefully characterized in order to study BSA adsorption at optimal binding conditions. The surface charges of the species were analyzed using zeta potential measurements, from which the isoelectric points (pI) were determined. The results from the zeta potential analysis for BSA and MPS are shown in Fig. 1(a) and Fig. 1(b). The pI of BSA and MPS were calculated to be pH 4.64 and pH 3.64, respectively. The sizes (hydrodynamic radii) of BSA and MPS at different pH values were also determined to examine their influence on protein adsorption. The hydrodynamic diameters of BSA and MPS were strongly dependent on the pH of the buffer; the diameters increased as the buffer pH was reduced towards the pI. However, BSA achieved a maximum size of ~7.8 nm (polydispersity index = 0.627 ± 0.032) at its pI point and the size decreased again, while the zeta potential/surface charge increased for pH values below the pI point. Minimum hydrodynamic diameter of BSA reached 2.23 nm (polydispersity index = 0.427 ± 0.084) at pH 7.03. Expansion and contraction of the hydrodynamic diameter of BSA at different pH values are a result of the cohesive attractive and repulsive forces associated with the BSA molecule. Conversely, the hydrodynamic diameter of MPS continually increased for pH values below the pI point (up to 12 μm, polydispersity index = 0.885 ± 0.150). This was despite increases in the surface charge as the repulsive force between the MPS molecules was not sufficiently strong enough to prevent flocculation, thus stable agglomerates were formed. The mean particle size distribution of MPS is 0.84 ± 0.05 μm at pH 4.91. It was noticed that silica nanoparticles with an average diameter larger than 0.20 μm promote sedimentation at the cell surface, thus increasing the transfection efficiency.[5] Surface potential (zeta potential) gives an indication of the potential stability of the colloidal system. If all the particles in suspension have a large negative or positive zeta potential then they will tend to repel each other, thereby resulting in no tendency to flocculate. However, if the particles have low zeta potential values then there is no force to prevent the particles coming together and flocculating. The general dividing line between stable and unstable suspensions is generally taken at either +30 mV or −30 mV. Particles with absolute zeta potential values greater than 30 mV are normally considered stable.[23] The 'low' (<30 mV) absolute values of the MPS zeta potential for pH values below 3.5 indicates that the MPS colloidal system is unstable at these low pH values. This implies that the optimum pH to carry out adsorption of BSA to MPS is ~ pH 4. At this point, MPS is negatively charged and well dispersed, while BSA is positively charged and has a hydrodynamic radius around 6 nm. The hydrodynamic diameters of BSA range from 2.23 nm at pH 7.03 up to 7.80 nm at pH 4.74, hence BSA is sufficiently small at all pH levels that were examined to diffuse into the pores of MPS, which are ~17.5 nm, as confirmed by the BJH method.[10] Such diffusion is enhanced by a smaller hydrodynamic diameter, which gives a reduced solute molar volume.[24]

Adsorption studies

The isoelectric point (pI) of BSA is pH 4.64 hence, BSA has a net positive charge below the pI value and a net negative charge above the pI value. The dominant driving forces responsible for the interaction between BSA and MPS are van der Waals attraction and electrostatic attraction between the amino acid residues on the surface of BSA and silanol groups on the surface of MPS.[25] Under the condition of 10 mmol L^{-1} sodium acetate buffer (pH 4.2), the net charge of BSA molecules is low. Consequently, binding to the MPS surface can be considered analogous to a neutralized precipitation between the BSA molecules and the MPS, for which closer packing of the BSA molecule is possible. Thus, the dominant adsorption mechanism will be

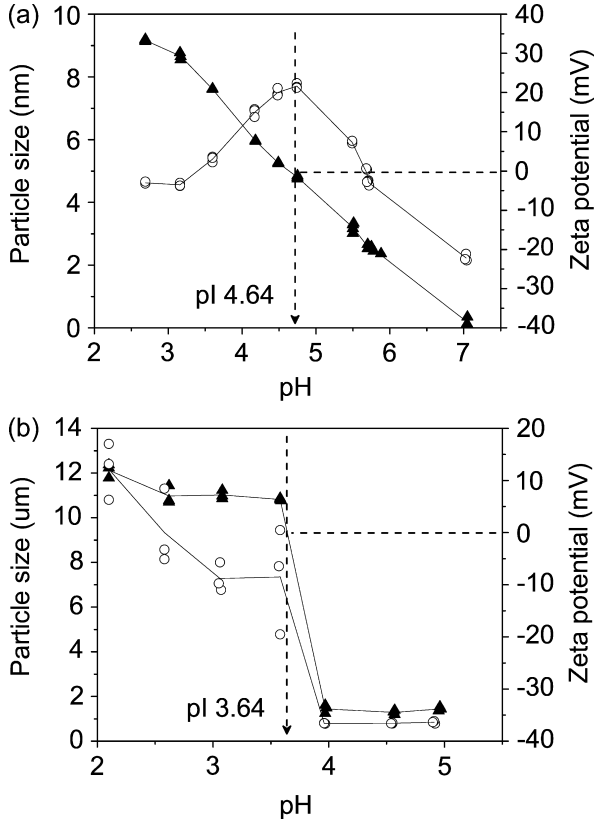

Figure 1. Plot of zeta potentials (▲) and sizes (○) of (a) BSA and (b) MPS versus pH. The pI values of BSA and MPS are pH 4.64 and pH 3.64, respectively.

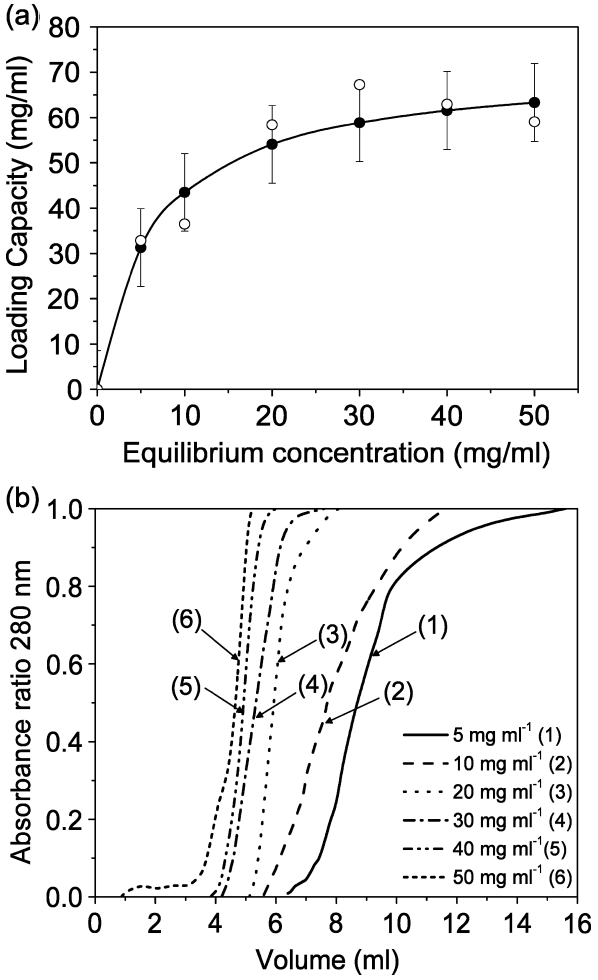

Figure 2. (a) Adsorption isotherm of BSA onto MPS in 10 mmol L^{-1} CH_3COONa buffer (pH 4.2) at 25 °C. A flowrate of 0.2 mL min^{-1} was used for all experiments: experimental data employing the Langmuir model (solid) and experimental data (open). (b) Break through curve for different concentrations of BSA under continuous loading onto a chromatography column packed with MPS (1 mL).

the attraction of the non-polar side chains of the amino acid residues on the surface of the BSA to the silanol groups on the MPS surface. Decreasing the pH value results in an increasing net positive charge for the protein molecule and causes an increase in the repulsion between amino acid residues. This will cause the protein molecules to repel each other, hence the monolayer binding capacity decreases. The adsorption isotherm (Fig. 2(a)) appears to be an L-type isotherm,[26] implying a strong interaction between the BSA molecule and the MPS surface. The isotherm shows a sharp initial rise, suggesting fast adsorption kinetics between the BSA and the MPS surface. The solid line in this figure represents a fit of the experimental data employing the Langmuir model. The monolayer adsorption capacity was calculated using the Langmuir equation:

$$q^* = \frac{q_{\max} C^*}{K_D + C^*} \tag{1}$$

where K_D is the Langmuir constant, C^* is the concentration of BSA solution, $q_{\max}$ is the maximum monolayer adsorption capacity and q^* is the amount of BSA adsorbed on the MPS. K_D and $q_{\max}$ obtained from this correlation are 6.42 mg mL^{-1} of MPS (9.88×10^{-5} mol L^{-1}) and 71.43 mg mL^{-1} of MPS, respectively, which is a higher maximum binding capacity than found in previous studies.[9,10,27] The K_D value displayed by BSA for MPS indicates the suitability of MPS as a protein delivery platform, as the K_D value dictates the strength of binding and indicates ratios of dissociation and association rates of the protein for the adsorbent. Figure 2(b) shows the breakthrough curve for several concentrations of BSA that were loaded onto chromatography columns packed with MPS. The maximum BSA binding capacity (column saturation) was obtained most quickly (22 min) for a BSA feed concentration of 50 mg mL^{-1}. Trace amounts of BSA (<5% of maximum absorbance at 280 nm) were detected in the deionized water used to leach out protein molecules that were loosely bound to the MPS surface after column saturation. Continuous loading and real-time measurements of BSA concentration in the outlet minimized the errors associated with mixing and washing in batch mode, thus the effectiveness and efficiency of BSA loading on MPS in a scalable, continuous process was displayed. Moreover, continuous loading also reduced the time needed to reach equilibrium adsorption,[28] which was less than 2 h on average.

Characterization of support after adsorption studies

Figures 3 and 4 show the characteristics of the MPS before and after BSA adsorption. Nitrogen adsorption/desorption isotherms before and after loading with BSA (feed concentration of 40 mg mL^{-1}) are shown in Fig. 3. The hysteresis loops clearly show a mesoporous structure in the silica spheres. The amount of nitrogen adsorbed decreased after BSA loading. The pore volume decreased from 0.22 to 0.16 $cm^3\,g^{-1}$, the mean pore diameter decreased from 17.5 to 12.5 nm (insets in Fig. 3) and the surface area reduced from 56.7 to 39.9 $m^2\,g^{-1}$ upon the adsorption of 61.55 mg mL^{-1} BSA. Figure 4 compares the structure and conformation of the MPS before (Fig. 4(a)) and after (Fig. 4(b)) BSA loading. The SEM images show that the MPS retained spherical shape, and were highly dispersible after BSA adsorption.

In vitro release profile of BSA

One of the main purposes of this work was to determine the feasibility of using MPS synthesized from colloids as a platform for controlled biopharmaceutical/protein delivery. Comparisons of the cumulative release profiles of BSA for the first 72 h are displayed in Fig. 5, which shows that each concentration has a similar delivery profile. In general, the delivery profiles

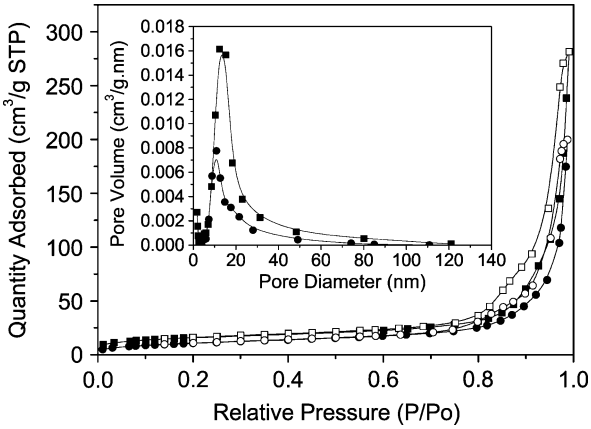

Figure 3. Nitrogen adsorption (solid) and desorption (open) isotherms and pore size distribution (insets) of MPS before and after BSA adsorption: ■, original; ●, 61.55 mg mL^{-1}. All the isotherms show the feature of Type IV isotherm that indicated the pore structure of mesoporous solids.

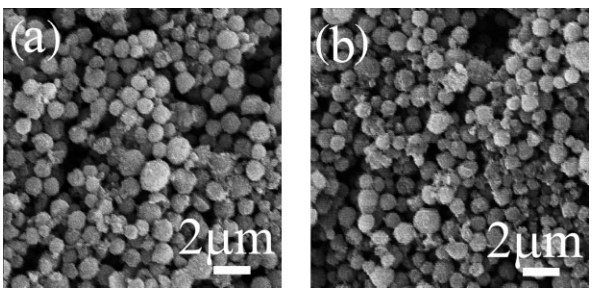

Figure 4. SEM images of MPS before (a) and after (b) BSA adsorption.

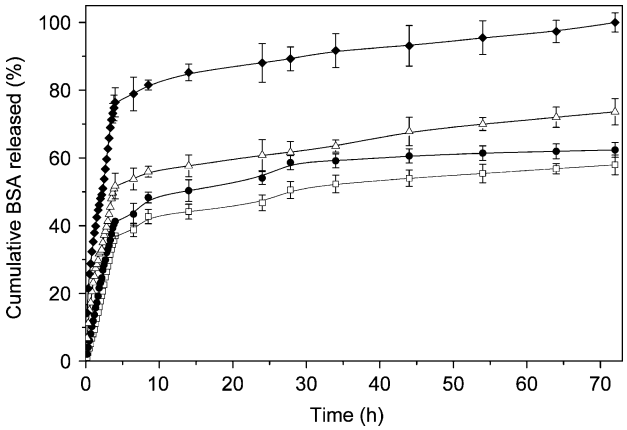

Figure 5. Delivery of BSA *in vitro* under physiological conditions (PBS buffer, 37 °C, 200 rpm) from MPS. MPS loaded with different concentrations of BSA (31.27 mg mL^{-1}: □, 43.50 mg mL^{-1}: ●, 61.55 mg mL^{-1}: △ and 63.30 mg mL^{-1}: ♦) were used for the delivery studies. Protein concentration was determined via a Bradford Reagent assay. The averages from three runs are shown ($n = 3$).

start to plateau after 4 h and released 95.0 ± 2.5% of total BSA loaded within one week (data not shown). However, higher concentrations resulted in a higher burst rate, possibly due to the faster dissolution rate of the surface localized BSA near the MPS surface when closer to its saturated loading capacity. MPS with 63.30 mg mL^{-1} BSA exhibited a burst effect amounting to 35.3% and 48.0% released in 1 and 2 h. A very rapid BSA release, corresponding to about 76.4% compared with others was observed after 4 h (initial burst period). In contrast, MPS with 31.27 mg mL^{-1} and 43.50 mg mL^{-1} BSA released only around 37.0% and 41.3% of the BSA, respectively, in the burst period. Results obtained from the automated electrophoresis gel (Fig. 6) revealed no clear difference in the conformation and size (in kDa) of BSA between before adsorption in MPS and after desorption from them (percentage of dimers observed was <1.5% of total). This indicates that protein structure can remain intact upon desorption from a MPS delivery platform and was not influenced by the adsorption in MPS. Figure 6 also shows a comparison of the size of BSA in different buffer solutions (PBS buffer, deionized water and sodium acetate buffer).

The influence of ionic strength on the BSA delivery profile was also investigated. As shown in Fig. 7, the hydrodynamic diameter of BSA increases when the ionic strength of the buffer increases. Protein macromolecules are hydrophilic in aqueous media; however, they contain hydrophobic sites. Electric charges at the surface are neutralized by the counterions from the ambient solution, resulting in the formation of an electrical double layer.[23] When the thickness of electrical double layers decrease, protein molecules tend to approach each other and the energy barrier for stabilization is reduced. This leads to the agglomeration of protein molecules when the buffer ionic strength is increased, and this neutralizes the charges at the C-terminus and N-terminus. The delivery profiles of BSA from MPS in

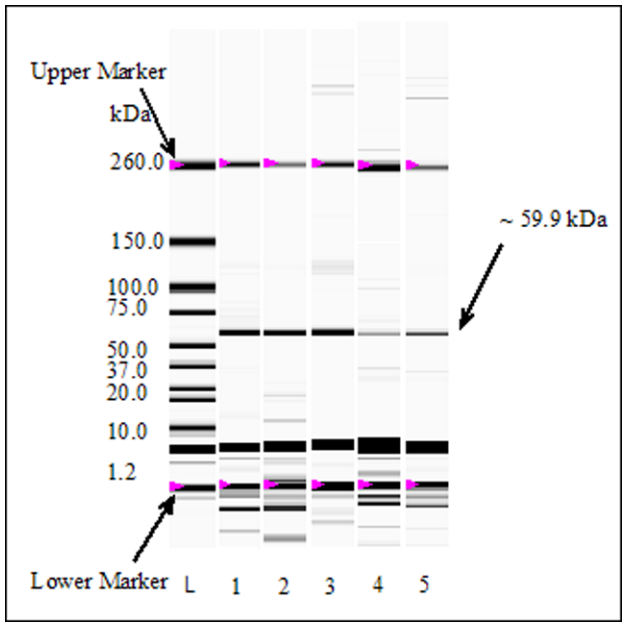

Figure 6. Result from automated electrophoresis gel for BSA in different conditions. L: Ladder; 1: BSA in PBS buffer (pH 7.4); 2: BSA in 10 mmol L^{-1} sodium acetate buffer (pH 4); 3: BSA in deionized water (0.22 µm filtered); 4: BSA from *in vitro* studies (PBS buffer, pH 7.4, 37 °C and 200 rpm) of MPS loaded with 61.55 mg mL^{-1}; 5: BSA from *in vitro* studies (PBS buffer, pH 7.4, 37 °C and 200 rpm) of MPS loaded with 63.30 mg mL^{-1}.

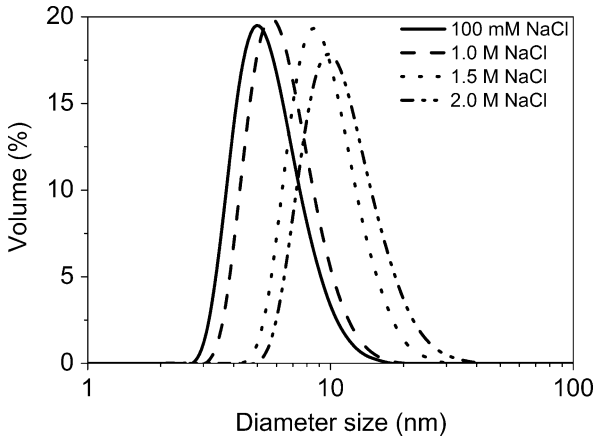

Figure 7. Hydrodynamic diameter of BSA in PBS buffer with different ionic strength (100 mmol L^{-1}, 1.0 mol L^{-1}, 1.5 mol L^{-1} and 2.0 mol L^{-1} NaCl).

buffers with an ionic concentration similar to human physiological fluid (~100 mmol L^{-1}) and higher ionic strength (200 mmol L^{-1}) are displayed in Fig. 8. As can be seen from Fig. 8(a) and Fig. 8(b), MPS loaded with 31.27 mg mL^{-1} and 43.50 mg mL^{-1} BSA has a lower delivery rate in buffer containing 200 mmol L^{-1} NaCl than in 100 mmol L^{-1} NaCl buffer, which amounted to 54.3% and 67.3% released in the first 72 h, respectively. This can be explained by protein molecules coagulation by the formation of hydrophobic interactions with each other analogous to a salting out effect, which delays the delivery rate of BSA from the pores of the MPS. The adsorption values are highly dependent upon the self-organized structure of BSA macromolecules in aqueous solution,[29] which tends to attach to the hydrophobic sites on the adsorbent surface via intramolecular hydrophobic sections within the macromolecules. This also explains the low release rate of BSA in higher ionic strength conditions. This assumption is further supported by the results of the automated electrophoresis gel (Fig. 9), which shows agglomeration of BSA.

CONCLUSION

A strategy to characterize and enhance the adsorption of a protein to MPS has been investigated. The dissociation constant (K_D) of BSA for MPS was shown to be 6.42 mg mL^{-1} of MPS (9.88×10^{-5} mol L^{-1}), and the maximum binding capacity (q_{max}) of 71.43 mg mL^{-1} of MPS was higher than in previously reported studies. The dimensions of MPS pores and surface charges are crucial for protein adsorption into the mesoporous networks. BSA is a small, compact protein with a low isoelectric focusing point and with physico-chemical properties suitable for adsorption onto MPS. It was shown that the adsorption of protein onto MPS requires the surface charges of MPS and of the protein to be compatible. The adsorption of protein onto MPS

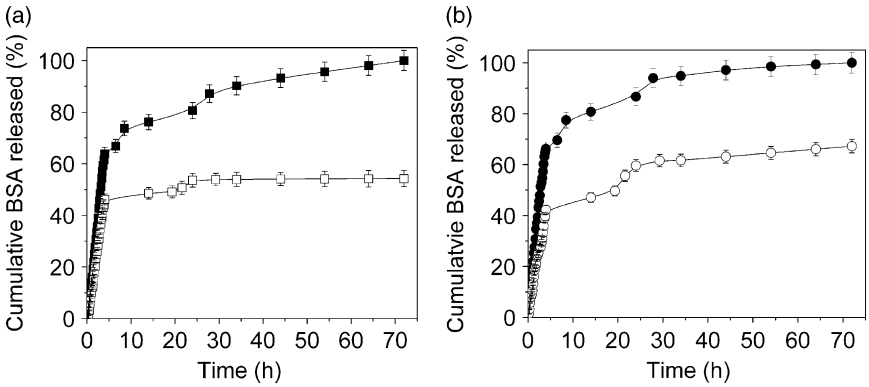

Figure 8. Comparison delivery profiles of BSA, *in vitro* under physiological conditions (PBS buffer, pH 7.4, 37 °C, 200 rpm) from MPS under different ionic concentrations: 100 mmol L^{-1} NaCl (solid) and 200 mmol L^{-1} NaCl (open). MPS loaded with different concentrations of BSA: (a) 31.27 mg mL^{-1}: ■ and (b) 43.50 mg mL^{-1}: ● were used for the delivery studies. Protein concentration was determined via a Bradford Reagent assay. The averages from three runs are shown ($n = 3$).

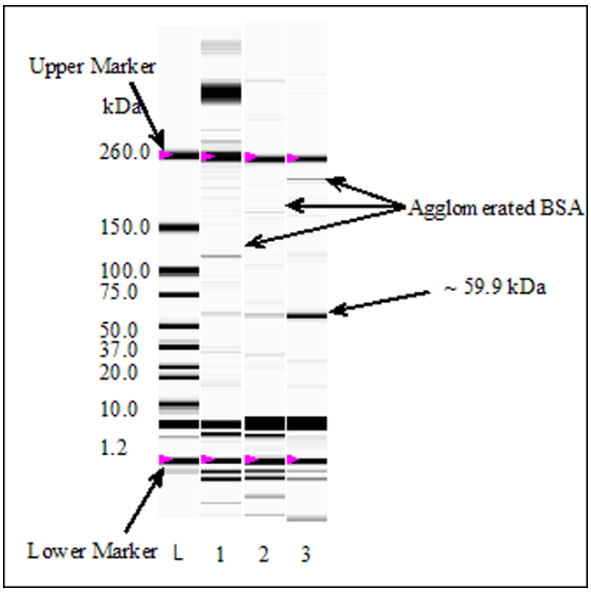

Figure 9. Result from automated electrophoresis gel for BSA from *in vitro* studies (PBS buffer, 200 mmol L^{-1} NaCl, pH 7.4, 37 °C and 200 rpm). L: Ladder; 1: BSA from MPS loaded with 31.27 mg mL^{-1}; 2: BSA from MPS loaded with 43.50 mg mL^{-1}; 3: BSA from MPS loaded with 63.30 mg mL^{-1}. The figure shows bands of high molecular weight protein which may be attributed to agglomerated BSA.

was displayed in a continuous, scale chromatography column packed with the MPS. *In vitro* delivery studies revealed that MPS from colloids are suitable for use as a controlled delivery platform for proteins. The novel synthesis of MPS at the micrometer scale with tailored pore size using simple electrolyte and inexpensive commercial inorganic silica is easily scalable to produce large quantities of silica spheres suitable as a controlled delivery system for biomolecules or biopharmaceuticals.

ACKNOWLEDGEMENTS

This work was supported by Monash University. GMF thanks the Victorian Endowment for Science, Knowledge and Innovation (VESKI) for the Innovation Fellowship and support of this research. HW thanks the Australian Research Council for the QEII Fellowship. JH and MKD gratefully acknowledge the financial support from the Monash University Research Graduate Scholarship. We thank SNOWTEX®, Nissan Chemical Industries, Tokyo, Japan for providing silica colloids.

REFERENCES

1 Frost & Sullivan, *Strategic Analysis of the World Biogenerics Market* (2005). http://www.frost.com/prod/servlet/report-overview.pag?repid=B613-01-00-00-00 [accessed 13 July 2007].
2 Kneuer C, Sameti M, Haltner EG, Schiestel T, Schirra H, Schmidt H, *et al.*, Silica nanoparticles modified with aminosilanes as carriers for plasmid DNA. *Int J Pharmacol* **196**:257–261 (2000).
3 Luo D and Saltzman WM, Synthetic DNA delivery systems. *Nat Biotechnol* **18**:33–37 (2000).
4 Lei J, Fan J, Yu CZ, Zhang LY, Jiang SY, Tu B, *et al.*, Immobilization of enzymes in mesoporous materials: controlling the entrance to nanospace. *Microporous Mesoporous Mater* **73**:121–128 (2004).
5 Luo D, Han E, Belcheva N and Saltzman WM, A self-assembled, modular DNA delivery system mediated by silica nanoparticles. *J Control Release* **95**:333–341 (2004).
6 Wang YJ and Caruso F, Mesoporous silica spheres as supports for enzyme immobilization and encapsulation. *Chem Mater* **17**:953–961 (2005).
7 Luo D and Saltzman WM, Nonviral gene delivery – thinking of silica. *Gene Therapy* **13**:585–586 (2006).
8 Weetall HH, Preparation of immobilized proteins covalently coupled through silane coupling agents to inorganic supports. *Appl Biochem Biotechnol* **41**:157–188 (1993).
9 Deere J, Magner E, Wall JG and Hodnett BK, Adsorption and activity of cytochrome c on mesoporous silicates. *Chem Commun* 465–466 (2001).
10 Deere J, Magner E, Wall JG and Hodnett BK, Mechanistic and structural features of protein adsorption onto mesoporous silicates. *J Phys Chem B* **106**:7340–7347 (2002).
11 Hudson S, Magner E, Cooney J and Hodnett BK, Methodology for the immobilization of enzymes onto mesoporous materials. *J Phys Chem B* **109**:19496–19506 (2005).
12 Diaz JF and Balkus KJ, Enzyme immobilization in MCM-41 molecular sieve. *J Mol Catal B-Enzym* **2**:115–126 (1996).
13 Washmon-Kriel L, Jimenez VL and Balkus KJ, Cytochrome c immobilization into mesoporous molecular sieves. *J Mol Catal B-Enzym* **10**:453–469 (2000).
14 Han YJ, Stucky GD and Butler A, Mesoporous silicate sequestration and release of proteins. *J Am Chem Soc* **121**:9897–9898 (1999).
15 Fan J, Lei J, Wang LM, Yu CZ, Tu B and Zhao DY, Rapid and high-capacity immobilization of enzymes based on mesoporous silicas with controlled morphologies. *Chem Commun* 2140–2141 (2003).
16 Vinu A and Miyahara Mand Ariga K, Biomaterial immobilization in nanoporous carbon molecular sieves: Influence of solution pH, pore volume, and pore diameter. *J Phys Chem B* **109**:6436–6441 (2005).
17 Beck JS, Vartuli JC, Roth WJ, Leonowicz ME, Kresge CT, Schmitt KD, *et al.*, A new family of mesoporous molecular-sieves prepared with liquid-crystal templates. *J Am Chem Soc* **114**:10834–10843 (1992).
18 Zhao DY, Feng JL, Huo QS, Melosh N, Fredrickson GH, Chmelka BF, *et al.*, Triblock copolymer syntheses of mesoporous silica with periodic 50 to 300 angstrom pores. *Science* **279**:548–552 (1998).
19 Ho J, Zhu W, Wang H and Forde GM, Mesoporous silica spheres from colloids. *J Colloid Interface Sci* **308**:374–380 (2007).
20 Peters T, *All about Albumin: Biochemistry, Genetics, and Medical Applications* Academic Press, San Diego (1996).
21 Kneuer C, Sameti M, Bakowsky U, Schiestel T, Schirra H, Schmidt H, *et al.*, A nonviral DNA delivery system based on surface modified silica-nanoparticles can efficiently transfect cells *in vitro*. *Bioconjugate Chem* **11**:926–932 (2000).
22 Xu ZP, Zeng QH, Lu GQ and Yu AB, Inorganic nanoparticles as carriers for efficient cellular delivery. *Chem Eng Sci* **61**:1027–1040 (2006).
23 Myers D, Wiley InterScience (Online Service), and John Wiley & Sons, *Surfaces, Interfaces, and Colloids: Principles and Applications*. 2nd edn. Wiley-VCH, pp. 214–252 (1999).
24 Geankoplis CJ and Geankoplis CJ, *Transport Processes and Separation Process Principles (includes unit operations)*, 4th edn. Prentice Hall PTR, Upper Saddle River, NJ, pp. 1026 (2003).
25 Vinu A and Hartmann M, Adsorption of cytochrome c on MCM-41 and SBA-15: Influence of pH, in *Recent Advances in the Science and Technology of Zeolites and Related Materials, Pts A – C*. Elsevier Science Bv, Amsterdam, pp. 2987–2994 (2004).

26 Schmidt-Traub H, *Preparative Chromatography of Fine Chemicals and Pharmaceutical Agents*, Wiley-VCH, Weinheim (2005).
27 Paredes B, Suarez E, Rendueles M, Villa-Garcia MA and Diaz JM, Ammonia-functionalized particulate poly(glycidyl methacrylate-co-ethylene dimethacrylate)-based polymers as stationary phase for protein retention. *J Chem Technol Biotechnol* **76**:1171–1178 (2001).
28 Yang J, Daehler A, Stevens GW and O'Connor AJ, Adsorption of lysozyme and trypsin onto mesoporous silica materials, in *Nanotechnology in Mesostructured Materials*. Elsevier Science Bv, Amsterdam, pp. 775–778 (2003).
29 Eltekov AY and Eltekova NA, Mesoporous molecular sieves for albumin, in *Impact of Zeolites and Other Porous Materials on the New Technologies at the Beginning of the New Millennium, Pts A and B*. Elsevier Science Bv, Amsterdam, pp. 1537–1544 (2002).

CHAPTER FOUR

ENGINEERING ASPECTS OF SYNTHESIS OF MICROSPHERES ENCAPSULATING PLASMID DNA VIA ULTRASONIC ATOMIZATION

Process considerations related to the microencapsulation of plasmid DNA via ultrasonic atomization

Jenny Ho, Huanting Wang, Gareth M. Forde

Biotechnology and Bioengineering

101 (1) (2008) 172 – 181

Monash University

Declaration for Thesis Chapter Four

Declaration by candidate

In the case of Chapter 4, the nature and extent of my contribution to the work was the following:

Nature of contribution	Extent of contribution (%)
Initiation, Key ideas, Experimental works, Development, Data analysis, Writing up	90

The following co-authors contributed to the work. Co-authors who are students at Monash University must also indicate the extent of their contribution in percentage terms:

Name	Nature of contribution
Dr Gareth M. Forde	Initiation, Key ideas, Development, Review
Dr. Huanting Wang	Key ideas, Development, Review

Candidate's signature		**Date**

Declaration by co-authors

The undersigned hereby certify that:

(1) the above declaration correctly reflects the nature and extent of the candidate's contribution to this work, and the nature of the contribution of each of the co-authors.
(2) they meet the criteria for authorship in that they have participated in the conception, execution, or interpretation, of at least that part of the publication in their field of expertise;
(3) they take public responsibility for their part of the publication, except for the responsible author who accepts overall responsibility for the publication;
(4) there are no other authors of the publication according to these criteria;
(5) potential conflicts of interest have been disclosed to (a) granting bodies, (b) the editor or publisher of journals or other publications, and (c) the head of the responsible academic unit; and
(6) the original data are stored at the following location(s) and will be held for at least five years from the date indicated below:

Location	Department of Chemical Engineering, Monash University – Clayton campus, Australia.

Signature		**Date**
Signature		**Date**

ARTICLE

BIOTECHNOLOGY and BIOENGINEERING

Process Considerations Related to the Microencapsulation of Plasmid DNA Via Ultrasonic Atomization

Jenny Ho, Huanting Wang, Gareth M. Forde

Department of Chemical Engineering, Monash University, Clayton, 3800 VIC, Australia; telephone: +61-3-9905-1867; fax: +61-3-9905-5686; e-mail: jenny.ho@eng.monash.edu.au

Received 4 January 2008; revision received 14 February 2008; accepted 27 February 2008

Published online 7 March 2008 in Wiley InterScience (www.interscience.wiley.com). DOI 10.1002/bit.21876

ABSTRACT: An effective means of facilitating DNA vaccine delivery to antigen presenting cells is through biodegradable microspheres. Microspheres offer distinct advantages over other delivery technologies by providing release of DNA vaccine in its bioactive form in a controlled fashion. In this study, biodegradable poly(D,L-lactide-*co*-glycolide) (PLGA) microspheres containing polyethylenimine (PEI) condensed plasmid DNA (pDNA) were prepared using a 40 kHz ultrasonic atomization system. Process synthesis parameters, which are important to the scale-up of microspheres that are suitable for nasal delivery (i.e., less than 20 μm), were studied. These parameters include polymer concentration; feed flowrate; volumetric ratio of polymer and pDNA-PEI (plasmid DNA-polyethylenimine) complexes; and nitrogen to phosphorous (N/P) ratio. PDNA encapsulation efficiencies were predominantly in the range 82–96%, and the mean sizes of the particle were between 6 and 15 μm. The ultrasonic synthesis method was shown to have excellent reproducibility. PEI affected morphology of the microspheres, as it induced the formation of porous particles that accelerate the release rate of pDNA. The PLGA microspheres displayed an in vitro release of pDNA of 95–99% within 30 days and demonstrated zero order release kinetics without an initial spike of pDNA. Agarose electrophoresis confirmed conservation of the supercoiled form of pDNA throughout the synthesis and in vitro release stages. It was concluded that ultrasonic atomization is an efficient technique to overcome the key obstacles in scaling-up the manufacture of encapsulated vaccine for clinical trials and ultimately, commercial applications.

Biotechnol. Bioeng. 2008;101: 172–181.

KEYWORDS: ultrasonic atomization; microspheres; plasmid DNA; poly(D,L-lactide-*co*-glycolide); polyethylenimine

Introduction

Unwanted side effects of toxicity and multi-drug resistance associated with larger dose administration can be overcome via improved delivery systems. As a result, controlled release delivery systems using biodegradable polymer are being developed to address many of the difficulties associated with the conventional methods of administration (Edlund and Albertsson, 2002). Poly(D,L-lactide-*co*-glycolide) (PLGA) has been studied extensively as a candidate for vaccine delivery systems using parenteral administration and has displayed considerable potential in animal models for intranasal administration (Alpar et al., 2005; Eyles et al., 1998; Turker et al., 2004). In the last decade, nasal vaccination has been recognized as a very promising route, as it offers a faster and more effective therapeutic effect (Davis, 2001). Deposition of particles in the nasal cavity region is most common for larger particles, and it takes place via inertial impaction. Both theory and experimental studies have indicated that particles of <20 μm in diameter favor deposition in the upper airways during nasal inhalation and minimize deposition in the lungs and gastro-intestinal tract (Kippax and Fracassi, 2003; Newman et al., 2004).

Currently, the most commonly used method to embed biopharmaceutical compounds into biodegradable microspheres is emulsion–solvent extraction/evaporation (Castellanos et al., 2001; Freitas et al., 2005); however, this method is inherently seen as a batch operation; therefore, this method makes large scale production difficult and costly. In addition, bioactivity of biopharmaceutical can be eliminated due to the presence of organic solvents, and the solvents are also difficult to remove completely (Freitas et al., 2005). Spray drying is frequently being employed to prepare microspheres (Atuah et al., 2003; Johansen et al., 2000); but, there are drawbacks to this method that makes it ineffective. These drawbacks include: it is infeasible for temperature sensitive compounds; it has considerable product lost due to inefficient separation in the collecting process (Johansen et al., 2000). Demand of aseptic

Correspondence to: J. Ho

microencapsulation is increasing because heat-sterilization and sterilization by gamma rays may harm the encapsulated biopharmaceutical and degrade the polymer. The use of ultrasonic atomization in producing microspheres containing biopharmaceuticals is comparatively new, and shows promising results to obtain micron and submicron monodispersed particles (Felder et al., 2003; Forde et al., 2006; Freitas et al., 2004). Ultrasonic atomization creates cavities and shock waves in the liquid to form particles. Since the cavitational collapse only lasts a few microseconds, the amount of energy released by each individual bubble during ultrasonic atomization is minute, that is, less than 1 $J\,s^{-1}$ (Avvaru et al., 2006). Ultrasonic atomization is feasible for heat liable biopharmaceuticals and the heat produced can transfer to surrounding easily via air circulation during the fast processing time. Therefore, this method is a scaleable and commercially viable production method, and it can be tailored to synthesize particles with certain size distribution to match particular applications.

The aim of this study was to evaluate the potential of ultrasonic atomization process in the preparation of plasmid DNA (pDNA) loaded PLGA microspheres, which has a range of suitable particle size for vaccination in the nasal cavity. To the best of our knowledge, ultrasonic atomization system has not been utilized in the production of microparticle containing pDNA. This study can be viewed as a preliminary work for a possible technology transfer and a more engineered-guided DNA vaccine carrier production process. PUC19 was chosen as a model plasmid DNA, because it is a small and high copy number *E. coli* plasmid cloning vector. In recent years, polyethylenimine (PEI) has been proven to be an efficient cationic polymer for gene delivery. PEI is capable of acting as a proton sponge and DNA condensed agent to enhance transgene delivery of pDNA into the nucleus of cells (Lungwitz et al., 2005). In this study, we observed the effect of PEI as a DNA condensed agent during the formation of PLGA microspheres. The influence of various processes and formulation parameters includes polymer concentration; feed flowrate; volumetric ratio of polymer and pDNA-PEI complexes; and nitrogen to phosphorous ratio (N/P). These influences on the characteristics of the resulting microspheres were studied.

Materials and Methods

Materials

The poly(D,L-lactide-*co*-glycolide) (PLGA 50:50, M_W = 15,000 Da), polyethylenimine (PEI, M_W = 25,000 Da, branched), poly(vinyl alcohol) (PVA, M_W = 50,000 Da, 87–90% hydrolyzed) and phosphate buffered saline (PBS) were purchased from Sigma–Aldrich (Sydney, Australia). Other materials include acetone (99.5%, LabScan, Dublin), agarose (Promega, Sydney, Australia), ethidium bromide (Sigma–Aldrich; M_W 394.31, 10 $mg\,mL^{-1}$) and 1 kbp DNA ladder (New England Bio-Labs, Ipswich, MA).

Purification of Plasmid DNA

Concentrated frozen *E. coli* DH5α-pUC19 cells, which were obtained from a fed-batch fermentation of *E. coli* harboring pUC19 plasmid (2,686 bp, $\sim 1.8 \times 10^6$ $g\,mol^{-1}$) at 37°C and pH 8 in a 20 L fermentor (BioFlo 410, New Brunswick Scientific, Edison, NJ), were thawed. The cells were purified with PureYield™ Plasmid Maxiprep System according to the manufacturer's instructions (Promega).

Characterization of Polymer Solution

The PLGA polymeric solutions with concentrations varying from 0.25% to 4.0% (w/v) were prepared by dissolving PLGA 50:50 in acetone. The viscosity of the polymer solutions was measured at 20°C using a calibrated BS/U-tube glass capillary viscometer (Series 9724-E50, size A, Cannon Instrument Company, State College, PA) with an approximate constant at 0.003 $cSt\,s^{-1}$. The kinematic viscosity (υ) and dynamic viscosity (η) were determined and expressed as the mean of three experimental runs ($n = 3$). The surface tension was measured at 23°C using the capillary rise method ($n = 3$) via a Volac disposable glass pasteur pipettes (D812, Bacto Laboratories, NSW, Australia), and calibrated with hexadecane (Sigma–Aldrich). The density was measured using a dry and clean pycnometer (V 726/T, Technotest®, Modena, Italy), where the ratio of the mass and the volume gives the density ($n = 3$).

Formation of pDNA-PEI Complexes

Ten percent (w/v) of polyethylenimine (PEI) stock solution was prepared by adding 5.0 mL of PEI (M_W = 25 kDa, branched) into 35 mL of PBS (0.01 $mol\,L^{-1}$, pH 7.4). The pH of solution was adjusted to pH 7.9 with concentrated hydrochloric acid (HCl), and the final volume was adjusted to 50 mL with PBS (Lungwitz et al., 2005). This was followed by filtration with a 0.22 μm pore-size cellulose acetate membrane filter (Sartorius, Goettingen, Germany), and then stored at 4°C for subsequent dilution. Complexes of PEI and plasmid DNA were formed by first diluting plasmid DNA and polymer separately with PBS buffer into the appropriate volumes (based on the desired N/P ratio). The plasmid DNA solution was then added to the PEI solution in dropwise. The mixture was vortexed immediately for 2 min; and it was incubated for 10 min prior to the zeta potential measurements. The polymer concentrations were calculated from the desired N/P ratio and the amount of plasmid—assuming that 43.1 $g\,mol^{-1}$ corresponds to each repeating unit of PEI containing one nitrogen atom, and 330 $g\,mol^{-1}$ corresponds to each repeating unit of DNA containing one phosphorous atom. The resulting charge ratio is expressed as PEI nitrogen: DNA phosphorous.

Preparation of Microsphere Via Ultrasonic Atomization

The polymeric solutions were prepared by dissolving PLGA 50:50 in acetone. The resulting polymeric solutions varied in concentration from 0.25% to 4.0% (w/v). The plasmid solution was prepared from the DNA condensation as described above. Feedstocks were prepared by mixing the pDNA-PEI solutions to the PLGA polymeric solutions at several volumetric ratios: 100 PLGA:1 pDNA-PEI (v/v), 100:2, 100:5, and 100:10; and this mixing process continued until a homogenous mixture was obtained. A 40 kHz ultrasonic atomization system (VCX134 AT, Sonics, USA) with a 6 mm full wave atomization probe was used to create the microspheres. The atomization probe was energized at an amplitude of 100%. Feedstocks were fed to the nozzle of ultrasonic atomizer via a syringe peristaltic pump (KDS 100, KD Scientific, Holliston, MA) at a constant flowrate of 18 $mL\,h^{-1}$; however, varying flowrates were used in the experiments that determined the effect of flowrate on the microspheres. The atomizer tip was fixed at 15 cm above the surface of the hardening agent (0.1% (w/v) PVA). This height enabled sufficient time for the volatile acetone solvent to evaporate from the fine droplets formed by the ultrasonic head (Felder et al., 2003; Forde et al., 2006). The atomized droplets were collected in defined volumes (i.e., 5 mL in a 50 mL glass measuring cylinder, FORTUNA®, Wertheim, Germany) of hardening agent (0.1% (w/v) PVA) under continuous stirring at 500 rpm. After the atomization, the stirring continued for another 30 min. The final products were stored at 4°C for subsequent analysis. For each formulation or set of parameter, three batches were prepared.

Microsphere Size Distribution and Morphology

The particle size distributions were determined directly after preparation using a Malvern Mastersizer 2000 (Malvern Instruments Ltd., Worcestershire, UK), which utilizes laser diffraction to determine a frequency of size distribution. The instrument was equipped with a series of photosensitive detectors which were positioned to allow accurate sizing across the widest possible range of particle sizes; and the particle size distributions were accurately predicted by the Mie scattering model. Herein, particle sizes or diameters are presented in the volume-weighted mode with the mean diameter as $D[4,3]$. The $D[4,3]$ indicates where the volume of the system lies by assuming all the particles are spherical. $D[4,3]$ was calculated by multiplying each particle diameter by the total volume of material in all the particles of that size, then summing up. The summing value is then divided by the total volume of all particles. Where d is the diameter of a spherical particle, $D[4,3]$ is defined as

$$D[4,3] = \frac{\sum d^4}{\sum d^3} \quad (1)$$

The focus in this study is on the hydrodynamic diameter of microspheres, with the aim to prepare different microsphere formulations suspensions for nasal inhalation (Kippax and Fracassi, 2003). The microsphere shape and morphology were analyzed by scanning electron microscopy (SEM). Samples of microspheres were placed on a double-sided adhesive carbon tape that fixed to an aluminum stage and dried at 30°C for 30 min. The dried samples were then coated with 6 nm of gold, and characterized with a JEOL JSM-6300F field emission scanning electron microscope (FESEM), which was operated at an accelerating voltage of 10 kV.

pDNA Encapsulation Efficiency and Structural Integrity

The amount of encapsulated pDNA in the microspheres was calculated by performing a mass balance over the amount of pDNA in the feedstock and the measured unencapsulated pDNA remained in the hardening agent after microspheres formation (Forde et al., 2006). After microspheres formation, the microspheres suspension was centrifuged for 10 min at 14,000 rpm, and the supernatant was checked for the unencapsulated pDNA concentration. The concentration of pDNA sample was determined by a spectrophotofluorometer (RF-1501, Shimadzu, Kyoto, Japan) with a Quant-iT™ PicoGreen® dsDNA quantitation assay reagent (Invitrogen, Mount Waverley (VIC), Australia) (Bivas-Benita et al., 2004). pDNA samples were also analyzed for potential alterations in the plasmid structure by 0.8% agarose gel electrophoresis that uses 1 kbp DNA ladder and ethidium bromide (EtBr) staining. The gel was made up of 0.8 g agarose in 50× dilution of TAE buffer (242 g of Tris base, 57.1 mL CH_3COOH, 9.305 g of EDTA). The gel was stained with 3 $\mu g\,mL^{-1}$ ethidium bromide and the stained gel was run at 60 V for 90 min. The resulting fractioned nucleic acid gel was analyzed and photographed in a Molecular Imager Gel Doc XR System (BIORAD, Segrate (MI), Italy). The ratio of supercoiled to degraded linear pDNA was quantified via densitometry studies using the Quantity One® software (BIORAD).

Zeta Potential Measurements

Zeta potential and size distribution of pDNA samples, which condensed with PEI, were determined using a Malvern Zetasizer Nano ZS series (ZEN 3600). Samples of pDNA-PEI were prepared in the PBS buffer as described above, and 1.0 mL aliquot of these solutions was then filled into the clear disposable zeta cell for measurement. The zeta potential and size distribution were determined in triplicate for each sample. The measurement values were analyzed by using the system software (Dispersion Technology Software, version 4.20, Malvern Instruments Ltd.).

In Vitro Release Study

A study was conducted in a Mk X Incubator-Shaker (LH fermentation, Stoke Poges, UK) to determine the release rate

of pDNA from microspheres under physiological condition in vitro (phosphate buffered saline (PBS), 37°C, pH7.4, 200 rpm). Thirty milligrams of microspheres for each formulation were suspended in 2.0 mL of PBS buffer (0.01 mol L^{-1}) along with 0.05% (w/v) PVA. At predetermined time intervals (every 24 h for 30 days), the samples were subjected to centrifugation (10,000 rpm for 10 min in a Heraeus Multifuge® 3 S-R centrifuge) to pellet the microspheres. The 2.0 mL supernatant was removed, and the concentration of released pDNA was determined by using a spectrophotofluorometer (RF-1501, Shimadzu) with a Quant-iT™ PicoGreen® dsDNA quantitation assay reagent (Invitrogen). The volume of supernatant removed was then replaced with fresh PBS. Release experiments were performed in triplicate ($n = 3$), and the results were averaged.

Mass Loss Study

Thirty milligrams of blank microspheres were added to 2.0 mL of PBS buffer (0.01 mol L^{-1}, pH 7.4). The sample was incubated at 37°C and 200 rpm in a Mk X Incubator-Shaker (LH Fermentation). At predetermined time intervals (every 24 h for 30 days), the microspheres were collected on a 0.22 μm mixed cellulose esters membrane filter (Millipore®). The microspheres were dried and weighed. The experiments were performed in triplicate ($n = 3$).

Statistical Analysis

The analysis of variance (ANOVA) using a single factor was performed to determine if observed differences in microsphere diameters due to the changes in the ultrasonic atomization process parameters were statistically significant. In all experiments, when $P < 0.05$, then the difference will be considered statistically significant.

Results and Discussion

DNA Condensation

In general, the cellular uptake of naked DNA is inefficient. The primary cause of this deficiency is the electrostatic repulsion between the phosphate backbone of DNA molecules and negatively charged cell surface (Patil et al., 2005). The condensation of polyanionic pDNA molecules into small and positively charged complexes is an important prerequisite for gene delivery. The cationic polymer PEI has been widely used for non-viral transfection. PEI has an advantage over other polycations because PEI combines strong DNA compaction capacity with an intrinsic endosomolytic activity (Lungwitz et al., 2005). In this study, we have condensed pUC19 by using PEI ($M_W = 25$ kDa) with a consequent reduction in the hydrodynamic diameter of pDNA (Fig. 1)—with the result of pUC19 forming into a toroidal structure (Lungwitz et al., 2005). The number of cationic charges of the nitrogen of PEI divided by the number of anionic charges of the phosphorous of DNA yields the N/P ratio. The pUC19 pDNA molecules exhibited highly negative zeta potential (−66.6 mV) and a mean hydrodynamic diameter of 190.3 nm in PBS buffer, pH 7.4 ($n = 3$). At low N/P ratios (<1), a net negative charge complex existed (−41.8 mV). Upon increasing the N/P ratio, the pDNA-PEI complex became larger (~592.7 nm), and polydisperse aggregations were formed at a value close to N/P = 1. This is due to the lowered overall surface charge, which was confirmed via zeta potential measurement (−19.9 mV). Further increased in the N/P ratios (>2) reduced the size of the complexes due to the electrostatic repulsion. For example, at a N/P ratio of 10, the zeta potential was 29.5 mV with a resultant hydrodynamic diameter of 110.7 nm. Another important merit of PEI condensation is that the pDNA is protected from shear-induced degradation associated with the ultrasonic atomization process. Studies (Densmore et al., 2000; Gautam et al., 2000; Lengsfeld and Anchordoquy, 2002) have shown that

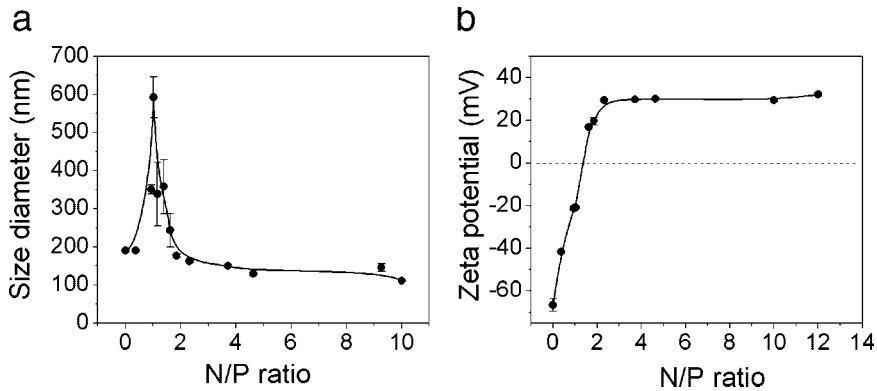

Figure 1. The influence of N/P ratio on (**a**) the hydrodynamic diameter and (**b**) zeta potentials of plasmid DNA-PEI complexes ($n = 3$).

reduction of hydrodynamic diameter of pDNA via PEI condensation can reduce the effective force imparted on the particle. This helps to lower the possibility of shear-induced degradation onto the plasmid DNA to a greater extent. From our observations, PEI can effectively condense the pDNA at a ratio of N/P = 10 to form positively charged complexes which favors cellular transfection (Lungwitz et al., 2005).

Effect of Various Process Parameters on the Microspheres Size and Morphology

In this study, the polymer concentrations in the range of 0.25–4.0% (w/v) have been studied for their effect on the microspheres. The physiochemical properties of PLGA in acetone and the mean microspheres diameter obtained are reported in Table I. The volume-weighted mean diameter ($D[4,3]$) of the PLGA microspheres increased from 9.02 to 22.89 μm, with a parallel increase in the standard deviation when the polymer content was increased from 0.25% to 4.0% (w/v). This result can be attributed to the increased viscosity. This observation is not uncommon as observed by previous studies (Forde et al., 2006; Freitas et al., 2004). Since the growth rate of the capillary wave amplitude is low in viscous liquid, the liquid will not be atomized immediately when it comes out from the atomizer nozzle (Bellman and Pennington, 1954). In addition, the hydraulic shock wave, which is produced upon the implosive collapse of cavitation bubbles on the vibrating surface, is unable to tear the viscous liquid capillary wave crest due to the higher viscous energy dissipation (Avvaru et al., 2006). Besides this, the surface tension and density of the liquid also have an impact on the mean droplet size that was produced by an ultrasonic atomizer (Lang, 1962). The failure of uniform atomization is expected because of the nonlinear interaction between viscosity, surface tension and density. ANOVA analysis shows $P < 0.001$, which indicates the physiochemical properties of polymer solution have statistically significant effects on the particle size distribution in the ultrasonic atomization.

The increase in the amount of PEI-pDNA complex in the polymer feedstock affected the particle size distribution, $D[4,3]$. As seen in Figure 2, the particle size distribution shifted to a larger size range and became more dispersed when the volumetric ratio was changed from 100 PLGA:1 pDNA-PEI (v/v) ($D[4,3] = 11.42$ μm, span = 1.22) to 100:2 (v/v) ($D[4,3] = 14.14$ μm, span = 1.26). However, the $D[4,3]$ of microspheres dropped to 6.33 μm (span = 0.67) and 5.69 μm (span = 1.06) for ratios 100 PLGA:5 pDNA-PEI (v/v) and 100 PLGA:10 pDNA-PEI (v/v), respectively. This can be explained by the addition of PEI in the aqueous phase (pDNA-PEI complex) and this addition led to an increase in the feedstock stability (De Rosa et al., 2002). Subsequently, this resulted to a more homogeneous and uniform atomization, as displayed by the experimental results. According to statistical analysis, $P < 0.001$ revealed that the differences of the average $D[4,3]$ are statistically significant at a statistical probability >95%.

Another operating consideration is the feed flowrate. With increased feed flowrate, a significant shift to larger range of sizes and a wider particle size distribution were observed (Fig. 3). These observations can be attributed to collision and subsequent coalescence of droplets in close vicinity of the atomizing tip, shortly after the atomization. This claim is further supported by the fact that agglomerations and lower yield have been noticed at higher feed flowrate. Nevertheless, the effect of feed flowrate was less significant for feedstock with less solid contents (i.e., lower volumetric ratio of plasmid DNA to polymer). This was probably due to a more uniform atomization despite the higher flowrate. However, $P > 0.05$ with a statistical probability of <95% indicated that when the feed flowrates varied, the differences between the averages ($D[4,3]$) were not statistically significant. Based on our observation, the feed flowrate of 18 mL h^{-1} gave the narrowest and smallest particle size distribution; thus this value will be further used as the base case flowrate for subsequent studies. In general, the reproducibility of the particle size distribution for repeated production, under several conditions being considered, was highly satisfactory as reflected by the moderate standard deviation.

Effect of PEI Content

One of the purposes of the present work was to study the effect of encapsulating pDNA condensed by cationic polymer (PEI) into the PLGA microspheres. As discussed

Table I. Properties of poly(D,L-lactide-*co*-glycolide) in acetone.

PLGA (%, w/v) in acetone	Density (kg m^{-3})	Surface tension, σ^a (N m^{-1})	Viscosity, η^b (Pa · s)	Mean diameter*, $D[4,3]$ (μm)
0.25	761.8 ± 0.3	0.0238 ± 0.0006	3.31 ± 0.10	9.02 ± 0.20
0.5	780.9 ± 0.8	0.0252 ± 0.0004	3.42 ± 0.08	10.98 ± 0.15
1.0	797.7 ± 0.2	0.0260 ± 0.0008	3.53 ± 0.05	11.13 ± 0.24
2.0	800.1 ± 1.1	0.0243 ± 0.0015	4.21 ± 0.03	12.86 ± 0.52
3.0	809.3 ± 0.8	0.0240 ± 0.0012	4.91 ± 0.02	15.14 ± 0.69
4.0	827.5 ± 1.5	0.0267 ± 0.0009	5.25 ± 0.07	22.89 ± 1.63

Values are given as the mean of three runs ($n = 3$) ± standard deviation of the mean.
[a]Surface tension was measured via the capillary rise method at ambient conditions ($T = 23°C$).
[b]Viscosity was measured using a glass capillary viscometer at 20°C.
*ANOVA analysis shown that $P < 0.001$ with a statistical probability >95%.

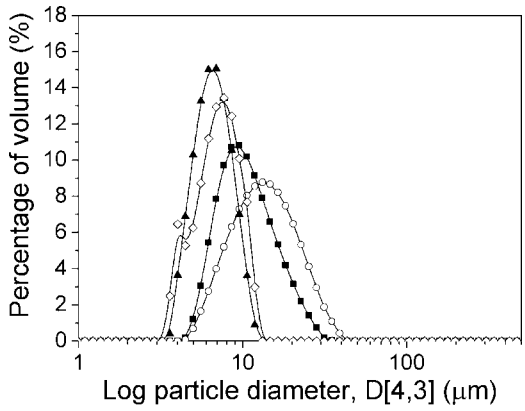

Figure 2. Particle distributions for 1% (w/v) PLGA in acetone with different volumetric ratios of pDNA-PEI complexes, which were pumped through a 40 kHz ultrasonic atomizer at 18 mL h^{-1} ($n = 3$). ■: 100 PLGA:1 pDNA-PEI (v/v); ○: 100:2 (v/v); ▲: 100:5 (v/v), and ◇: 100:10 (v/v).

in the previous section, the PEI is able to condense pDNA into smaller hydrodynamic diameter. Meanwhile, pDNA can acquire positive surface charge, which holds promise for intracellular transfection. Although increasing the amount of PEI can help condense pDNA into a more compact form, this increase was associated with the increased cytoxicity, which will decrease the cell viability (Godbey et al., 2001). Thus, the incorporation of pDNA-PEI complex into biodegradable polymer such as PLGA appeared to be safer, and this helped to increase the percentage of cell viability (Kim et al., 2005). However, the addition of PEI into the formulation strongly affects the morphology of microspheres. The scanning electron microscopy images (Fig. 4) revealed that the microspheres produced were spherical in shape, but the microspheres exhibited numerous surface pores. The porosity increased at higher N/P ratios. It has been reported that the osmotic pressure created by the inner aqueous phase (pDNA-PEI in this case) and the rate of solidification of microspheres have contributed to the formation of high porous surface (Crotts and Park, 1995). The higher amount of PEI in the formulation, which is an osmotically active polycation, will induce more influx of water into the internal aqueous phase during the microspheres hardening/solidified in the hardening agent (De Rosa et al., 2002; Freytag et al., 2000). This is associated with higher inner aqueous droplet volumes and eventually forms porous structure. On the other hand, the N/P ratio does not shown significant effect onto the microspheres size distribution (Fig. 4) when compared with the effect of volumetric ratio. During ultrasonic atomization, the droplets ejected from the ultrasonic nozzle, and the solvent evaporated. Then, the droplets shrank and formed a solid layer at the surface, which will determine the microspheres mean diameter. The subsequent solvent removal and influx of water, due to the increased of PEI contents, create pores inside the particles, but these will not significantly alter their dimension.

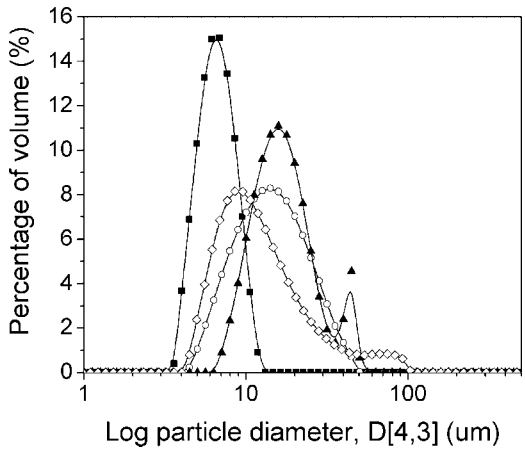

Figure 3. Percentage volume versus particle diameter for feedstocks of 1.0% (w/v) PLGA in acetone (100 PLGA:5 pDNA-PEI (v/v), N/P = 10) pumped through a 40 kHz ultrasonic atomizer at different feed flowrate ($n = 3$). ■: 18 mL h^{-1}; ○: 36 mL h^{-1}; ▲: 72 mL h^{-1}, and ◇: 90 mL h^{-1}.

Encapsulation Efficiency

The high encapsulation efficiencies of pDNA-PEI into PLGA microspheres via ultrasonic atomization have indicated the viability of this technology for large scale microspheres preparation. In general, the encapsulation efficiencies were higher for lower PLGA concentration and higher volumetric ratios of pDNA-PEI as shown in Figure 5. This coincides with the results obtained for the particle size distribution, where higher volumetric ratios tend to have more homogeneous atomization because the feedstock increased in stability. In addition, nonuniform atomizations for highly viscous polymer solutions have caused lower encapsulation efficiencies. An increase in polymer solution concentration from 0.5% to 2.0% (w/v) has caused the encapsulation efficiencies to drop from ~42% to ~24% and ~96% to ~82% for 100:1 (v/v) and 100:10 (v/v) formulations, respectively. The formulations prepared from 0.5% (w/v) PLGA with volumetric ratio of 100 PLGA:10 pDNA-PEI (v/v) have encapsulation efficiencies varying between 90% and 96%. In addition, the N/P ratios do not show significant effect on the encapsulation efficiencies of microspheres as claimed by De Rosa et al. (2002). In Figure 6, even though the polymer concentration was high (i.e., 2.0%, w/v), the encapsulation efficiencies for different N/P ratios at 100:10 (v/v) varied between 82% and 96%. According to De Rosa et al. (2002), encapsulation efficiencies will decrease due to a diffusional loss of the encapsulated compounds through the high surface porosity. However, this phenomenon was not observed in the ultrasonic atomization method. This can be best explained by the fact that fast atomization rate can reduce the probability of loss for encapsulated compounds during the synthesis process when

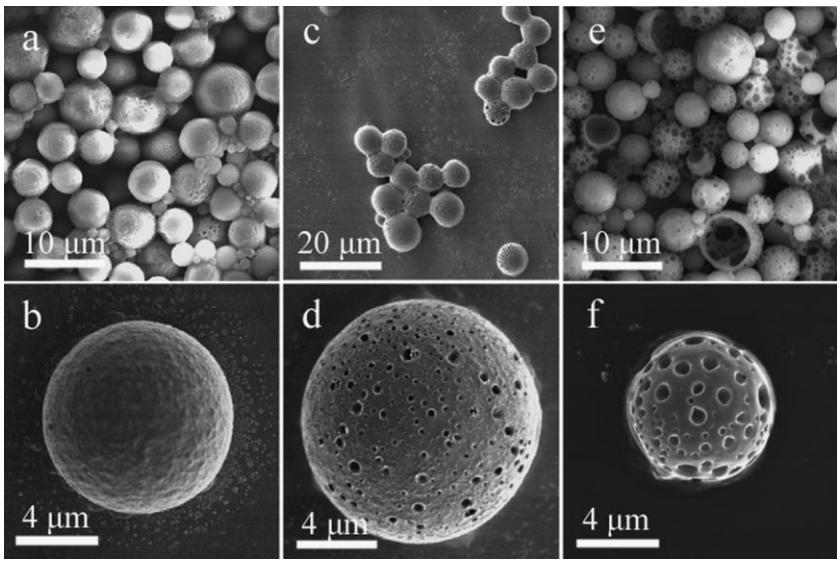

Figure 4. SEM images of microspheres containing pDNA-PEI complexes at several N/P ratios in 1% (w/v) PLGA with 100 PLGA:10 pDNA-PEI (v/v), where (**a**) and (**b**) are N/P = 2; (**c**) and (**d**) are N/P = 5; (**e**) and (**f**) are N/P = 10.

compared with the conventional methods (i.e., multiple emulsion/solvent evaporation method) (Freytag et al., 2000; Pistel and Kissel, 2000). On the other hand, increase of the feed flowrate also caused a decrease in the encapsulation efficiency, and this effect is particularly significant at lower volumetric ratio.

In Vitro pDNA Release

Release kinetics experiments were carried out in 0.01 mol L^{-1} phosphate buffered saline (pH 7.4) at 37°C. In general, the microspheres obtained via the use of ultrasonic atomization herein demonstrated zero order or near-zero order release kinetics without an initial spike of released pDNA. The release profiles that were obtained correlated with linear line and the correlation coefficients are shown in Table II. Most of the formulations have correlation coefficients greater than 0.96; thus, this indicates that zero order release kinetics is being followed (McGee et al., 1995). From Figure 7, we can see that the microspheres prepared with N/P = 10 in the formulation shows an 8.05% initial

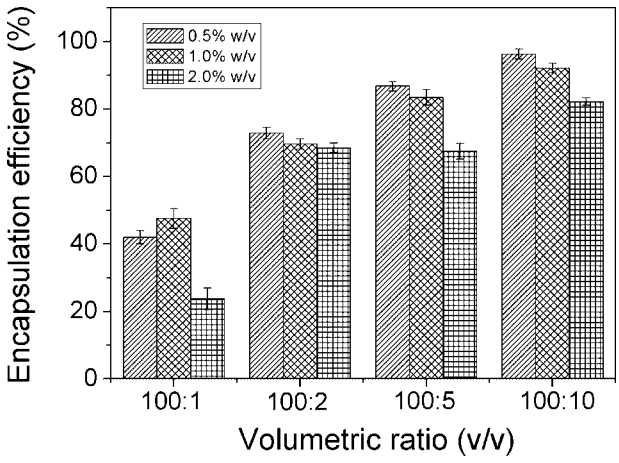

Figure 5. Encapsulation efficiencies of 0.5%, 1.0%, and 2.0% (w/v) PLGA in acetone with several volumetric ratios of pDNA-PEI (N/P = 2) complexes, which were pumped through the ultrasonic atomizer at 18 mL h^{-1}. The results are the mean of three experiments ± SD (standard deviation).

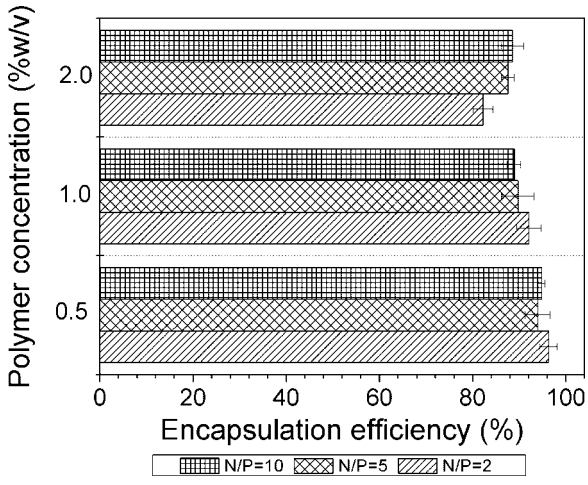

Figure 6. Effects of N/P ratio onto the encapsulation efficiencies for 0.5%, 1.0%, and 2.0% (w/v) PLGA in acetone (100 PLGA:10 pDNA-PEI (v/v)) pumped through the 40 kHz ultrasonic atomizer at 18 mL h^{-1}. The results are the mean of three experiments ± SD (standard deviation).

Table II. The correlation coefficients for different formulations of microspheres used in the in vitro studies by following fitting of a linear line of best fit to the release profiles.

Sample	Correlation coefficient
No PEI[a]	0.9697 ± 0.0015
N/P = 2[a]	0.9674 ± 0.0023
N/P = 5[a]	0.9751 ± 0.0057
N/P = 10[a]	0.9740 ± 0.0068
0.5% (w/v)[b]	0.9852 ± 0.0035
1.0% (w/v)[b]	0.9674 ± 0.0046
2.0% (w/v)[b]	0.9927 ± 0.0038

Values are given as mean of three microspheres batches ($n = 3$).
[a]The formulations were prepared with 1.0% (w/v) PLGA in acetone and consist of 100 PLGA:10 pDNA-PEI (v/v) or 100 PLGA:10 pDNA, atomized through a 40 kHz ultrasonic atomizer at 18 mL h^{-1}.
[b]The formulations were prepared with 100 PLGA:10 pDNA-PEI (v/v) at N/P = 2, atomized through a 40 kHz ultrasonic atomizer at 18 mL h^{-1}.

release of the encapsulated pDNA over the first 5 days, which is relatively high when compared with other formulations. In fact, the microspheres prepared without PEI in the formulation only showed an initial release of 3.84% within the same period of time. This can be best explained by the high porous surface, which will form much more readily in the microspheres with higher amounts of PEI. However, the initial release herein is small compared to previous published studies, which reported burst effects corresponding to 40–80% (De Rosa et al., 2002). Microencapsulation of pDNA via ultrasonic atomization has yielded microspheres with the majority of pDNA entrapped within the core, and with very little surface localized pDNA in compared with multiple emulsion methods.

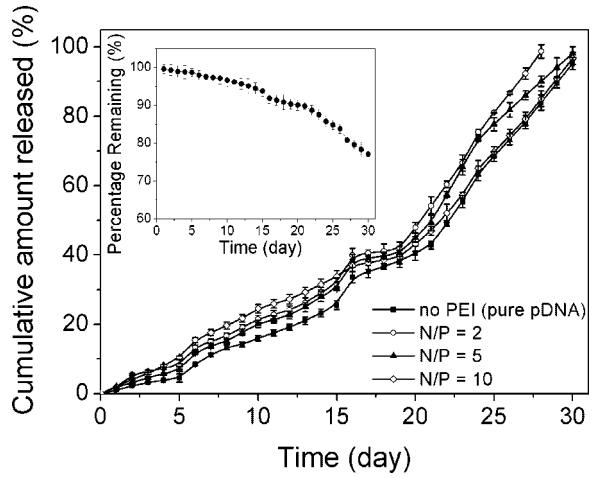

Figure 7. The delivery profiles of pDNA and pDNA-PEI in vitro under physiological conditions (PBS buffer, pH 7.4, 37°C, 200 rpm) from microspheres obtained from 1.0% (w/v) PLGA in acetone (100PLGA:10 pDNA-PEI (v/v)). Plasmid DNA concentrations were determined via the use of Quant-iT™ PicoGreen® dsDNA reagent. The mass loss of blank microspheres obtained under the same in vitro condition is shown in the inset ($n = 3$).

Following the continuous release of pDNA over the first 16 days, the microspheres displayed a short lag phase, which lasted for 4 days (Fig. 7), and after the lag phase it showed a more rapid release kinetics. These observations were as expected and are consistent with the finding from the blank microspheres mass loss (inset Fig. 7). The blank microspheres showed a more rapid bulk erosion and break up of polymer after 21 days. The in vitro release profiles of microspheres prepared with different polymer concentrations are shown in Figure 8. The release profiles also showed biphasic, which supports the fact that the first phase of release was ascribed to the diffusion of pDNA through the pores. In contrast, the following phase was mainly attributed to the degradation and solubilization of microspheres. Meanwhile, the higher polymer concentrations have shown slower release kinetics. Nonuniform atomization for highly viscous polymer solutions (i.e., 2.0%, w/v) has caused more pDNA close to the surface of microspheres; and these microspheres exhibited faster release rate in initial stage and slower release profile in the following phase. Generally, microspheres with different formulations have released between 95% and 99% of the encapsulated pDNA within 30 days. The SEM images in Figure 9 display the PLGA microspheres at different stages of in vitro studies. The microspheres are slightly crenate, and the increased bulk erosion over time can be seen. After 30 days incubation, the microspheres lost their spherical shape and only porous remnants of microspheres remained.

Integrity of pDNA

Shear induced degradation of plasmid DNA is a major problem in the processing of plasmid-based therapeutics. Several studies (Lengsfeld and Anchordoquy, 2002; Lentz et al., 2006) have investigated the mechanism governing the

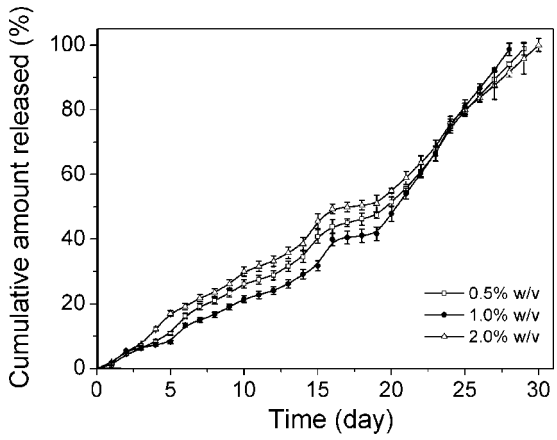

Figure 8. The delivery profiles of pDNA-PEI in vitro under physiological conditions (PBS buffer, pH 7.4, 37°C, 200 rpm) from microspheres, which have different polymer concentrations, and volumetric ratio of 100 PLGA:10 pDNA-PEI (v/v), $n = 3$.

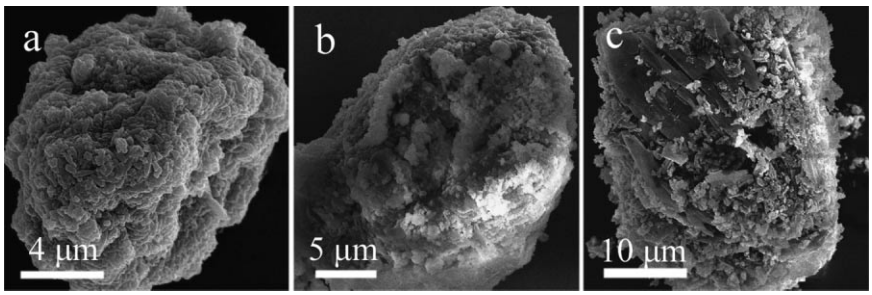

Figure 9. SEM images of PLGA microspheres at different degradation stages. (**a**) 10 days, (**b**) 20 days, and (**c**) 30 days in PBS buffer at 37°C.

degradation of pDNA, and strategies have been suggested to circumvent and minimize this effect during the myriad of processing steps used in the development of plasmid-based therapeutics. Strain rates of approximately 10^5–10^6 s^{-1} can fragment the pDNA; however, mitigation strategies such as the employment of cationic condensation agent can enhance molecular integrity (Murphy et al., 2006). In the current study, polyethylenimine (PEI) 25 kDa was used to condense and protect the pUC19 from mechanical shear developed during the ultrasonic atomization. The complexing of pUC19 with PEI can reduce the hydrodynamic diameter (~110.7 nm) and result in a lower probability of shear-induced degradation. As shown in Figure 10, the pDNA retained supercoiled conformation (~80.5%) after being released from PLGA microspheres. The naked pDNA has been degraded into smaller undesirable fragments after it was pumped through the 40 kHz ultrasonic atomizer, but only ~8.40% of the pDNA remained supercoiled. Based upon these observations, cationic polymer can be applied to protect the shear sensitive plasmids during microencapsulation process.

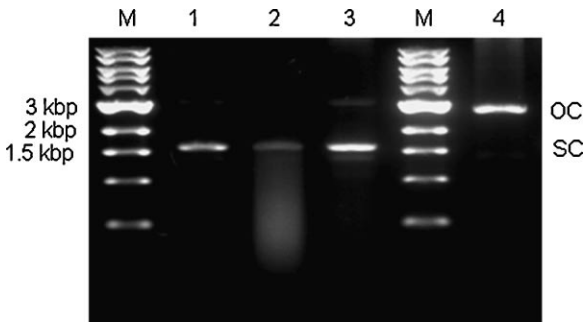

Figure 10. Result of ethidium bromide agarose gel electrophoresis for the assessment of the pDNA structural integrity after ultrasonic atomization. Analysis was performed using 0.8% agarose in TAE 1x buffer and 3 μg mL^{-1} EtBr at 60 V for 90 min. Lane M: 1 kbp DNA ladder; lane 1: 0.33 μg pDNA; lane 2: naked pDNA which was pumped through a 40 kHz ultrasonic atomizer; lane 3: pDNA recovered from in vitro release studies; lane 4: open circular pDNA obtained from 16 h and 37°C digestion study with *Eco*RI (New England BioLabs, Ipswich, MA). Lane 2 shows that the pDNA was partially covalently cleaved into smaller DNA fragments, whilst lane 3 shows that the majority (~80.5%) of the pDNA remain intact in a supercoiled form with minimal cleavage into a linearized or fragmented state.

Conclusions

A novel microencapsulation method has been developed for the preparation of biodegradable microspheres containing plasmid DNA, which was condensed with cationic polymer. It is clear that by manipulation and optimization of the synthesis parameters, microspheres in the size range suitable for vaccination in the nasal cavity can be produced with comparable narrow distribution. It was shown that the best method to synthesize microspheres that are less than 20 μm and display high encapsulation efficiencies (84–96%) is to pump the feedstocks containing 100 parts of 0.50% or 1.0% (w/v) PLGA in acetone with 5 or 10 parts of pDNA-PEI complex (v/v) through the 40 kHz ultrasonic atomizer at 18 mL h^{-1}. ANOVA analysis indicated that polymer concentrations and volumetric ratios have more statistical significant effects on the microspheres size distribution in comparison to the feed flowrate. The amount of PEI being used to condense pDNA has a significant effect on the surface morphology of microspheres. The in vitro release profiles obtained within 30 days appeared to follow the zero order release kinetics for 95–99% of the encapsulated pDNA with a minimal initial burst rate. 80.5% of plasmids DNA remained to be supercoiled after being released from the microspheres. The production method presented herein is easily scalable to produce large quantities of microspheres, which were shown to be a suitable controlled delivery system for biomolecules such as pDNA. The controlled delivery mechanism has applications in the areas of DNA therapeutics and gene therapy.

G.M.F. thanks the Victorian Endowment for Science, Knowledge and Innovation (VESKI) for the Innovation Fellowship and support of this research. HW thanks the Australian Research Council for the QEII Fellowship. J.H. gratefully acknowledges the financial support from the Monash University Research Graduate Scholarship.

References

Alpar HO, Somavarapu S, Atuah KN, Bramwell V. 2005. Biodegradable mucoadhesive particulates for nasal and pulmonary antigen and DNA delivery. Adv Drug Deliv Rev 57(3):411–430.

Atuah KN, Walter E, Merkle HP, Alpar HO. 2003. Encapsulation of plasmid DNA in PLGA-stearylamine microspheres: A comparison of solvent

evaporation and spray-drying methods. J Microencapsul 20(3):387–399.

Avvaru B, Patil MN, Gogate PR, Pandit AB. 2006. Ultrasonic atomization: Effect of liquid phase properties. Ultrasonics 44(2):146–158.

Bellman R, Pennington RH. 1954. Effects of surface tension and viscosity on Taylor instability. Q Appl Math 12(2):151–162.

Bivas-Benita M, Romeijn S, Junginger HE, Borchard G. 2004. PLGA-PEI nanoparticles for gene delivery to pulmonary epithelium. Eur J Pharm Biopharm 58(1):1–6.

Castellanos IJ, Carrasquillo KG, Lopez JD, Alvarez M, Griebenow K. 2001. Encapsulation of bovine serum albumin in poly(lactide-*co*-glycolide) microspheres by the solid-in-oil-in-water technique. J Pharm Pharmacol 53(2):167–178.

Crotts G, Park TG. 1995. Preparation of porous and nonporous biodegradable polymeric hollow microspheres. J Control Release 35(2–3):91–105.

Davis SS. 2001. Nasal vaccines. Adv Drug Deliv Rev 51(1–3):21–42.

De Rosa G, Quaglia F, La Rotonda MI, Appel M, Alphandary H, Fattal E. 2002. Poly(lactide-*co*-glycolide) microspheres for the controlled release of oligonucleotide/polyethylenimine complexes. J Pharm Sci 91(3): 790–799.

Densmore CL, Orson FM, Xu B, Kinsey BM, Waldrep JC, Hua P, Bhogal B, Knight V. 2000. Aerosol delivery of robust polyethyleneimine-DNA complexes for gene therapy and genetic immunization. Mol Ther 1(2): 180–188.

Edlund U, Albertsson AC. 2002. Degradable polymer microspheres for controlled drug delivery. Degradable aliphatic polyesters. Berlin: Springer-Verlag. p 67–112.

Eyles JE, Sharp GJE, Williamson ED, Spiers ID, Alpar HO. 1998. Intra nasal administration of poly-lactic acid microsphere co-encapsulated Yersinia pestis subunits confers protection from pneumonic plague in the mouse. Vaccine 16(7):698–707.

Felder CB, Blanco-Prieto MJ, Heizmann J, Merkle HP, Gander B. 2003. Ultrasonic atomization and subsequent polymer desolvation for peptide and protein microencapsulation into biodegradable polyesters. J Microencapsul 20(5):553–567.

Forde GM, Coomes AD, Giliam FK, J Ho , Horsfall MJ. 2006. Creation of protein loaded biodegradable microparticles via ultrasonic atomization suitable for nasal delivery. Chem Eng Res Des 84(A3):178–184.

Freitas S, Merkle HP, Gander B. 2004. Ultrasonic atomisation into reduced pressure atmosphere - envisaging aseptic spray-drying for microencapsulation. J Control Release 95(2):185–195.

Freitas S, Merkle HP, Gander B. 2005. Microencapsulation by solvent extraction/evaporation: Reviewing the state of the art of microsphere preparation process technology. J Control Release 102(2):313–332.

Freytag T, Dashevsky A, Tillman L, Hardee GE, Bodmeier R. 2000. Improvement of the encapsulation efficiency of oligonucleotide-containing biodegradable microspheres. J Control Release 69(1):197–207.

Gautam A, Densmore CL, Xu B, Waldrep JC. 2000. Enhanced gene expression in mouse lung after PEI-DNA aerosol delivery. Mol Ther 2(1):63–70.

Godbey WT, Wu KK, Mikos AG. 2001. Poly(ethylenimine)-mediated gene delivery affects endothelial cell function and viability. Biomaterials 22(5):471–480.

Johansen P, Merkle HP, Gander B. 2000. Technological considerations related to the up-scaling of protein microencapsulation by spray-drying. Eur J Pharm Biopharm 50(3):413–417.

Kim IS, Lee SK, Park YM, Lee YB, Shin SC, Lee KC, Oh IJ. 2005. Physicochemical characterization of poly(L-lactic acid) and poly(D,L-lactide-*co*-glycolide) nanoparticles with polyethylenimine as gene delivery carrier. Int J Pharm 298(1):255–262.

Kippax P, Fracassi J. 2003. Particle size characterisation in nasal sprays and aerosols. Walnut Creek, CA: LabPlus International.

Lang RJ. 1962. Ultrasonic atomization of liquids. J Acoust Soc Am 34(1): 6–8.

Lengsfeld CS, Anchordoquy TJ. 2002. Shear-induced degradation of plasmid DNA. J Pharm Sci 91(7):1581–1589.

Lentz YK, Anchordoquy TJ, Lengsfeld CS. 2006. Rationale for the selection of an aerosol delivery system for gene delivery. J Aerosol Med-Depos Clear Eff Lung 19(3):372–384.

Lungwitz U, Breunig M, Blunk T, Gopferich A. 2005. Polyethylenimine-based non-viral gene delivery systems. Eur J Pharm Biopharm 60(2): 247–266.

McGee JP, Davis SS, Ohagan DT. 1995. Zero-order release of protein from poly(D,L-lactide-*co*-glycolide) microparticles prepared using a modified phase-separation technique. J Control Release 34(2):77–86.

Murphy JC, Cano T, Fox GE, Willson RC. 2006. Compaction agent protection of nucleic acids during mechanical lysis. Biotechnol Prog 22(2):519–522.

Newman SP, Pitcairn GR, Dalby RN. 2004. Drug delivery to the nasal cavity: In vitro and in vivo assessment. Crit Rev Ther Drug Carr Syst 21(1):21–66.

Patil SD, Rhodes DG, Burgess DJ. 2005. DNA-based therapeutics and DNA delivery systems: A comprehensive review. AAPS J 7(1):E61–E77.

Pistel KF, Kissel T. 2000. Effects of salt addition on the microencapsulation of proteins using W/O/W double emulsion technique. J Microencapsul 17(4):467–483.

Turker S, Onur E, Ozer Y. 2004. Nasal route and drug delivery systems. Pharm World Sci 26(3):137–142.

CHAPTER FIVE

SYNTHESIS AND APPLICATION OF INORGANIC-BIODEGRADABLE POLYMER COMPOSITE MICROSPHERES FOR CONTROLLED DELIVERY OF A PRIME-BOOST VACCINE

Biodegradable polymer-mesoporous silica composite microspheres for DNA prime-protein boost vaccination

Jenny Ho, Huanting Wang, Gareth M. Forde

Journal of Controlled Release

Manuscript number:

JCR-D-08-00460

Monash University

Declaration for Thesis Chapter Five

Declaration by candidate

In the case of Chapter 5, the nature and extent of my contribution to the work was the following:

Nature of contribution	Extent of contribution (%)
Initiation, Key ideas, Experimental works, Development, Data analysis, Writing up	90

The following co-authors contributed to the work. Co-authors who are students at Monash University must also indicate the extent of their contribution in percentage terms:

Name	Nature of contribution
Dr Gareth M. Forde	Initiation, Key ideas, Development, Review
Dr. Huanting Wang	Key ideas, Development, Review

Candidate's signature		**Date**

Declaration by co-authors

The undersigned hereby certify that:

(1) the above declaration correctly reflects the nature and extent of the candidate's contribution to this work, and the nature of the contribution of each of the co-authors.
(2) they meet the criteria for authorship in that they have participated in the conception, execution, or interpretation, of at least that part of the publication in their field of expertise;
(3) they take public responsibility for their part of the publication, except for the responsible author who accepts overall responsibility for the publication;
(4) there are no other authors of the publication according to these criteria;
(5) potential conflicts of interest have been disclosed to (a) granting bodies, (b) the editor or publisher of journals or other publications, and (c) the head of the responsible academic unit; and
(6) the original data are stored at the following location(s) and will be held for at least five years from the date indicated below:

Location	Department of Chemical Engineering, Monash University – Clayton campus, Australia.

Signature		**Date**
Signature		**Date**

Biodegradable Polymer-Mesoporous Silica Composite Microspheres for DNA Prime-Protein Boost Vaccination

Jenny Ho, Huanting Wang and Gareth M. Forde*

Department of Chemical Engineering, Monash University, Clayton, 3800, VIC, Australia.

*Corresponding author: Jenny Ho, Phone: +61 3 9905 1867, Fax: +61 3 9905 5686, email: jenny.ho@eng.monash.edu.au

ABSTRACT

A composite microsphere formulation, composed of mesoporous silica spheres (MPS) and PLGA, enables the controlled delivery of a prime-boost vaccine via the encapsulation of plasmid DNA (pDNA) and protein in different segments was developed. Method with modified dual-concentric-feeding needles attached to a 40 kHz ultrasonic atomizer was studied. These needles focus the flow of two different solutions, which passed through the ultrasonic atomizer. The process synthesis parameters, which are important to the scale-up of composite microspheres, were also studied. These

parameters include polymer concentration, feed flowrate, and volumetric ratio of polymer and pDNA/MPS. This fabrication technique produced composite microspheres with mean D[4,3] ranging from 6 – 34 μm, depending upon the microsphere preparation. The resultant physical morphology of composite microspheres was largely influenced by the volumetric ratio of pDNA/MPS to polymer, and this was due to the precipitation of MPS at the surface of the microspheres. The encapsulation efficiencies were predominantly in the range of 93 – 98 % for pDNA and 46 – 68 % for MPS. In the *in vitro* studies, the pDNA and protein showed different release kinetics in a 40 day time frame. The dual-concentric-feeding in ultrasonic atomization was shown to have excellent reproducibility. It was concluded that this fabrication technique is an effective method to prepare formulations containing a heterologous prime-boost vaccine in a single delivery system.

KEY WORDS: Mesoporous silica spheres; Composite microspheres; Plasmid DNA; Prime-boost vaccine; PLGA.

1. Introduction

DNA-based immunisation utilises an approach in which plasmid DNA encoding an antigen is introduced into the host. Consequently, the immune responses are generated following *in vivo* expression of the antigenic gene product [1]. Strong antibody and T-cell responses against antigens induced by the DNA vaccines have been demonstrated in animal models. However, the levels of antibodies induced are often low or modest, and this is particularly true in human recipients [2]. Therefore, there is an urgent need to develop potent and efficient DNA vaccines to enable DNA to be employed as an

effective tool in human health applications. A number of strategies have been proposed as possible means to improve DNA vaccines. These include delivery systems; administration of adjuvants; targeting strategies; boosting strategies; and immunising by different routes [3]. Prime-boost strategies have been shown to successfully generate impressive cell-mediated immunity against a variety of encoded antigens [4-7]. Homologous and heterologous boosting are the prime-boost mechanisms being used to enhance the immune responses. However, repeated immunisation with the same vaccine (homologous boosting) has been shown to be ineffective at boosting the level of specific T-cell responses [8]. Nevertheless, heterologous prime-boost immunisation strategies have been shown to induce very high levels of protection and specific $CD8^+$ T-cell responses [9, 10]. As a result, most DNA and protein vaccines need to be administered at least twice for the induction of protective immune responses. Unwanted side effects of toxicity and multi-drug resistance associated with larger dose administration can be overcome via improved delivery systems. As a result, improved delivery systems that provide sustained release of biomolecules over time while simultaneously protecting them from degradation are increasing importance.

Numerous materials and methods have been developed to maximise the therapeutic effects and convenience of administration of biopharmaceuticals [11-13]. Among these, inorganic silica has become attractive as a biomaterial because of its good biocompatibility, low cytotoxicity and excellent ability for functionalisation [14-16]. Mesoporous silica derived by using triblock copolymers [17] or silica colloids [18] have been identified to have the potential to act as convenient reservoirs for controlled delivery systems. Poly(D,L-lactide-co-glycolide) (PLGA)/mesoporous silica hybrids have helped to delay the release period of gentamicin to as long as 5 weeks, and this has

helped to further the development of a controlled reservoir [19]. Currently, the most commonly used method to embed biopharmaceutical compounds into biodegradable microspheres is emulsion-solvent extraction/evaporation [20, 21]. However, this method is inherently a batch operation which makes scale-up and large scale production difficult, inefficient and costly. In addition, the bioactivity of biopharmaceuticals can be greatly impaired or completely eliminated due to the presence of organic solvents and high shear; simultaneously, the solvents are difficult to remove completely [21]. Demand of aseptic microencapsulation is increasing because heat-sterilisation and sterilisation by gamma rays may harm the encapsulated biopharmaceuticals and degrade the polymer. The use of ultrasonic atomization in producing microspheres containing biopharmaceuticals is comparatively new, and this method shows promising results for the synthesis of micron and submicron monodispersed particles [22-25]. Importantly, this fabrication technique is readily accommodated within a laminar air-flow cabinet for aseptic processing. Continuing from previous study that reported the method for microencapsulating pDNA into uniform polymer microspheres via ultrasonic atomization [26], a modified apparatus utilising dual-concentric-feeding needles, which enabling the formation of inorganic-organic composite microspheres, was studied.

The aim of this study was to evaluate the potential of an ultrasonic atomization process for the preparation of mesoporous silica spheres (MPS)-PLGA composite microspheres, which are suitable for controlled delivery of a plasmid DNA (pDNA) prime and protein boost vaccine. Microspheres with a prime-boost vaccine in a single formulation have not previously been reported in the literature. This study can be viewed as a preliminary work for a possible platform technology employing an engineered-guided vaccine carrier production process. pEGFP-N1, an *E.coli* plasmid

cloning vector, was chosen as a model plasmid DNA, because it has been optimised for higher expression in mammalian cells, and it has a representable size (kbp) compared to most of the pDNA currently in clinical use. The influences of various processing and formulation parameters where considered, including: polymer concentration; feed flowrate; volumetric ratio of feedstocks; and nitrogen to phosphorous ratio (N/P) when condensing the pDNA. The influences on the characteristics of the resulting composite microspheres were studied. The deliveries of pDNA and protein from the resulting composite microspheres were also observed and analysed. This novel fabrication technique is shown to be a potential synthesis method for particulates that facilitate an effective prime-boost delivery system to improve and homogenise the overall immune responses to vaccines.

2. Materials and methods

2.1. Materials

The poly(D,L-lactide-co-glycolide) (PLGA 50:50, M_W = 15,000 Da); polyethylenimine (PEI, M_W = 25,000 Da, branched); poly(vinyl alcohol) (PVA, M_W = 50,000 Da, 87-90 % hydrolysed); and phosphate buffered saline (PBS) were purchased from Sigma-Aldrich (Sydney, Australia). SNOWTEX® silica colloid (ST-20L: 40 – 50 nm) was provided by Nissan Chemical Industries (Tokyo, Japan) and was diluted into a 10wt % aqueous before use. Bovine serum albumin (BSA, 98%, MW ~ 66 kDa, Sigma-Aldrich) stock solutions were prepared by dissolving in an acetic buffer (10 mM CH_3COONa, ~ pH 4.2). Other materials include pEGFP-N1 plasmid, 4733 bp, ~1.8 x 10^6 g mol^{-1} (Clontech Laboratories Inc., Melbourne, Australia); acetone

(99.5 %, LabScan, Dublin); agarose (Promega, Sydney, Australia); ethidium bromide (Sigma-Aldrich; MW 394.31, 10 mg ml^{-1}); and 1 kbp DNA ladder (New England Bio-Labs, Ipswich, MA, USA).

2.2. Synthesis of mesoporous silica spheres and adsorption of BSA

Mesoporous silica spheres (MPS) were produced using the method we have reported [18]. Briefly, mesoporous silica spheres were synthesised from 10 wt % commercially available silica colloids (SNOWTEX® ST-20L), and 0.25 mol L^{-1} ammonium nitrate (NH_4NO_3, 99 %, Ajax Chemicals) was used as an electrolyte to destabilise the silica colloids. Monomer acrylamide, (AM, CH_2=$CHCONH_2$, 99%, Sigma-Aldrich), crosslinker *N,N'*- methylenebisacrylamide, (MBAM, $(CH_2$=$CHCONH_2)_2CH_2$, 99%, Sigma-Aldrich), and initiator ammonium persulfate, ($(NH_4)_2S_2O_8$, >98%, Sigma-Aldrich) (2 AM : 0.02 MBAM : 0.01 $(NH_4)_2S_2O_8$: 1 SiO_2 by weight) were added to the resulting suspension to produce a temporary polymer barrier during the synthesis of mesoporous silica spheres (MPS). The obtained suspension was then heated at 90 °C for 30 min to form a polymer hydrogel, which was left to dry overnight at 90 °C. The resulting solids were carbonised under N_2 for 2 h and calcined under O_2 for 5 h at 500 °C to yield mesoporous silica spheres. A BSA adsorption isotherm was generated by loading 30.0 mg ml^{-1} BSA solution in a continuous flow at a flowrate of 0.2 ml min^{-1} onto 1.0 ml of MPS which were packed in an Econo-Pac column (1.5 cm inside diameter, BIO-RAD) at 25 °C. The outlet concentrations of BSA were measured with a UV spectrophotometer at 280 nm. The resulting mesoporous silica spheres loaded with BSA were then washed continuously with deionised water (1.0 ml min^{-1}) for 20 min in

order to leach out loosely bound BSA from the silica surface. The total amount of BSA bound was calculated by performing a mass balance over the BSA by using data from the breakthrough curve and leaching stage [27].

2.3. Formation of pDNA-PEI complexes

10 %w/v of polyethylenimine (PEI) stock solution was prepared by adding 5.0 ml of PEI (M_W = 25 kDa, branched) into 35 ml of deionised water. The pH of the solution was adjusted to 7.9 with concentrated hydrochloric acid (HCl), and the final volume of the solution was adjusted to 50 ml with deionised water [28]. This was followed by filtration with a 0.22 μm pore-size cellulose acetate membrane filter (Sartorius, Goettingen, Germany), and the filtered solution was then stored at 4 °C for subsequent dilution. Complexes of PEI and pDNA were formed by first diluting pDNA and polymer separately with deionised water into the appropriate volumes (based on the desired N/P ratio). The pDNA solution was then added dropwise into the PEI solution. The mixture was vortexed immediately for 2 min; and it was incubated for 10 min prior to the zeta potential measurements. The polymer concentrations were calculated from the desired N/P ratio and the amount of plasmid – assuming that 43.1 g mol^{-1} corresponds to each repeating unit of PEI containing one nitrogen atom, and 330 g mol^{-1} corresponds to each repeating unit of pDNA containing one phosphorous atom. The resulting charge ratio is expressed as PEI nitrogen : DNA phosphorous. The zeta potential and the size distribution of pDNA samples, which condensed with PEI, were determined in triplicate for each sample by using a Malvern Zetasizer Nano ZS series (ZEN 3600).

2.4. Preparation of microspheres via dual-concentric-feeding ultrasonic atomization

Solutions containing various concentrations of PLGA 50:50 (0.5 – 5.0 %w/v) were prepared in acetone. The viscosity of the polymer solutions was measured at 20 °C using a calibrated BS/U-tube glass capillary viscometer (Series 9724-E50, size A, Cannon Instrument Company,PA, USA) with an approximate constant at 0.003 cSt s^{-1}. The MPS adsorbed with BSA were suspended into the pDNA-PEI solutions at two weight ratios, 100 pDNA-PEI : 5 MPS (w/w) and 100 : 10; and this mixing process continued until a homogenous mixture was obtained. The composite microspheres were prepared by using a modified method for the production of plasmid encapsulated microspheres [26]. Briefly, two concentric needles were used to feed the feedstocks to a 40 kHz ultrasonic atomization system (VCX134 AT, Sonics, USA) with a 6 mm full wave atomization probe. The atomized droplets were collected in defined volumes (i.e. 5 ml in a 50 ml glass measuring cylinder) of hardening agent (0.1 %w/v PVA in deionised water) under continuous stirring at 500 rpm. After atomization, the stirring was continued for another 30 min. The final products were stored at 4 °C for subsequent analysis. Three batches were prepared for each formulation or set of parameter.

2.5. Microsphere size distribution and morphology

The particle size distributions were determined by using a Malvern Mastersizer 2000 (Malvern Instruments, UK), which utilises laser diffraction to determine the frequency of size distribution. The focus of this study is on the hydrodynamic diameter of microspheres in suspensions for nasal inhalation. As a result, particle sizes or

diameters are presented in the volume-weighted mode with a mean diameter of D[4,3]. The D[4,3] indicates where the volume of the system lies by assuming all the particles are spherical. Where *d* is the diameter of a spherical particle, D[4,3] is defined as:

$$D[4,3] = \frac{\sum d^4}{\sum d^3} \quad (1)$$

The microsphere shape and morphology were analysed by Scanning Electron Microscopy (SEM). Samples of microspheres were placed directly on an aluminium stage and dried at room temperature for 1 h. The dried samples were then coated with 1 nm of platinum, and characterised with a JEOL JSM-6300F field emission scanning electron microscope (FESEM), which was operated at an accelerating voltage of 5 kV.

2.6. pDNA and MPS encapsulation efficiency

The amount of encapsulated pDNA in the microspheres was calculated by performing a mass balance over the amount of pDNA in the feedstock and the measured unencapsulated pDNA remained in the hardening agent after composite microspheres formation [24]. After composite microspheres formation, the microspheres suspension was centrifuged for 30 min at 4000 rpm, and the supernatant was checked for the unencapsulated pDNA concentration. The concentration of pDNA sample was determined by a spectrophotofluorometer (RF-1501, Shimadzu, Japan) with a Quant-iT^{TM} PicoGreen$^{®}$ dsDNA quantitation assay reagent (Invitrogen, Australia) [29]. On the other hand, to determine the MPS encapsulation efficiencies into the composite microspheres, the unencapsulated MPS need to be removed from the microspheres suspension. This is achieved by filtrating with a 0.8 μm pore-size cellulose acetate membrane filter (Sartorius, Goettingen, Germany). The composite microspheres

retained by the membrane filter were dissolved in 2 ml chloroform (Sigma-Aldrich, Sydney, Australia), and kept at room temperature for about 2 h. After the composite microspheres were dissolved completely, the resulting mixture was centrifuged for 30 min at 4000 rpm – the white pellets precipitate at the bottom are MPS. The MPS were washed with deionised water to remove the organic solvent (n = 3). The MPS were dried in the oven overnight at 50 °C, and weighed. The encapsulation efficiency was calculated as the weight ratio of MPS content in the composite microspheres to that in the feedstock. The test was repeated three times and the results were averaged.

2.7. In vitro release study

A study was conducted in a Mk X Incubator-Shaker (LH fermentation, Stoke Poges, UK) to determine the release rate of pDNA and protein from the composite microspheres under physiological condition *in vitro* (phosphate buffered saline (PBS), 37 °C, pH7.4, 200 rpm). 200.0 mg of composite microspheres for each formulation were suspended in 2.0 ml of PBS buffer (0.01 mol L^{-1}) along with 0.05 %w/v PVA. At predetermined time intervals (every 24 h for 40 days), the samples were centrifugated (4000 rpm for 30 min in a Heraeus Multifuge® 3 S-R centrifuge) to cause the microspheres to precipitate. The 2.0 ml of supernatant was removed; the volume of the supernatant removed was then replaced with fresh PBS. The concentration of released pDNA was determined by using a spectrophotofluorometer (RF-1501, Shimadzu, Japan) with a Quant-iT™ PicoGreen® dsDNA quantitation assay reagent (Invitrogen). On the other hand, the concentration of the released BSA was determined using a Bradford Reagent (Sigma-Aldrich, Sydney, Australia) assay, which is 0.900 ml of Bradford

Reagent was added to a 0.100 ml aliquot of sample. The optical density of the solution was measured at 595 nm using a UV-visible spectrophotometer (UV-2450, Shimadzu, Tokyo, Japan). Release experiments were performed in triplicate (n = 3), and the results were averaged. pDNA samples were also analysed for potential alterations in the plasmid structure by using 0.8 % agarose gel electrophoresis that uses 1 kbp DNA ladder and 3 μg ml^{-1} ethidium bromide (EtBr) staining. The gel ran at 60 V for 90 min. The resulting fractioned nucleic acid gel was analysed and photographed in a Molecular Imager Gel Doc XR System (BIORAD, Italy). The ratio of supercoiled to degraded linear pDNA was quantified via densitometry studies using the Quantity One® software (BIORAD). The molecular weight and conformation of BSA after the delivery studies were observed using an Experion Automated Electrophoresis System (BIORAD), which was used according to manufacturer's instructions.

2.8. Statistical analysis

A single factor analysis of variance (ANOVA) was performed to determine if observed differences in composite microsphere diameters due to the changes in the ultrasonic atomization process parameters were statistically significant. In all experiments, when $p < 0.05$, then the differences in the results obtained from different parameters were found to be statistically significant.

3. Results and discussion

3.1. Description of dual-concentric-feeding ultrasonic atomization

A process for fabricating microspheres encapsulated with plasmid DNA via an ultrasonic atomizer was reported previously [26]. In an extension of the reported method, feedstocks were fed to the nozzle of the ultrasonic atomizer through the dual-concentric-feeding needles (P/N 038110 internally and P/N 039847 externally, SGE Analytical Science, Ringwood, Australia). These needles were pumped via two syringe peristaltic pumps (KDS 100, KD Scientific, Holliston, MA) at two predetermined flowrates – this process is illustrated in Figure 1. From our previously reported study, the volumetric ratio and feed flowrate of feedstocks have shown to have significant effects on the weighted mean particle size (D[4,3]). Nevertheless, due to a more uniform atomization of the fluid, the effect of feed flowrate was less significant for feedstock with less solid contents. As a result, in this novel ultrasonic atomization which employs dual-concentric-feeding needles, the effect of feed flowrate can be further reduced by only controlling the internally delivered feed stream flowrate. The relative flowrates of each of these streams can be varied to control the volumetric ratio between the polymer solution and pDNA/MPS contents. The atomization probe was energised at an amplitude of 100 %. The atomizer tip was fixed at 15.0 cm above the surface of the hardening agent (0.1 %w/v PVA in deionised water). This height enabled sufficient time for the volatile acetone solvent to evaporate from the fine droplets, which were formed by the ultrasonic head. The feedstocks were acoustically excited when introduced onto the vibrational nozzle. The liquids absorbed the vibrational energy and created a unique wave pattern [30]. Liquid particles are ejected from the liquid surface into the

surrounding air. Under atomizing conditions, very fine dense fogs were formed. This fabrication technique has several advantages over conventional methods (e.g. emulsion-solvent extraction/evaporation) as it is easily scaled to produce large quantities of microspheres; less contacting time between biopharmaceuticals and organic solvents to minimise degradation/precipitation/agglomeration; and the microsphere content can be easily tailored by changing the feedstock flowrates.

3.2. Fabrication of PLGA-MPS composite microspheres

The goal of this work was to fabricate organic-inorganic composite microspheres containing plasmid DNA and protein in different segments, as a means to potentially achieve controlled delivery profiles. The role of polymer concentration and viscosity on the fabrication of the composite microspheres was investigated. The ultrasonic atomization process was shown to greatly depend upon the viscosity of the polymer solution. This is because the viscous liquids will not be atomized evenly and instantly, due to the relatively low growth rate of the capillary wave amplitude [31]. This failure of uniform atomization causes wider microsphere size distributions, and reduces the yield of microspheres. The reduction in the yield is also due to the intensive agglomeration at the hardening agent surface at higher polymer concentrations. The correlations between polymer concentration, viscosity and volume-weighted mean diameter (D[4,3]) are shown in Figure 2. ANOVA analysis shows $p < 0.001$, which indicates that the viscosity of polymer solutions has a statistically significant effect on the size distribution of microspheres produced by ultrasonic atomization.

The increase in the content of pDNA/MPS affected the size distribution and morphology of the composite microspheres. In this study, the D[4,3] shifted from 6.64 μm (*span* = 0.78) to 18.05 μm (*span* = 1.16) when the volumetric ratio changed from 5 pDNA/MPS : 100 PLGA (5 %v/v) to 10 pDNA/MPS : 100 PLGA (10 %v/v) for 1 %w/v PLGA pumped through the ultrasonic atomizer. The microsphere mean diameter (D[4,3]) further increased drastically to 31.75 μm (*span* = 2.35) when the ratio increased to 20 pDNA/MPS : 100 PLGA (20 %v/v). Wider size distributions were obtained due to the failure of homogeneous atomization and encapsulation (Figure 3). *Span* is the measurement of the width of the size distribution. A small *span* indicates a narrow particle size distribution. The *span* is calculated as:

$$\frac{d(0.9)-d(0.1)}{d(0.5)} \qquad (2)$$

where d(0.1), d(0.5) and d(0.9) are the sizes of particle below which 10 %, 50 % and 90 % respectively of the sample lies.

This outcome is due to the fact that most of the plasmid DNA and mesoporous silica spheres were not being embedded into the composite microspheres as observed from the low encapsulation efficiency. Intensive agglomeration phenomena of the resulting materials also occurred. Figure 4 show the microstructure of the microspheres loaded with 5, 10 and 20 % v/v pDNA-MPS, respectively. As shown in Figure 4 (a), only the PLGA microspheres with pDNA exhibited smooth surfaces and well-established spherical shapes. When 5 %v/v of content (pDNA/MPS) is loaded, it is observed from Figure 4 (b) that the composite microspheres also show a well-established spherical shape; however, the surfaces of the composite microspheres are rough and some mesoporous silica spheres (MPS) were observed on the surfaces of the composite

microspheres. The precipitation of the MPS on the surfaces is related to the hydrophilic nature of the MPS [19]. This also can due to the larger size of MPS compared to pDNA and creates higher tendency to migrate towards the aqueous hardening agent interface. With increasing pDNA/MPS loading to 10 and 20 %v/v, the resulting microspheres show similar microstructure to that of the composite microspheres with 5 %v/v content; even though their sphere size became larger and significant amount of MPS noticed at the surfaces of microspheres (Figure 4 c and d). When the weight ratio of pDNA-PEI complexes and MPS changed from 100:5 (w/w) to 100:10 (w/w), a similar phenomenon was observed. According to statistical analysis, when the solid content was increased, $p < 0.001$ revealed that the differences of the average D[4,3] are statistically significant at a statistical probability > 95 %.

In this study, the effect of two feedstock flowrates on the synthesis of composite microspheres was also studied. The polymer solution and pDNA/MPS mixture were passed through the ultrasonic atomizer at various flowrates, as indicated in Table I. With increased feed flowrate, a significant shift to a larger range of microsphere sizes and a wider microsphere size distribution were observed. These observations can be attributed to the collision and subsequent coalescence of droplets in close vicinity of the atomizing tip, shortly after the atomization. This is further supported by the fact that agglomerations and lower yield have been noticed at higher feed flowrate. Moreover, $p < 0.05$ with a statistical probability of < 95 % indicated that when the feed flowrates varied, the differences between the averages (D[4,3]) were statistically significant.

As reported previously [26], we have observed that polyethylenimine (PEI) can protect the pDNA from shear-induced degradation associated with ultrasonic

atomization. In this study, we condensed pEGFP-N1 by using PEI (MW = 25 kDa) with a consequent reduction in the hydrodynamic diameter of pDNA (Figure 5). The pEGFP-N1 formed into a toroidal structure and positively charged complexes – this transformation favours cellular transfection [28]. The N/P ratio equals to the number of cationic charges of the nitrogen of PEI divided by the number of anionic charges of the phosphorous of DNA. The pEGFP-N1 pDNA molecules exhibited highly negative zeta potential (-46.9 mV) and a mean hydrodynamic diameter of 198.0 nm in PBS buffer, pH 7.4 (n = 3). When the N/P ratio increased, the pDNA-PEI complex became larger (~ 462.0 nm), and formed polydisperse aggregations at a value close to N/P = 1. This is due to the lowered overall surface charge. Further increase in N/P ratios (> 2) reduced the size of the complexes due to the electrostatic repulsion. The increase in the content of nitrogen from PEI has rendered the effective surface charge of the complexes – causing it to become positive. When the complexes have large positive zeta potentials (≥ 30 mV), they tend to repel each other electrostatically; thereby, reducing the tendency to agglomerate or flocculate. While varying the N/P ratios from 5 to 20, the zeta potentials were maintained ~ 29.6 ± 1.2 mV, and the resultant hydrodynamic diameters were ~ 62.7 ± 5.0 nm. These two characteristics show that when N/P > 5, the pEGFP-N1 can be condensed into a compact form and acquired positive surface charges. On the other hand, the addition of PEI into the formulation strongly affects the morphology of the composite microspheres. The composite microspheres obtained were spherical in shape; however, the microspheres exhibited numerous surface pores (Figure 4). The osmotic pressure associated with pDNA-PEI complexes induced the influx of water into the microspheres during the hardening process in the hardening agent [32]. Interestingly, the N/P ratio does not show significant effect on the composite microsphere size distributions. This is mainly because the droplets shrank and formed a

solid layer at the surface after ejected from the nozzle. The subsequent influx of water does not significantly alter their dimension, but creates pores inside the particles.

3.3. Encapsulation efficiency

In general, this fabrication technique via dual-concentric-feeding in ultrasonic atomization showed high encapsulation efficiency for pDNA-PEI complexes; however, encapsulation efficiency appeared to be slightly lower for mesoporous silica spheres. An increase in polymer concentration from 1.0 %w/v to 3.0 %w/v caused the encapsulation efficiencies for pDNA to decrease slightly from 96.7 % to 91.4 % and 97.9 % to 95.1 % for 5 %v/v and 10 %v/v formulations respectively, due to the nonuniform atomization for highly viscous polymer solutions. Nevertheless, the overall encapsulation capability for pDNA in this fabrication method is higher than the single inlet feedstock that has been reported [26]. In addition, the N/P ratios do not show significant effect on the encapsulation efficiencies of the composite microspheres. In Figure 6, the formulations prepared from 1.0 %w/v and 2.0 %w/v PLGA at several volumetric ratios of pDNA/MPS have encapsulation efficiencies for pDNA varying between 93 – 98 %. On the other hand, encapsulation efficiencies for mesoporous silica spheres appeared relatively low, varied between 46 – 68 %. As shown in Figure 4, some MPS were observed on the surface of the composite microspheres. MPS are highly hydrophilic, and have a strong inclination to migrate towards the aqueous hardening agent during the formation of composite microspheres. As a result, MPS were precipitated on the outer surface of microspheres and partially lost into the hardening agent [19].

3.4. In vitro release studies

The *in vitro* release profiles of pEGFP-N1 and BSA from the composite microspheres have shown significantly different release kinetics. In general, the release profiles of pEGFP-N1 were triphasic (Figure 7). The first phase of release (the first 10 days) was attributed to the pDNA on or close to the microsphere surface during the fabrication process. The following short lag phase, which lasted for approximately one week, was mainly due to the diffusion of pDNA through the polymer matrix. The third phase of release can be ascribed to polymer degradation and solubilisation. In Figure 7, we can see that the microspheres prepared with 3.0 %w/v PLGA show a 27.17 % initial release of the encapsulated pDNA over the first 4 days; this percentage is relatively high when compared with other formulations. In fact, the composite microspheres prepared with 1 %w/v and 2 %w/v PLGA only showed an initial release of 6.52 % and 12.93 % respectively within the same period of time. This is because nonuniform atomization for highly viscous polymer solution caused more pDNA close to the surface of microspheres. The composite microspheres prepared with higher polymer concentrations showed slower release profile in the later stage, and more efficiently retained entrapped pDNA because only 67.24 % and 73.45 % of entrapped pDNA were released by day 40 for 2.0 %w/v and 3.0 %w/v PLGA respectively.

In contrast, the BSA adsorbed onto the mesoporous silica spheres in the composite microspheres herein demonstrated zero order or near-zero order release kinetics without an initial spike of the released protein. The release profiles that were obtained fit with linear line and the correlation coefficients are shown in Table II. Most of the formulations have correlation coefficients greater than 0.98; thus, this indicates that zero

order release kinetics is being followed. The hybrid structure between MPS and PLGA can provide sustained release for protein, and this largely depends on the degradation of polymer [19]. The release profiles of protein were shown to be different to the release profiles of pDNA, where the release of protein was delayed (Figure 8 in comparison to Figure 7; Figure 9a and 9b) and showed a less distinct triphasic release profile. MPS encapsulated by higher polymer concentrations showed more protein retained at the end of the release kinetics studies, and slower release rates as shown in Figure 8. Non-uniform atomization at higher polymer concentrations resulted in slightly higher initial release of protein which may be attributed to more MPS being precipitated at the surface of the composite microspheres.

Comparison of release kinetics between pDNA and protein are shown in Figure 9. The composite microspheres were prepared at several volumetric ratios of pDNA/MPS, and the weight ratios of pDNA to MPS are 5 (w/w). The volumetric ratio has significant effect on the release kinetics of the encapsulated pDNA and protein, due to the physical appearance of the composite microspheres obtained. Microspheres prepared using 5 %v/v of pDNA/MPS (Figure 9a) exhibited a burst effect for pDNA, which amount to ~ 6.69 % and ~ 25.00 % released in 1 and 5 days, respectively. The burst release can be explained by the surface localised pDNA. It appears that greater surface area of smaller microspheres formed as a result of low solid content (D[4,3] = 6.64 μm) results in microspheres having more surface-bound pDNA. On the other hand, less MPS precipitated at the composite microspheres surface also facilitated the diffusion of pDNA through the polymer matrix. This was further supported by the fact that ~ 94.03 % of encapsulated pDNAs were released at the end of 40 days. Microspheres prepared using 10 %v/v and 20 %v/v of pDNA/MPS exhibited a relatively slow release

rate of pDNA compared to microspheres prepared using 5 %v/v solid content. The release from microspheres prepared using 10 %v/v (D[4,3] = 18.05 μm) was higher than microspheres using 20 %v/v (D[4,3] = 31.75 μm) due to smaller microsphere sizes and higher surface areas. At day 40, the 10 %v/v and 20 %v/v solid content formulations released ~ 86.33 % and ~ 40.94 % of pDNA respectively. However, the release kinetics of protein showed opposite trends to pDNA in the first 10 days – formulations prepared with 20 % v/v pDNA/MPS exhibited a higher initial burst rate (~ 20.84 %) in 5 days compared to 10 %v/v and 5 %v/v. This is because more MPS have precipitated at the microsphere surface as discussed in the previous section. After day 10, the protein release profiles were similar to the release profiles of pDNA, which largely depends on the size distribution and surface area as mentioned above. Nevertheless, the delivery profiles of pDNA and protein when encapsulated individually in microspheres do not show significant differences (data not shown). pH of the supernatant collected throughout the *in vitro* release studies were around ~ 6 – 7, which do not showed high acidic condition.

One of the challenges in developing an effective delivery system is to retain bioactivity of the biopharmaceuticals by protecting them during all of the processing stages. It is necessary for pDNA and protein to be formulated in such a manner that it can be administered and it can remain stable for long periods of time. The integrities of pDNA and protein were studied at the end of *in vitro* studies. As shown in Figure 10, the pDNA retained a supercoiled conformation (~ 70.8 %) after being released from the composite microspheres. The feedstock pDNA was 91.5 % supercoiled before encapsulation. In addition, the electropherogram (Figure 11) obtained from the automated electrophoresis gel revealed no obvious differences in the conformation and

size (kDa) of BSA between the feedstock and after the delivery experiments. The percentage of dimers observed was < 4.5 % of the total, and this indicates that the protein structure remained predominantly intact upon desorption from the MPS in composite microspheres.

4. Conclusions

The development of dual-concentric-feeding ultrasonic atomization has allowed the production of composite microspheres to efficiently encapsulate a prime-boost vaccine in a single formulation. PLGA-mesoporous silica composite microspheres containing plasmid DNA and protein in different segments can be prepared with various particle sizes by changing the feedstock composition and processing parameters during the microsphere preparation. Characterisation of the microspheres showed that the volumetric ratio of pDNA/MPS to PLGA at 10 %v/v display a high encapsulation efficiency (96 % - 98 %) for pDNA while being encapsulated in 1.0 %w/v and 2.0 %w/v of PLGA. ANOVA analysis indicated that polymer concentrations, volumetric ratios and feed flowrates during microsphere preparation have statistically significant effects on the sizes of microspheres (D[4,3]). The *in vitro* release profiles obtained within 40 days showed pDNA and protein have different release kinetics. Protein appeared to follow the quasi-zero order release kinetics with a minimal initial burst rate. These release profiles showed an effective way to enhance immune responses by having a heterologous prime-boost immunisation strategy. The dual-concentric-feeding ultrasonic atomization method displayed simplicity, reproducibility, suitability for aseptic processing and convenience for scale-up. However, notable limitations remain, especially in controlling precipitation of MPS at the microsphere surface and

reproducible delivery rates of different antigens. Further work on the mechanism of prime-boost vaccines in one formulation will enable the creation of a vaccine delivery platform to combat a host of current and emerging infectious diseases.

Acknowledgments

G.M.F thanks the Victorian Endowment for Science, Knowledge and Innovation (VESKI) for the Innovation Fellowship and their support on this research. H.W thanks the Australian Research Council for the QEII fellowship. J.H gratefully acknowledges the financial support from the Monash University Research Graduate Scholarship. Lastly, the technical assistance from Dr. Tim Williams at the Monash Centre for Electron Microscopy is gratefully appreciated.

References

[1] J.B. Ulmer, J.C. Sadoff, M.A. Liu, DNA vaccines, Curr. Opin. Immunol. 8(4) (1996) 531-536.

[2] P. Moingeon, C. de Taisne, J. Almond, Delivery technologies for human vaccines, Br. Med. Bull. 62 (2002) 29-44.

[3] R.D. Weeratna, M.J. McCluskie, L. Comanita, T. Wu, H.L. Davis, Optimization strategies for DNA vaccines, Intervirology 43(4-6) (2000) 218-226.

[4] I.A. Ramshaw, A.J. Ramsay, The prime-boost strategy: exciting prospects for improved vaccination, Immunology Today 21(4) (2000) 163-165.

[5] S. Manoj, L.A. Babiuk, S.V. Littel-van den Hurk, Approaches to enhance the efficacy of DNA vaccines, Crit. Rev. Clin. Lab. Sci. 41(1) (2004) 1-39.

[6] Z.H. Chen, X. Guo, X.N. Ge, H. Jia, H.C. Yang, DNA priming and killed virus boosting vaccination strategy can augment the immune response to pseudorabies virus, Acta Virol. 51(3) (2007) 163-170.

[7] M.K. Hsieh, C.C. Wu, T.L. Lin, Priming with DNA vaccine and boosting with killed vaccine conferring protection of chickens against infectious bursal disease, Vaccine 25(29) (2007) 5417-5427.

[8] M. Sedegah, R. Hedstrom, P. Hobart, S.L. Hoffman, Protection against malaria by immunisation with plasmid DNA encoding circumsporozoite protien, Proc. Natl. Acad. Sci. U. S. A. 91(21) (1994) 9866-9870.

[9] J. Schneider, S.C. Gilbert, T.J. Blanchard, T. Hanke, K.J. Robson, C.M. Hannan, M. Becker, R. Sinden, G.L. Smith, A.V.S. Hill, Enhanced immunogenicity for CD8+ T cell induction and complete protective efficacy of malaria DNA

vaccination by boosting with modified vaccinia virus Ankara, Nat. Med. 4(4) (1998) 397-402.

[10] J. Schneider, S.C. Gilbert, C.M. Hannan, P. Degano, E. Prieur, E.G. Sheu, M. Plebanski, A.V.S. Hill, Induction of CD8(+) T cells using heterologous prime-boost immunisation strategies, Immunol. Rev. 170 (1999) 29-38.

[11] H.O. Alpar, V.W. Bramwell, Current status of DNA vaccines and their route of administration, Crit. Rev. Ther. Drug Carr. Syst. 19(4-5) (2002) 307-383.

[12] V.W. Bramwell, Y. Perrie, Particulate delivery systems for vaccines, Crit. Rev. Ther. Drug Carr. Syst. 22(2) (2005) 151-214.

[13] J.H. Hamman, G.M. Enslin, A.F. Kotze, Oral delivery of peptide drugs - Barriers and developments, Biodrugs 19(3) (2005) 165-177.

[14] D. Luo, W.M. Saltzman, Nonviral gene delivery - Thinking of silica, Gene Ther. 13(7) (2006) 585-586.

[15] C. Kneuer, M. Sameti, U. Bakowsky, T. Schiestel, H. Schirra, H. Schmidt, C.M. Lehr, A nonviral DNA delivery system based on surface modified silica-nanoparticles can efficiently transfect cells in vitro, Bioconjugate Chem. 11(6) (2000) 926-932.

[16] C. Kneuer, M. Sameti, E.G. Haltner, T. Schiestel, H. Schirra, H. Schmidt, C.M. Lehr, Silica nanoparticles modified with aminosilanes as carriers for plasmid DNA, Int. J. Pharm. 196(2) (2000) 257-261.

[17] D.Y. Zhao, J.L. Feng, Q.S. Huo, N. Melosh, G.H. Fredrickson, B.F. Chmelka, G.D. Stucky, Triblock copolymer syntheses of mesoporous silica with periodic 50 to 300 angstrom pores, Science 279(5350) (1998) 548-552.

[18] J. Ho, W. Zhu, H. Wang, G.M. Forde, Mesoporous silica spheres from colloids, J. Colloid Interface Sci. 308(2) (2007) 374-380.

[19] J.M. Xue, M. Shi, PLGA/mesoporous silica hybrid structure for controlled drug release, J. Control. Release 98(2) (2004) 209-217.

[20] I.J. Castellanos, K.G. Carrasquillo, J.D. Lopez, M. Alvarez, K. Griebenow, Encapsulation of bovine serum albumin in poly(lactide-co-glycolide) microspheres by the solid-in-oil-in-water technique, J. Pharm. Pharmacol. 53(2) (2001) 167-178.

[21] S. Freitas, H.P. Merkle, B. Gander, Microencapsulation by solvent extraction/evaporation: reviewing the state of the art of microsphere preparation process technology, J. Control. Release 102(2) (2005) 313-332.

[22] S. Freitas, H.P. Merkle, B. Gander, Ultrasonic atomisation into reduced pressure atmosphere - envisaging aseptic spray-drying for microencapsulation, J. Control. Release 95(2) (2004) 185-195.

[23] C.B. Felder, M.J. Blanco-Prieto, J. Heizmann, H.P. Merkle, B. Gander, Ultrasonic atomization and subsequent polymer desolvation for peptide and protein microencapsulation into biodegradable polyesters, J. Microencapsul. 20(5) (2003) 553-567.

[24] G.M. Forde, A.D. Coomes, F.K. Giliam, M.J. Horsfall, Creation of protein loaded biodegradable microparticles via ultrasonic atomization suitable for nasal delivery, Chem. Eng. Res. Des. 84(A3) (2006) 178-184.

[25] G.M. Forde, J. Friend, T. Williamson, Straightforward biodegradable nanoparticle generation through megahertz-order ultrasonic atomization, Appl. Phys. Lett. 89(6) (2006) 3.

[26] J. Ho, H.T. Wang, G.M. Forde, Process considerations related to the microencapsulation of plasmid DNA via ultrasonic atomization, Biotechnology and Bioengineering 101(1) (2008) 172 -181.

[27] J. Ho, M.K. Danquah, H.T. Wang, G.M. Forde, Protein loaded mesoporous silica spheres as a controlled delivery platform, J. Chem. Technol. Biotechnol. 83(3) (2008) 351-358.

[28] U. Lungwitz, M. Breunig, T. Blunk, A. Gopferich, Polyethylenimine-based non-viral gene delivery systems, Eur. J. Pharm. Biopharm. 60(2) (2005) 247-266.

[29] M. Bivas-Benita, S. Romeijn, H.E. Junginger, G. Borchard, PLGA-PEI nanoparticles for gene delivery to pulmonary epithelium, Eur. J. Pharm. Biopharm. 58(1) (2004) 1-6.

[30] B. Avvaru, M.N. Patil, P.R. Gogate, A.B. Pandit, Ultrasonic atomization: Effect of liquid phase properties, Ultrasonics 44(2) (2006) 146-158.

[31] R. Bellman, R.H. Pennington, Effects of surface tension and viscosity on Taylor instability, Q. Appl. Math. 12(2) (1954) 151-162.

[32] G. De Rosa, F. Quaglia, M.I. La Rotonda, M. Appel, H. Alphandary, E. Fattal, Poly(lactide-co-glycolide) microspheres for the controlled release of oligonucleotide/polyethylenimine complexes, J. Pharm. Sci. 91(3) (2002) 790-799.

Table I: The effect of formulation variables on the mean diameters (D[4,3]) and *span* of the composite microspheres

Theoretical ratio of pDNA-MPS : PLGA (% v/v) [a]	**Volumetric flowrate PLGA (ml h^{-1})**	**Volumetric flowrate pDNA-MPS (ml h^{-1})**	**Mean diameter, D[4,3] (µm)**	**Span**
5	18.0	0.9	6.64 ± 0.38	0.78 ± 0.12
10	18.0	1.8	17.86 ± 0.85	1.88 ± 0.33
20	18.0	3.6	30.92 ± 1.58	4.30 ± 0.68
5	36.0	1.8	7.78 ± 0.62	1.09 ± 0.34
10	36.0	3.6	19.25 ± 1.65	2.30 ± 0.46
20	36.0	7.2	38.27 ± 2.04	4.56 ± 0.88

Values are given as mean of three composite microspheres batches (n = 3). The standard deviation of the D[4,3] and *span* are the deviation values respectively from triplicate microspheres batches.

[a] The formulations were prepared with 1.0% w/v PLGA in acetone and consist of 100 pDNA-PEI : 10 MPS (w/w); and atomized through a 40 kHz ultrasonic atomizer. The plasmid DNA were condensed at N/P = 10.

Table II: The correlation coefficients by fitting a linear line of best fit to the overall 40 days release profiles of protein in the *in vitro* studies. The composite microspheres were prepared with different polymer concentration.

Sample	**Correlation coefficient**
1.0 % w/v	0.9949 ± 0.0035
2.0 % w/v	0.9942 ± 0.0042
3.0 % w/v	0.9854 ± 0.0065

Values are given as mean of three composite microspheres batches (n = 3). The formulations consist of 10 pDNA/MPS : 100 PLGA (10 %v/v); and the weight ratios are 100 pDNA-PEI : 5 MPS (w/w).

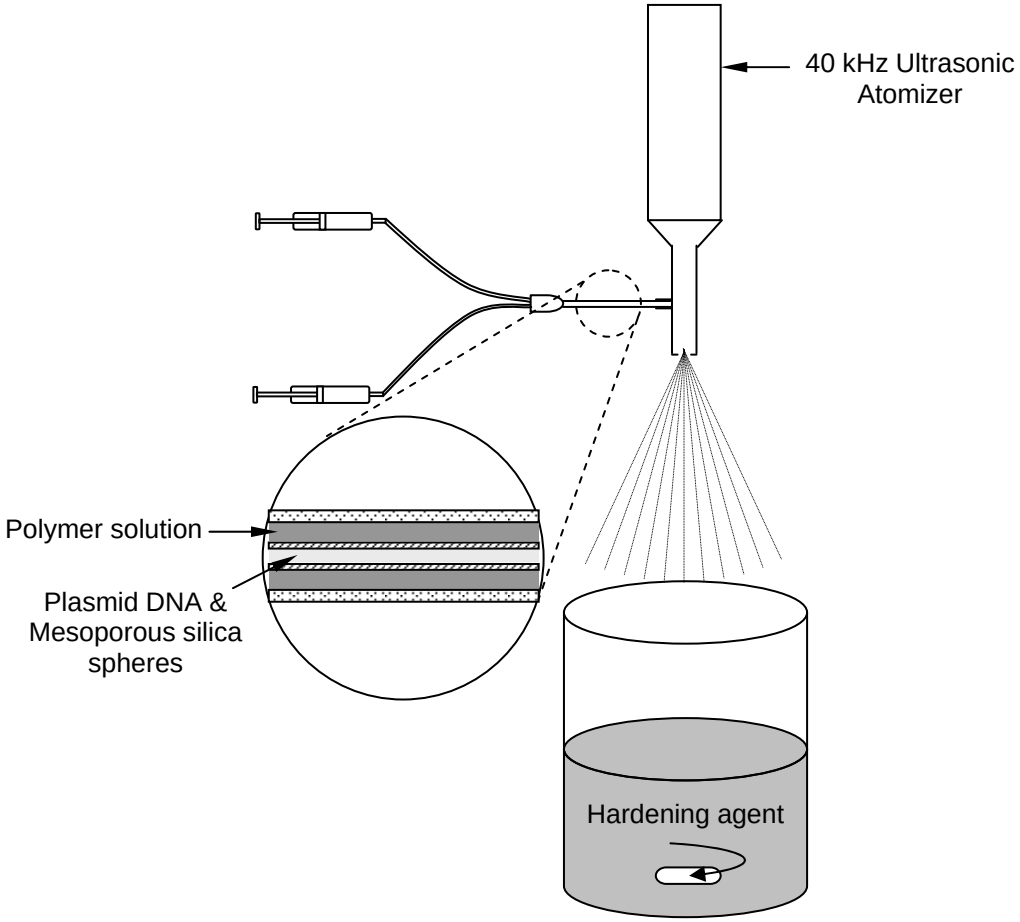

Fig. 1. Schematic illustration of setting for dual-concentric needles, which are feeding polymer solution and pDNA/MPS to a 40 kHz ultrasonic atomizer, to synthesise PLGA-mesoporous silica spheres composite microspheres.

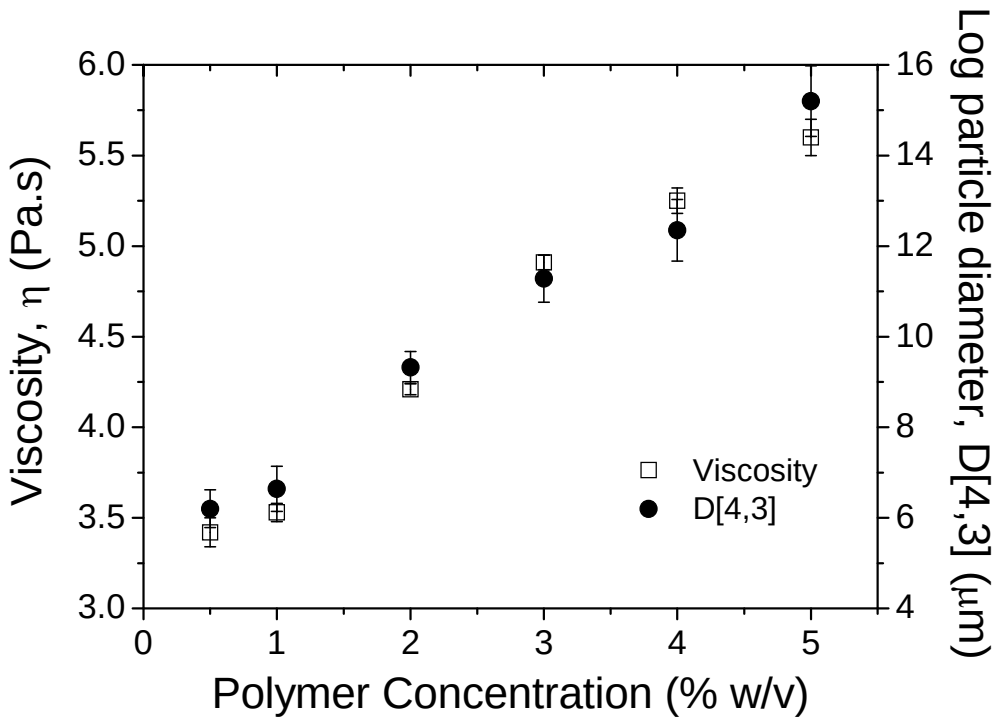

Fig. 2. Polymer concentration of PLGA 50:50 in acetone with respect to viscosity and the resulted volume-weighted mean diameter (D[4,3]) of composite microspheres (5 pDNA/MPS : 100 PLGA v/v). The composite microspheres within the size range being obtained (6 – 16 μm) could possibly be used for nasal cavity delivery of biomolecules.

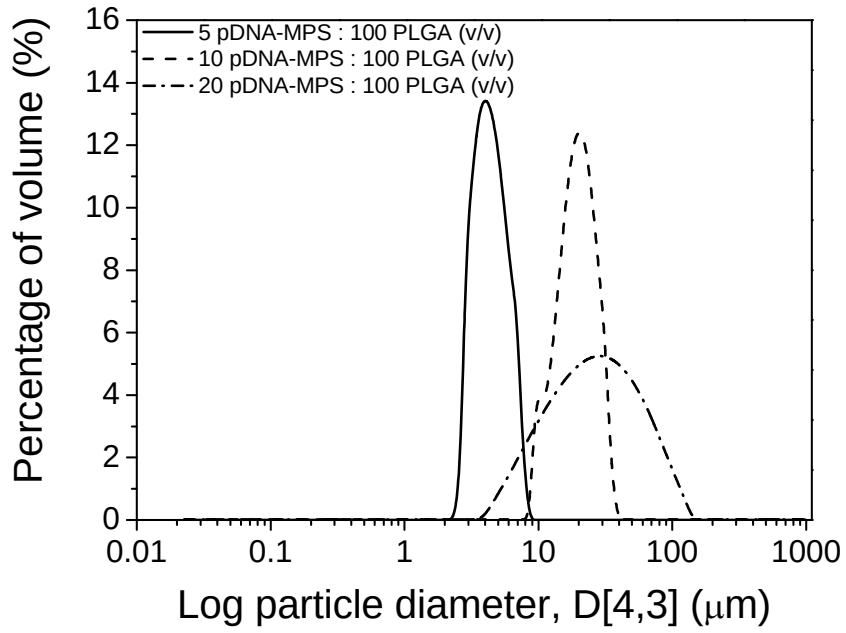

Fig. 3. Size distributions for 1 %w/v PLGA in acetone , which were pumped through a 40 kHz ultrasonic atomizer at 18 ml h^{-1} and consist of 100 pDNA-PEI: 5 MPS (w/w) at different volumetric ratios (n = 3).

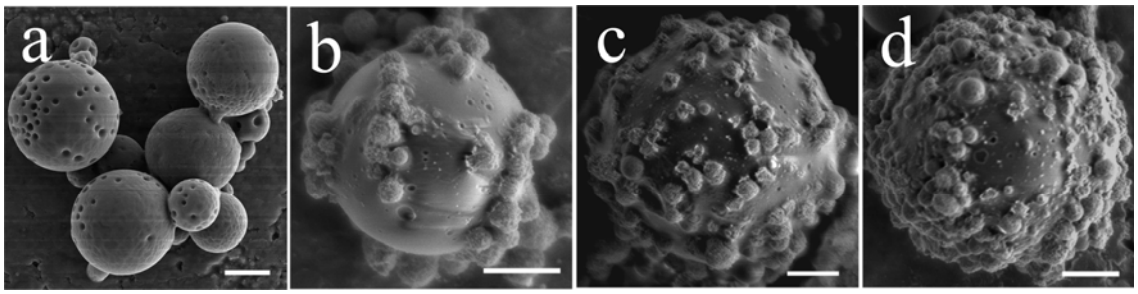

Fig. 4. SEM images of microspheres containing pDNA/MPS at several volumetric ratios in 1 % w/v PLGA with 100 pDNA-PEI: 5 MPS (w/w), where (a) is only pDNA; (b) is 5 %v/v {5 pDNA/MPS : 100 PLGA v/v}; (c) is 10 %v/v; and (d) is 20 %v/v. pDNA-PEI complexes were prepared at N/P = 5. Scale bar = 2.5 μm.

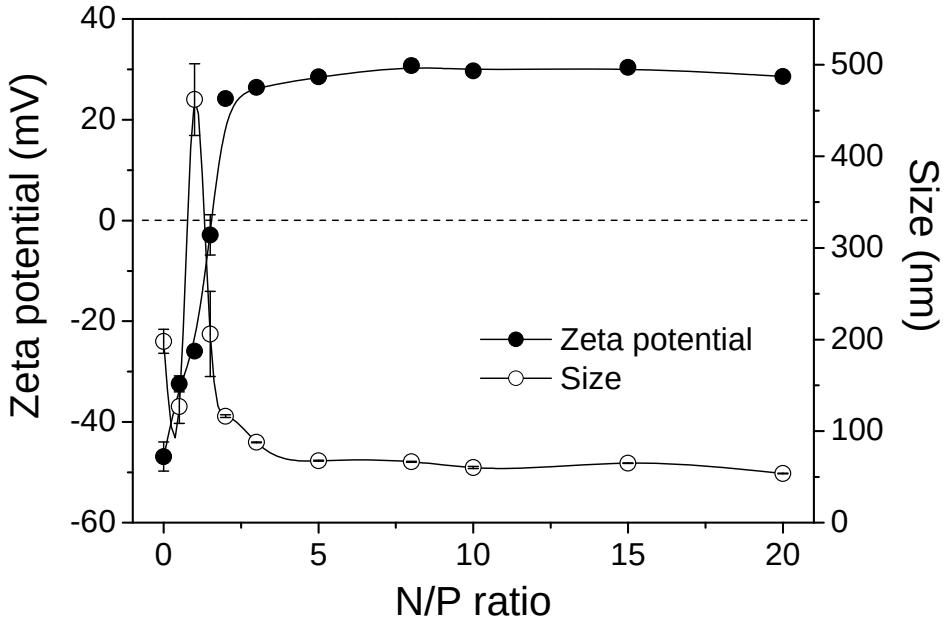

Fig. 5. The influence of N/P ratio on the hydrodynamic diameter and zeta potential of pDNA-PEI complexes (n =3).

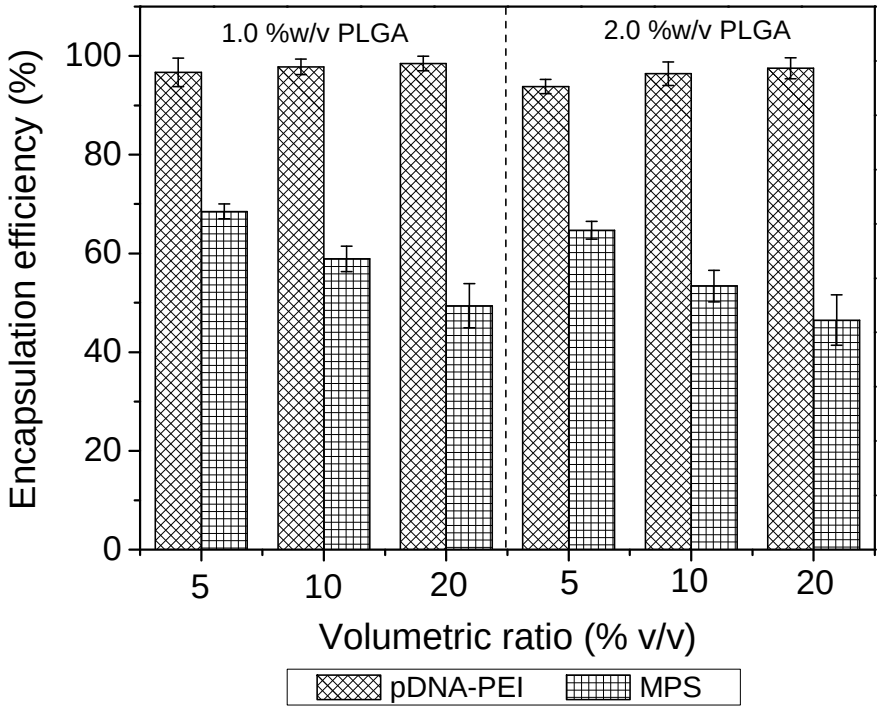

Fig. 6. Encapsulation efficiencies of 1.0 %w/v and 2.0 %w/v PLGA in acetone, which were pumped through the ultrasonic atomizer at 18 ml h^{-1}, with several volumetric ratios of pDNA/MPS. The results are the mean of three experiments ± SD (standard deviation).

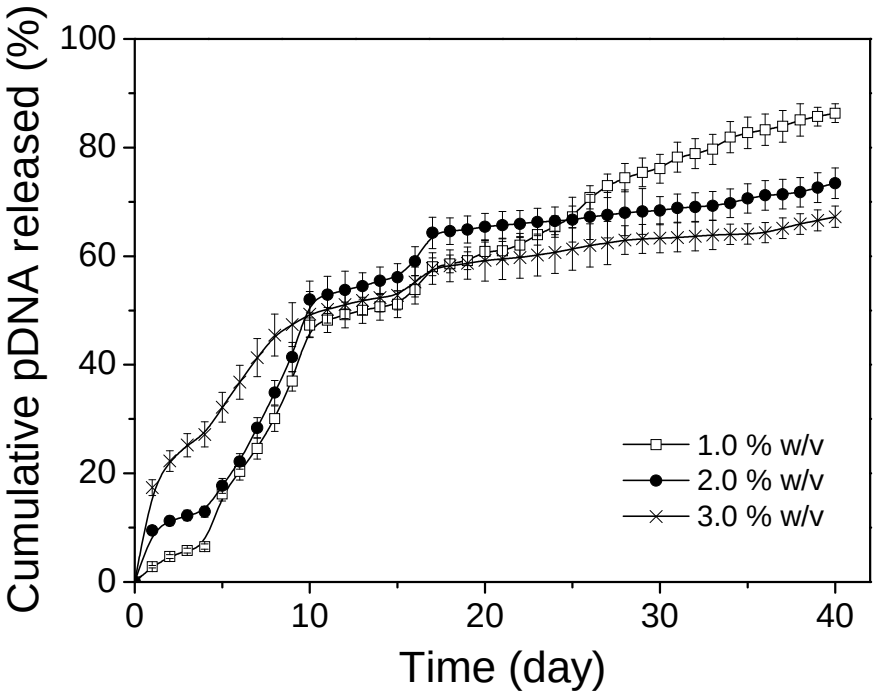

Fig. 7. The delivery profiles of pDNA-PEI complexes (N/P = 10) *in vitro* under physiological conditions (PBS buffer, pH 7.4, 37°C, 200 rpm) from composite microspheres, which have different polymer concentrations, and volumetric ratios of 10 %v/v pDNA/MPS, n = 3.

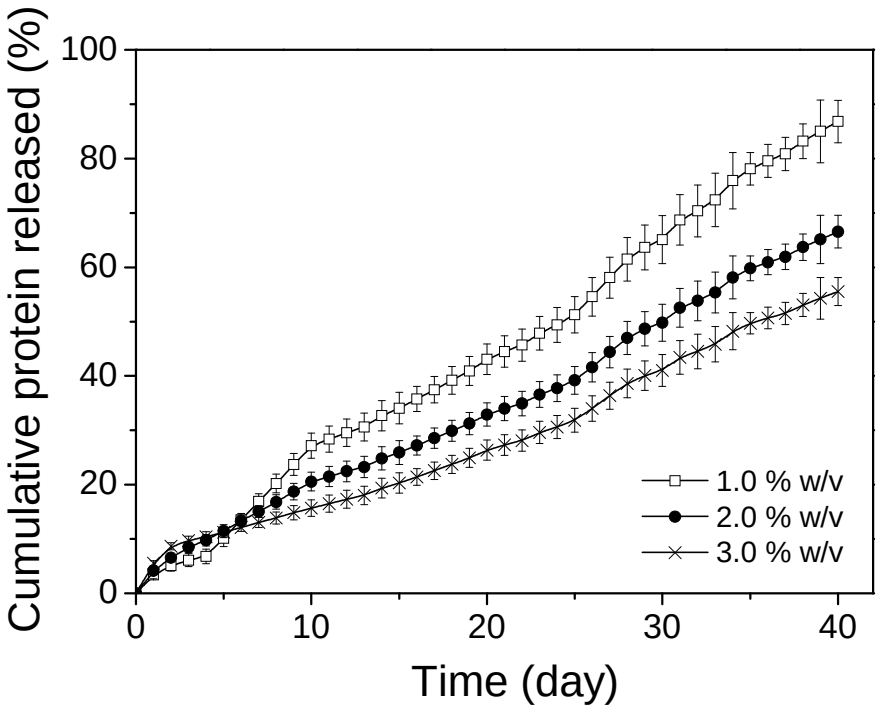

Fig. 8. *In vitro* (PBS buffer, pH 7.4, 37°C, 200 rpm) delivery profiles of protein adsorbed to MPS and encapsulated in composite microspheres. The delivery of microspheres with a volumetric ratio of 10 %v/v pDNA/MPS but different polymer concentrations is shown (n = 3).

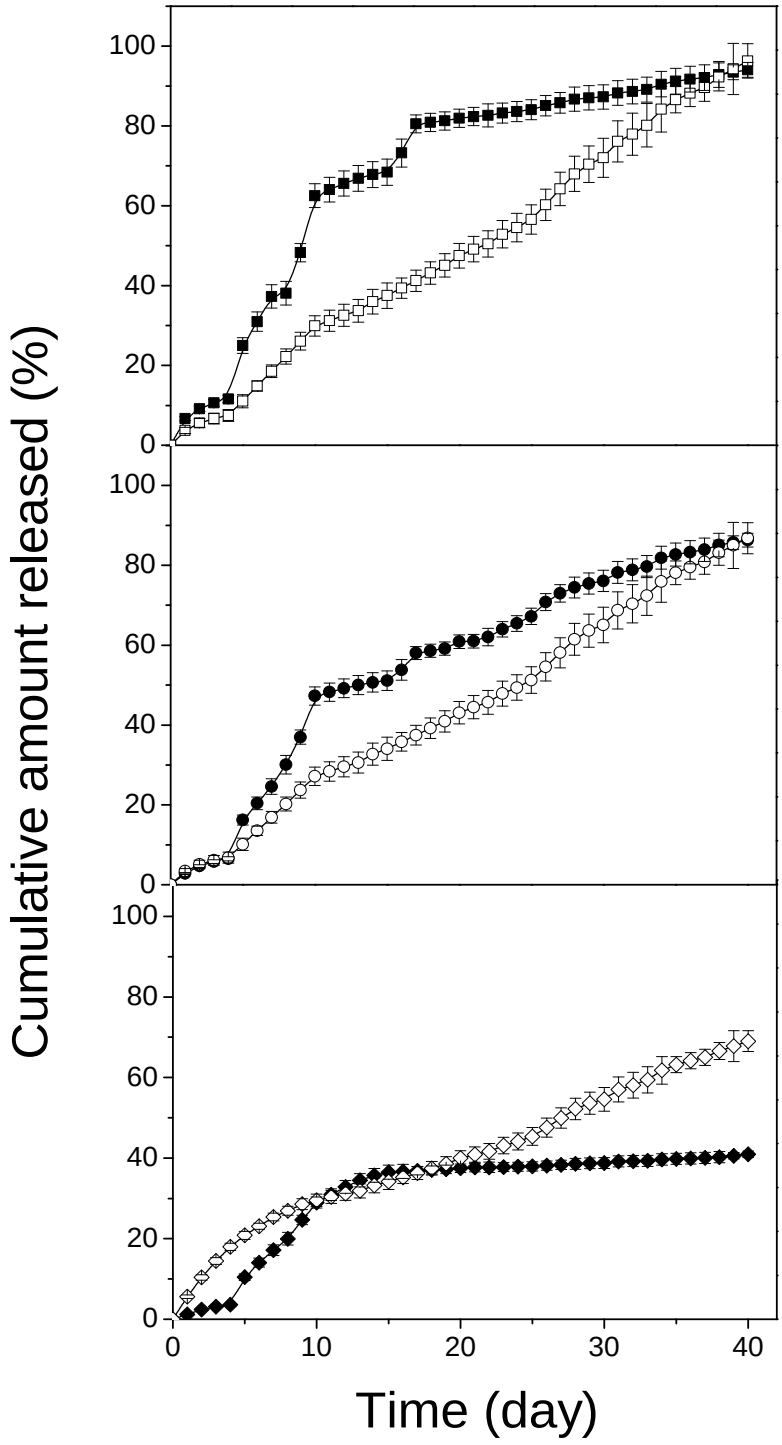

Fig. 9. Comparison of delivery profiles for composite microspheres containing pDNA-PEI complexes (solid) and protein (open) at several volumetric ratios of 1 % w/v PLGA and (a) 5 %; (b) 10 %; and (c) 20 % v/v pDNA/MPS (n = 3). A mass ratio of 100 pDNA-PEI : 5 MPS (w/w) was used throughout.

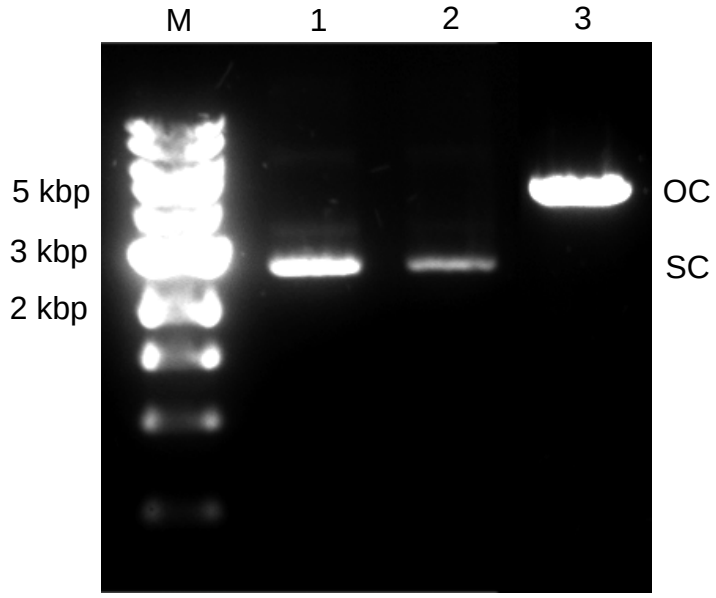

Fig. 10. Result of ethidium bromide agarose gel electrophoresis for the assessment of the pDNA structural integrity. Analysis was performed using 0.8 % agarose in TAE 1x buffer and 3 μg ml^{-1} EtBr at 60 V for 90 min. Lane M: 1 kbp DNA ladder; lane 1: 0.5 μg pDNA; lane 2: pDNA recovered from *in vitro* release studies; lane 3: lineraized pDNA obtained from 4 hours and 37 °C digestion study with EcoRI (BioLabs, New England). The intensity of the pDNA band in lane 2 is due to dilution caused by the release studies.

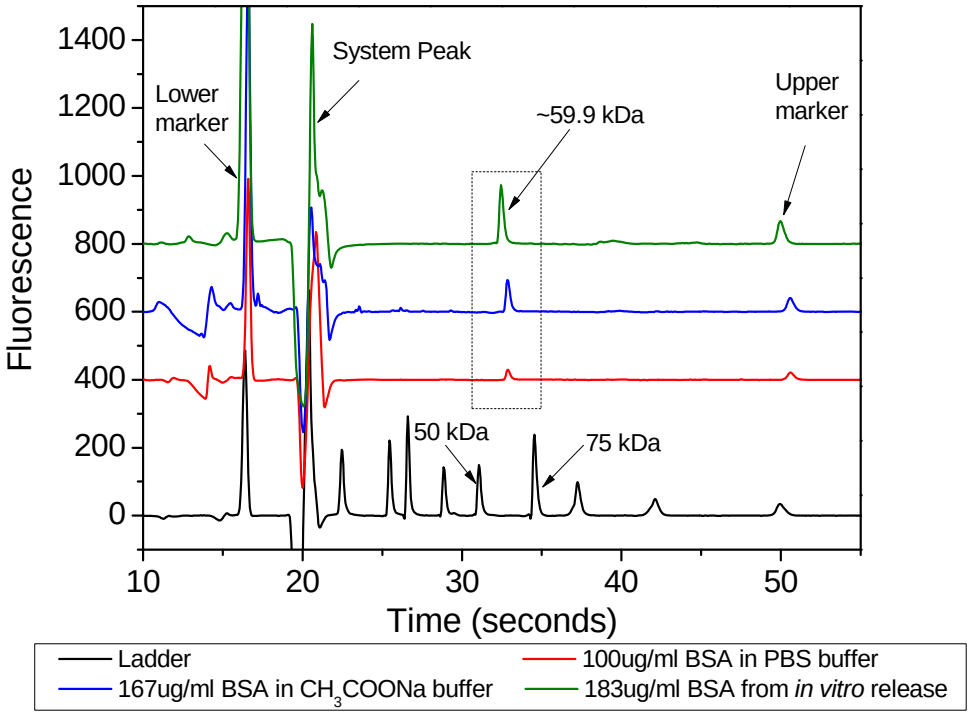

Fig. 11. Electropherogram obtained from automated electrophoresis gel shows the fluorescence intensity versus time for BSA.

CHAPTER SIX

CONCLUSIONS AND RECOMMENDATIONS FOR FUTURE WORK

6.1 Conclusions

In this research, a novel technique has been developed for the creation of an innovative mesoporous silica-biodegradable polymer based particulate system for intranasal administration of a pDNA prime-protein boost controlled delivery vaccine. The development of this technique has entailed the development of novel and scalable methods for synthesising new mesoporous material for bio-application and for encapsulating pDNA molecules into polymer microspheres. Results from the analysis of physiochemical parameters such as particle size, morphology, zeta potential, encapsulation/loading efficiency and *in vitro* release kinetics have proven the effectiveness of this delivery system.

The major outcomes of the body of research reported in this thesis can be summarized as follows.

1. An innovative synthesis method utilising silica colloids to create mesoporous silica spheres with diameters ranging from 0.5 to 1.6 μm has been developed offering the following features:
    - Greater flexibility in tailoring the pore size of mesoporous silica spheres from 14.1 to 28.8 nm by changing the size of precursor nanoparticles in colloids, and the concentration and type of electrolyte.
    - A scalable and cost effective method for producing mesoporous silica spheres with pore sizes not limited by the molecular size of the organic template.

- Flexibility in tailoring the pore size of the mesoporous silica spheres, which enables the loading of different therapeutic biomolecules; thereby, boosting the viability and versatility of particulate medicine.

2. A continuous and real-time adsorption measurement method for achieving optimum binding of biomolecules to mesoporous silica spheres has been developed. Specifically, it exhibit following advantages:
   - The mesoporous silica spheres demonstrated a high dynamic adsorption capacity of 71.43 mg ml^{-1} for protein based molecules.
   - The method is an effective, scalable and continuous method for large-scale protein adsorption, because it minimises the errors associated with mixing and washing in batch mode.
   - The enhanced loading capacity obtained opens up an opportunity to create a new biomaterial with pore sizes tailored for the delivery of specific biomolecules and leads to a reduced manufacturing cost via use of a more effective and efficient method.

3. A microencapsulation method to create an improved controlled delivery system for pDNA has been developed with the following characteristics:
   - This ultrasonic atomization system is an efficient and holistic approach to microencapsulate pDNA into biodegradable polymer.
   - Polymer microspheres obtained have highly reproducible and narrow size distributions, and are in the size range that makes them suitable for intranasal vaccination.
   - Process synthesis parameters such as polymer concentration, feed flowrate, volumetric ratio, and nitrogen to phosphorous ratio can be

easily monitored and controlled during the ultrasonic atomization to produce ideal polymer microspheres.

- This method achieves high encapsulation efficiency for pDNA and this characteristic is an important factor for commercial viability. This high-throughput method has comparatively higher encapsulation efficiencies and yield than previously reported technologies [78-80].
- This method enables the rapid production of large quantities of polymer microspheres to be used as pDNA vaccines carriers and in gene therapy. This new method has the potential to address major problems associated with pDNA vaccines encapsulation and its associated release from polymer microspheres. Comparing to previous study results [81], the smaller microsphere sizes obtained indicates that they are favourable for intranasal delivery whilst maintaining the supercoil structure of pDNA.
- The release kinetics and integrity of pDNA attained in this encapsulation method lay the foundation for creation of encapsulated vaccines suitable for commercial applications.

4. A technique for synthesising a composite microsphere, which is composed of mesoporous silica spheres and biodegradable polymer, has been developed. The following conclusions are drawn.
   - This ultrasonic atomization system coupled with a dual-concentric-feeding approach proved exceptionally functional in developing polymer microspheres with desired size distributions and tailored characteristics.
   - This is an effective technique to synthesise delivery system that enhance immune responses by facilitating different delivery regimes between the pDNA prime and protein boost through the advanced particle design.

- This fabrication technique is simple, and it is suitable for aseptic processing and convenient for scaling-up.

The scientific insights achieved in this study enhance the current understanding of biomolecule delivery systems, particularly for pDNA delivery. The preclinical-scale novel delivery technologies presented in this research represent a platform to achieve the ultimate goal of an economically viable method for the production of genetic vaccination and therapy formulations. Scale-up considerations show that this current Good Manufacturing Practices (cGMP) compatible technique can easily be advanced to a commercial scale. The use of high-throughput systems for production of newer delivery systems will also provide a tremendous impetus in developing newer potent vaccines with specific features and improved efficacy. In conclusion, this study reveals the great potential of inorganic-biodegradable polymer composite microspheres for administrating a heterologous prime-boost vaccine via the use of a single dose. The easy, safe and cheap vaccination technique described would represent a major breakthrough for global vaccination programs, especially for areas with limited medical services.

6.2 Recommendations for future work

New materials and delivery approaches for pDNA vaccines are being developed to not only improve the safety, acceptability, efficacy and ease of use of these vaccines but also reduce cost by administrating smaller doses. Such techniques enable the rapid development of plasmid-based products, both as prophylactic vaccines and immunotherapies. The transition of these plasmid-based molecules into vaccines to combat infectious diseases is still in its infancy, but offers considerable potential for

effective vaccination with the development of novel delivery platforms that prevent their degradation and increase their potency. However, the commercial application of a prime-boost vaccine in a single formulation will rely on overcoming several challenges. Outlined below, are the future research areas that should be considered.

- The chemical functionalisation of mesoporous silica spheres could be investigated for conjugation of protein molecules. Though partly covered in this study (as shown in appendix A), a detailed and optimised study of the thiol-hydroxyl conjugation between protein and mesoporous silica spheres would ideally result in a better-controlled release profile for protein. This immobilisation through thiol-hydroxyl conjugation is stable, and protein can be delivered under physiological condition via the *in vivo* enzymatic hydrolysis of the sulphur-sulphur bridge between the silica surface and the protein. However, there are issues with the scalability and commercial viability of this method, mainly due to the cost of thiol-disulphide exchange coupling reagents. In addition, the direct linking of protein molecules onto the mesoporous silica surface may lead to a decrease in biological activity if the thiol group is present within an active region. Thus, for the production of a commercially viable delivery platform for conjugated protein, this thiol-hydroxyl conjugation requires further development.

- The heterologous prime-boost immunization strategy in a single formulation could be further optimised; in particular, the delivery rates of different antigens need to be tailored in order to achieve staged delivery of antigens within a specific time span, or to meet specific timing or rate of delivery goals for specific applications (e.g. malaria DNA vaccine). Further to this, it may be

desirable to have a much more immediate pDNA prime that occurs over a shorter period coupled with a longer delay before the protein boost occurs. This would also help the development of systematic depot administration of vaccines. The goal of this local release system in the targeted site would be to maintain the plasma concentration of vaccine in the desired range with just a single dose; to localise delivery of the vaccine to a particular body compartment; to reduce the need for follow-up care; and to increase patient comfort or improve compliance.

- The performance of inorganic-biodegradable polymer composite microspheres developed in this study has been tested under *in vitro* physiological conditions and shown to be promising. However, before further scale-up to commercial applications and clinical trials, *in vivo* immunisations need to be investigated. The initial stage would be an *ex vivo* cell line transfection and this is follow by instillation into the nostrils of rodents. Such a study would provide information for the manipulation and optimisation of the production of inorganic-biodegradable polymer composite microspheres.

- There are several problems associated with PLGA microspheres such as low glass transition temperature (T_g), the relatively hydrophobic interface and the production of acidic degradation products. To circumvent these problems, further research into blending the PLGA with more amorphous polymers, such as polyethylene glycol (PEG) could be investigated. It has been claimed that PEG has a mucoadhesion promoting effect and that it is able to increase the stability of antigens on the nasal mucosa [82]. In addition, PEG also improves

the release rate of the encapsulated antigens and serves to protect the antigens from degrading polymer products and proteases [83].

- Functional moieties such as peptides or antibodies could also be incorporated into the composite microspheres for tissue targeting purposes or for altering *in vivo* behaviour of composite microspheres. For example, site directed microspheres with a coating or immobilised ligands (antigens, antibodies, monoclonal antibodies) could be used to target specific sites of disease or tissues.

REFERENCES

[1] R.G. Webster, H.L. Robinson, DNA vaccines - A review of developments, Biodrugs 8(4) (1997) 273-292.

[2] M.A. Liu, DNA vaccines: a review, J. Intern. Med. 253(4) (2003) 402-410.

[3] WHO, The World Health Report 2004: changing history. in: R. Beaglehole (Ed.), Vol. 2006, WHO, 2004.

[4] J.J. Donnelly, J.B. Ulmer, J.W. Shiver, M.A. Liu, DNA vaccines, Annu. Rev. Immunol. 15 (1997) 617-648.

[5] D. Luo, W.M. Saltzman, Synthetic DNA delivery systems, Nat. Biotechnol. 18(1) (2000) 33-37.

[6] J.A. Wolff, R.W. Malone, P. Williams, W. Chong, G. Acsadi, A. Jani, P.L. Felgner, Direct gene-transfer into mouse muscle in vivo, Science 247(4949) (1990) 1465-1468.

[7] J.B. Ulmer, J.J. Donnelly, S.E. Parker, G.H. Rhodes, P.L. Felgner, V.J. Dwarki, S.H. Gromkowski, R.R. Deck, C.M. Dewitt, A. Friedman, L.A. Hawe, K.R. Leander, D. Martinez, H.C. Perry, J.W. Shiver, D.L. Montgomery, M.A. Liu, Heterologous protection against influenza by injection of DNA encoding a viral protein, Science 259(5102) (1993) 1745-1749.

[8] A. Bouchie, In Brief, Nat. Biotechnol. 21(1) (2003) 9-11.

[9] R.J. Drape, M.D. Macklin, L.J. Barr, S. Jones, J.R. Haynes, H.J. Dean, Epidermal DNA vaccine for influenza is immunogenic in humans, Vaccine 24(21) (2006) 4475-4481.

[10] G.M. Forde, Rapid-response vaccines - does DNA offer a solution?, Nat. Biotechnol. 23(9) (2005) 1059-1062.

[11] M.A. Liu, B. Wahren, G.B.K. Hedestam, DNA vaccines: Recent developments and future possibilities, Hum. Gene Ther. 17(11) (2006) 1051-1061.

[12] R.R. Sinden, DNA structure and function, Academic Press, San Diego, 1994.

[13] D.L. Montgomery, J.B. Ulmer, J.J. Donnelly, M.A. Liu, DNA vaccines, Pharmacol. Ther. 74(2) (1997) 195-205.

[14] M.A. Liu, J.B. Ulmer, Advances in Genetics, Vol. 55, Elsevier Academic Press Inc, San Diego, 2005, pp. 25-40.

[15] J.R. Greenland, N.L. Letvin, Chemical adjuvants for plasmid DNA vaccines, 25(19) (2007) 3731-3741.

[16] F.D. Ledley, Pharmaceutical approach to somatic gene therapy, Pharm. Res. 13(11) (1996) 1595-1614.

[17] S.D. Patil, D.G. Rhodes, D.J. Burgess, DNA-based therapeutics and DNA delivery systems: A comprehensive review, AAPS Journal 7(1) (2005) E61-E77.

[18] A.R. Thierry, E. Vives, J.P. Richard, P. Prevot, C. Martinand-Mari, I. Robbins, B. Lebleu, Cellular uptake and intracellular fate of antisense oligonucleotides, Curr. Opin. Mol. Ther. 5(2) (2003) 133-138.

[19] J.J. Donnelly, J.B. Ulmer, M.A. Liu, DNA vaccines, Life Sci. 60(3) (1996) 163-172.

[20] M.N.V.R. Kumar, U. Bakowsky, C.-M. Lehr, in: C. M. Niemeyer and C. A. Mirkin (Eds.), Nanobiotechnology: Concepts, Applications and Perspectives, Wiley-VCH, British, 2004, pp. 319-342.

[21] D. Luo, Nanotechnology and DNA delivery, MRS Bull. 30(9) (2005) 654-658.

[22] M. Dupuis, K. Denis-Mize, C. Woo, C. Goldbeck, M.J. Selby, M.C. Chen, G.R. Otten, J.B. Ulmer, J.J. Donnelly, G. Ott, D.M. McDonald, Distribution of DNA vaccines determines their immunogenicity after intramuscular injection in mice, J. Immunol. 165(5) (2000) 2850-2858.

[23] Y.J.F. Hutin, R.T. Chen, Injection safety: a global challenge, Bull. World Health Organ. 77(10) (1999) 787-788.

[24] A. Battersby, R. Feilden, C. Nelson, Sterilizable syringes: excessive risk or cost-effective option?, Bull. World Health Organ. 77(10) (1999) 812-819.

[25] L. Simonsen, A. Kane, J. Lloyd, M. Zaffran, M. Kane, Unsafe injections in the developing world and transmission of bloodborne pathogens: a review, Bull. World Health Organ. 77(10) (1999) 789-800.

[26] A. Kane, J. Lloyd, M. Zaffran, L. Simonsen, M. Kane, Transmission of hepatitis B, hepatitis C and human immunodeficiency viruses through unsafe injections in the developing world: model-based regional estimates, Bull. World Health Organ. 77(10) (1999) 801-807.

[27] M.A. Miller, E. Pisani, The cost of unsafe injections, Bull. World Health Organ. 77(10) (1999) 808-811.

[28] S. Manoj, L.A. Babiuk, S. van Drunen Littel-van den Hurk, Approaches to enhance the efficacy of DNA vaccines, Crit. Rev. Clin. Lab. Sci. 41(1) (2004) 1-39.

[29] U.K. Griffiths, L. Botham, B.D. Schoub, The cost-effectiveness of alternative polio immunisation policies in South Africa, Vaccine 24(29-30) (2006) 5670-5678.

[30] J.E. Herrmann, DNA vaccines against enteric infections, Vaccine 24(18) (2006) 3705-3708.

[31] S.A. Galindo-Rodriguez, E. Allemann, H. Fessi, E. Doelker, Polymeric nanoparticles for oral delivery of drugs and vaccines: A critical evaluation of in vivo studies, Crit. Rev. Ther. Drug Carr. Syst. 22(5) (2005) 419-463.

[32] R.B. MacGregor, R. Ginsberg, K.E. Ugen, Y. Baine, C.U. Kang, X.M. Tu, T. Higgins, D.B. Weiner, J.D. Boyer, T-cell responses induced in normal volunteers immunized with a DNA-based vaccine containing HIV-1 env and rev, Aids 16(16) (2002) 2137-2143.

[33] J. Schultz, G. Dollenmaier, K. Molling, Update on antiviral DNA vaccine research (1998-2000), Intervirology 43(4-6) (2000) 197-217.

[34] P. Moingeon, C. de Taisne, J. Almond, Delivery technologies for human vaccines, Br. Med. Bull. 62 (2002) 29-44.

[35] R.D. Weeratna, M.J. McCluskie, L. Comanita, T. Wu, H.L. Davis, Optimization strategies for DNA vaccines, Intervirology 43(4-6) (2000) 218-226.

[36] I.A. Ramshaw, A.J. Ramsay, The prime-boost strategy: exciting prospects for improved vaccination, Immunol. Today 21(4) (2000) 163-165.

[37] S. Manoj, L.A. Babiuk, S.V. Littel-van den Hurk, Approaches to enhance the efficacy of DNA vaccines, Crit. Rev. Clin. Lab. Sci. 41(1) (2004) 1-39.

[38] Z.H. Chen, X. Guo, X.N. Ge, H. Jia, H.C. Yang, DNA priming and killed virus boosting vaccination strategy can augment the immune response to pseudorabies virus, Acta Virol. 51(3) (2007) 163-170.

[39] M.K. Hsieh, C.C. Wu, T.L. Lin, Priming with DNA vaccine and boosting with killed vaccine conferring protection of chickens against infectious bursal disease, Vaccine 25(29) (2007) 5417-5427.

[40] M. Sedegah, R. Hedstrom, P. Hobart, S.L. Hoffman, Protection against malaria by immunisation with plasmid DNA encoding circumsporozoite protien, Proc. Natl. Acad. Sci. U. S. A. 91(21) (1994) 9866-9870.

[41] J. Schneider, S.C. Gilbert, T.J. Blanchard, T. Hanke, K.J. Robson, C.M. Hannan, M. Becker, R. Sinden, G.L. Smith, A.V.S. Hill, Enhanced immunogenicity for CD8+ T cell induction and complete protective efficacy of malaria DNA vaccination by boosting with modified vaccinia virus Ankara, Nat. Med. 4(4) (1998) 397-402.

[42] J. Schneider, S.C. Gilbert, C.M. Hannan, P. Degano, E. Prieur, E.G. Sheu, M. Plebanski, A.V.S. Hill, Induction of CD8(+) T cells using heterologous prime-boost immunisation strategies, Immunol. Rev. 170 (1999) 29-38.

[43] S.L. Epstein, W.P. Kong, J.A. Misplon, C.Y. Lo, T.M. Tumpey, L. Xu, G.J. Nabel, Protection against multiple influenza A subtypes by vaccination with highly conserved nucleoprotein, Vaccine 23(46-47) (2005) 5404-5410.

[44] P.C.Y. Woo, S.K.P. Lau, H.W. Tsoi, Z.W. Chen, B.H.L. Wong, L.Q. Zhang, J.K.H. Chan, L.P. Wong, W. He, C. Ma, K.H. Chan, D.D. Ho, K.Y. Yuen, SARS coronavirus spike polypeptide DNA vaccine priming with recombinant spike polypeptide from Escherichia coli as booster induces high titer of neutralizing antibody against SARS coronavirus, Vaccine 23(42) (2005) 4959-4968.

[45] M.K. Song, S.W. Lee, Y.S. Suh, K.J. Lee, Y.C.F. Sung, Enhancement of immunoglobulin G2A and cytotoxic T-lymphocyte responses by a booster immunisation with recombinant hepatitis C virus E2 protein in E2 DNA-primed mice, J. Virol. 74(6) (2000) 2920-2925.

[46] J.S. Lee, A.G. Hadjipanayis, M.D. Parker, Viral vectors for use in the development of biodefense vaccines, Adv. Drug Deliv. Rev. 57(9) (2005) 1293-1314.

[47] A.N. Zakhartchouk, Q. Liu, M. Petric, L.A. Babiuk, Augmentation of immune responses to SARS coronavirus by a combination of DNA and whole killed virus vaccines, Vaccine 23(35) (2005) 4385-4391.

[48] S.S. Davis, Nasal vaccines, Adv. Drug Deliv. Rev. 51(1-3) (2001) 21-42.

[49] P.N. Boyaka, A. Tafaro, R. Fischer, K. Fujihashi, E. Jirillo, J.R. McGhee, Therapeutic manipulation of the immune system: enhancement of innate and adaptive mucosal immunity, Curr. Pharm. Design 9(24) (2003) 1965-1972.

[50] C.D. Partidos, Intranasal vaccines: forthcoming challenges, 3(8) (2000) 273-281.

[51] C.F. Kuper, P.J. Koornstra, D.M.H. Hameleers, J. Biewenga, B.J. Spit, A.M. Duijvestijn, P. Vriesman, T. Sminia, The Role of Nasopharyngeal Lymphoid-Tissue, Immunol. Today 13(6) (1992) 219-224.

[52] S. Turker, E. Onur, Y. Ozer, Nasal route and drug delivery systems, Pharm. World Sci. 26(3) (2004) 137-142.

[53] P. Kippax, J. Fracassi, Particle size characterisation in nasal sprays and aerosols, LabPlus International, February/March 2003.

[54] S.P. Newman, G.R. Pitcairn, R.N. Dalby, Drug delivery to the nasal cavity: In vitro and in vivo assessment, Crit. Rev. Ther. Drug Carr. Syst. 21(1) (2004) 21-66.

[55] A.R. Clark, M. Egan, Modelling the deposition of inhaled powdered drug aerosols, J. Aerosol. Sci. 25(1) (1994) 175-186.

[56] C. Kneuer, M. Sameti, E.G. Haltner, T. Schiestel, H. Schirra, H. Schmidt, C.M. Lehr, Silica nanoparticles modified with aminosilanes as carriers for plasmid DNA, Int. J. Pharm. 196(2) (2000) 257-261.

[57] D. Luo, W.M. Saltzman, Nonviral gene delivery - Thinking of silica, Gene Ther. 13(7) (2006) 585-586.

[58] H. Vallhov, S. Gabrielsson, M. Stromme, A. Scheynius, A.E. Garcia-Bennett, Mesoporous silica particles induce size dependent effects on human dendritic cells, Nano Lett. 7(12) (2007) 3576-3582.

[59] M. Fujiwara, F. Yamamoto, K. Okamoto, K. Shiokawa, R. Nomura, Adsorption of duplex DNA on mesoporous silicas: Possibility of inclusion of DNA into their mesopores, Anal. Chem. 77(24) (2005) 8138-8145.

[60] C. Kneuer, M. Sameti, U. Bakowsky, T. Schiestel, H. Schirra, H. Schmidt, C.M. Lehr, A nonviral DNA delivery system based on surface modified silica-nanoparticles can efficiently transfect cells in vitro, Bioconjugate Chem. 11(6) (2000) 926-932.

[61] D.R. Radu, C.Y. Lai, K. Jeftinija, E.W. Rowe, S. Jeftinija, V.S.Y. Lin, A polyamidoamine dendrimer-capped mesoporous silica nanosphere-based gene transfection reagent, J. Am. Chem. Soc. 126(41) (2004) 13216-13217.

[62] C.Y. Lai, B.G. Trewyn, D.M. Jeftinija, K. Jeftinija, S. Xu, S. Jeftinija, V.S.Y. Lin, A mesoporous silica nanosphere-based carrier system with chemically removable CdS nanoparticle caps for stimuli-responsive controlled release of neurotransmitters and drug molecules, J. Am. Chem. Soc. 125(15) (2003) 4451-4459.

[63] Y.J. Wang, F. Caruso, Mesoporous silica spheres as supports for enzyme immobilization and encapsulation, Chem. Mat. 17(5) (2005) 953-961.

[64] L. Ji, A. Katiyar, N.G. Pinto, M. Jaroniec, P.G. Smirniotis, Al-MCM-41 sorbents for bovine serum albumin: relation between Al content and performance, Microporous Mesoporous Mat. 75(3) (2004) 221-229.

[65] H.H.P. Yiu, C.H. Botting, N.P. Botting, P.A. Wright, Size selective protein adsorption on thiol-functionalised SBA-15 mesoporous molecular sieve, Phys. Chem. Chem. Phys. 3(15) (2001) 2983-2985.

[66] D.Y. Zhao, J.L. Feng, Q.S. Huo, N. Melosh, G.H. Fredrickson, B.F. Chmelka, G.D. Stucky, Triblock copolymer syntheses of mesoporous silica with periodic 50 to 300 angstrom pores, Science 279(5350) (1998) 548-552.

[67] J.S. Beck, J.C. Vartuli, W.J. Roth, M.E. Leonowicz, C.T. Kresge, K.D. Schmitt, C.T.W. Chu, D.H. Olson, E.W. Sheppard, S.B. McCullen, J.B. Higgins, J.L. Schlenker, A new family of mesoporous molecular-sieves prepared with liquid-crystal templates, J. Am. Chem. Soc. 114(27) (1992) 10834-10843.

[68] N. Baccile, D. Grosso, C. Sanchez, Aerosol generated mesoporous silica particles, J. Mater. Chem. 13(12) (2003) 3011-3016.

[69] O. Pillai, R. Panchagnula, Polymers in drug delivery, Curr. Opin. Chem. Biol. 5(4) (2001) 447-451.

[70] U. Edlund, A.C. Albertsson, Degradable Aliphatic Polyesters, Vol. 157, Springer-Verlag Berlin, Berlin, 2002, pp. 67-112.

[71] I.J. Castellanos, K.G. Carrasquillo, J.D. Lopez, M. Alvarez, K. Griebenow, Encapsulation of bovine serum albumin in poly(lactide-co-glycolide) microspheres by the solid-in-oil-in-water technique, J. Pharm. Pharmacol. 53(2) (2001) 167-178.

[72] S. Freitas, H.P. Merkle, B. Gander, Microencapsulation by solvent extraction/evaporation: reviewing the state of the art of microsphere preparation process technology, J. Control. Release 102(2) (2005) 313-332.

[73] K.N. Atuah, E. Walter, H.P. Merkle, H.O. Alpar, Encapsulation of plasmid DNA in PLGA-stearylamine microspheres: a comparison of solvent evaporation and spray-drying methods, J. Microencapsul. 20(3) (2003) 387-399.

[74] P. Johansen, H.P. Merkle, B. Gander, Technological considerations related to the up-scaling of protein microencapsulation by spray-drying, Eur. J. Pharm. Biopharm. 50(3) (2000) 413-417.

[75] C.L. Densmore, F.M. Orson, B. Xu, B.M. Kinsey, J.C. Waldrep, P. Hua, B. Bhogal, V. Knight, Aerosol delivery of robust polyethyleneimine-DNA complexes for gene therapy and genetic immunisation, Mol. Ther. 1(2) (2000) 180-188.

[76] S. Ando, D. Putnam, D.W. Pack, R. Langer, PLGA microspheres containing plasmid DNA: Preservation of supercoiled DNA via cryopreparation and carbohydrate stabilization, J. Pharm. Sci. 88(1) (1999) 126-130.

[77] E. Walter, K. Moelling, J. Pavlovic, H.P. Merkle, Microencapsulation of DNA using poly(DL-lactide-co-glycolide): stability issues and release characteristics, J. Control. Release 61(3) (1999) 361-374.

[78] C. Berkland, A. Cox, K. Kim, D.W. Pack, Three-month, zero-order piroxicam release from monodispersed double-walled microspheres of controlled shell thickness, J. Biomed. Mater. Res. Part A 70A(4) (2004) 576-584.

[79] C. Berkland, K. Kim, D.W. Pack, PLG microsphere size controls drug release rate through several competing factors, Pharm. Res. 20(7) (2003) 1055-1062.

[80] C. Berkland, M. King, A. Cox, K. Kim, D.W. Pack, Precise control of PLG microsphere size provides enhanced control of drug release rate, J. Control. Release 82(1) (2002) 137-147.

[81] N.K. Varde, D.W. Pack, Influence of particle size and antacid on release and stability of plasmid DNA from uniform PLGA microspheres, J. Control. Release 124(3) (2007) 172-180.

[82] A. Vila, A. Sanchez, C. Evora, I. Soriano, J.L.V. Jato, M.J. Alonso, PEG-PLA nanoparticles as carriers for nasal vaccine delivery, J. Aerosol Med.-Depos. Clear. Eff. Lung 17(2) (2004) 174-185.

[83] H. Tamber, P. Johansen, H.P. Merkle, B. Gander, Formulation aspects of biodegradable polymeric microspheres for antigen delivery, Adv. Drug Deliv. Rev. 57(3) (2005) 357-376.

APPENDIX

PEER-REVIEWED CONFERENCE PAPERS

A 1: Synthesis of mesoporous silica for controlled biomolecule delivery

A 2: Inorganic-organic composite particle as a staged delivery platform for plasmid DNA-based biopharmaceuticals

A 3: Production of nano and micro particles via ultrasonication for biopharmaceutical delivery

A 4: Spotlight featured article - Delivering a new generation of potential biopharmaceutical blockbusters: ultrasonic process engineering of plasmid DNA

APPENDIX 1

Synthesis of mesoporous silica for controlled biomolecule delivery

Jenny Ho, Gareth M. Forde and Huanting Wang

CHEMECA 2007 Proceeding

pp. 160 – 167

Synthesis of Mesoporous Silica for Controlled Biomolecule Delivery

Jenny Ho, Gareth M. Forde and Huanting Wang
Department of Chemical Engineering
Monash University
P.O. Box 36, Melbourne, VIC, 3800,
AUSTRALIA
E-mail: jenny.ho@eng.monash.edu.au

Abstract

Presented in this paper is a novel method for preparing mesoporous silica spheres from commercial silica colloids and its utilization for biomolecule delivery. This mesoporous material is mainly aimed at nasal delivery of drugs/vaccines, which has been an area of interest for the pharmaceutical industries in recent years. Nasal delivery is to overcome the alarming pattern of unsafe injection practices and the poor availability of orally administered vaccines. Novel synthesis of mesoporous silica spheres with a diameter at 0.5 to 1.6 μm and a tailored pore size (14.1 to 28.8 nm) has been developed by using a simple electrolyte and inexpensive commercial inorganic silica colloids. The effects of synthesis conditions, which include solution composition and calcination temperature on the formation of the mesoporous silica particles, were systematically investigated. This novel method offers great flexibility in tailoring the pore size and is easily scalable to produce large quantities of mesoporous silica spheres for potential use in bio-nanotechnology, drug delivery and inorganic adsorbent applications. The adsorption of protein onto these particles and the in vitro release profiles are discussed. Moreover, the incorporation of protein into the mesoporous silica utilized thiol coupling was investigated. This conjugation can protect protein against degradation and enable its controlled release. The release mechanism will be further compared to those obtained from the physical adsorption.

1. INTRODUCTION

Discover of the mesoporous silica opened up new possibilities in many areas of chemistry and material science. It possesses high specific surface areas, high specific pore volumes, and well-ordered pore structures (Hartmann, M., 2005). Great progress has recently been made in the utilization of mesoporous silica as a nonviral gene delivery vector (Fujiwara, M. et al., 2005, Kneuer, C. et al., 2000a, Kneuer, C. et al., 2000b), as well as its good immobilization capacity for various materials (*e.g.* enzymes and macromolecules) (Wang, Y. J. and Caruso, F., 2005, Yu, A. M. et al., 2005). Mesoporous silica exhibits its diversity and potential applications in many facets of biological science.

Biopharmaceuticals represent a new generation of therapeutics that will account for a market worth billions of dollars in the near future: biogenerics in the US and Europe alone are predicted to generate sales of $16.39 billion by 2011 at an average annual growth rate of 69.8 % (Frost & Sullivan, 2005). However, more research needs to be done to synthesize effective delivery systems for biopharmaceuticals. This is to overcome the alarming pattern of unsafe injection practices and the poor availability of orally administered drugs/vaccines. There is an increasing number of drugs/vaccines being administered to humans via the nasal route. The nasal route is an important arm of the mucosal immune system since it is often the first point of contact for inhaled antigens. After intranasal immunisation, both humoral and cellular immune responses can occur (Davis, S. S., 2001). Easier and safer administration in addition to a decreased total cost of treatment would represent a major breakthrough for the global vaccination programs. This is especially true for developing countries.

Methods such as solution growth (Beck, J. S. et al., 1992, Zhao, D. Y. et al., 1998) and aerosol self assembly (Baccile, N. et al., 2003) have been developed to synthesize mesoporous silica. Organosilicates such as tetraethyl orthosilicate (TEOS) are used in these syntheses and particularly organic templates are essential for generating the mesoporous structures of silica spheres. Presented in this paper is a novel and alternative

method for preparing mesoporous silica spheres and its utilization for protein imobilization which is mainly aimed at nasal delivery of drugs/vaccines. Commercial silica colloids (SNOWTEX®) are used as starting materials and the spherical agglomerates of silica nanoparticles are formed by adding inorganic salts (electrolytes) into the colloids (Ho, J. et al., 2007). The interstices within the mesoporous silica spheres obtained in this study are formed by agglomerated precursor nanoparticles and readily adjusted to form different pore sizes. This can be achieved by using silica colloids with different precursor particle diameters. The preparation and characterization of mesoporous silica spheres (MPS) will be described in detail in this paper. This paper will also reports the immobilization of Bovine Serum Albumin (BSA), which was chosen as a model protein, onto MPS via physical adsorption and covalent binding.

2. EXPERIMENTAL

2.1. Synthesis and Characterization of Mesoporous Silica Spheres

Mesoporous silica spheres were produced using the method we have reported (Ho, J. et al., 2007). Briefly, MPS were synthesized from commercially available silica colloids (SNOWTEX® ST-50: 20-30 nm, ST-20L: 40-50 nm, and ST-ZL: 70-100 nm) with simple electrolytes (NH_4NO_3 or NaCl). Water-soluble monomer acrylamide, crosslinker *N,N'*- methylenebisacrylamide and initiator ammonium persulfate (2 AM : 0.02 MBAM : 0.01 $(NH_4)_2S_2O_8$: 1 SiO_2 by weight) were added to the resulting suspension while stirring. After the monomer, crosslinker and initiator were dissolved, the obtained suspension was then heated at 90 °C for 30 min to form polyacrylamide hydrogel. This was followed by drying overnight at 90 °C. The resulting solids were carbonized and calcined at 500 ° C or 700 °C to yield MPS. As a comparison, a number of samples were also prepared without using polyacrylamide hydrogel. The MPS prepared with NaCl were washed with deionized water to remove residual NaCl and collected via centrifugation. Nitrogen sorption measurements for the MPS were performed at -196 °C using a Micromeritics ASAP 2020MC analyser. Surface areas were calculated by the BET (Brumauer-Emmett-Teller) method and the pore-size distributions were obtained from the desorption branch calculated by the BJH (Barrett-Joyner-Halenda) method. The pore volumes were estimated from the desorption branch of the isotherm at $P/P_0 = 0.98$ by assuming complete pore saturation. The MPS samples were also characterized with a JEOL JSM-6300F field emission scanning electron microscope (FESEM) which is operated at an accelerating voltage of 15 kV.

2.2. Protein Adsorption and *In vitro* Delivery Studies

In the present work, the characteristics (sizes, pore sizes, isoelectric points and zeta potentials) of BSA and MPS were determined to probe the interactions between the protein and MPS prior the adsorption studies. The adsorption of Bovine Serum Albumin (BSA) onto MPS synthesized from silica colloids was studied employing real time *in situ* measurements. BSA loading was performed in a continuous flow fashion at a flowrate of 0.2 ml min^{-1} onto 1.0 ml of mesoporous silica spheres packed in an Econo-Pac column (ID 1.5 cm, BIO-RAD) at 25 °C. The outlet concentrations of BSA were measured with a UV spectrophotometer at 280 nm. A study was undertaken to determine whether the MPS with adsorbed BSA (MPS-BSA) particles were capable of delivering the adsorbed protein under physiological condition *in vitro* (phosphate buffered saline (PBS), 37 °C, 100 rpm). 20.0 mg of MPS-BSA particles were suspended in 10.0 ml of PBS buffer (0.01 mol L^{-1}). At predetermined time, samples of 300 µl were collected and replaced with 300 µl of fresh PBS. The diluting effect of the fresh PBS was taken into account during the analysis.

2.3. Thiol Coupling of Protein

5.0 mg of MPS were added into 1.0 ml of 0.1 M *N*-hydroxysuccinimide (NHS)/0.4 M 1-Ethyl-3-(3-dimethylaminopropyl)-carbodiimide hydrochloride (EDC), 1:1 (v:v) mixture to activate the surface by modification of the hydroxyl groups. After incubation on the shaker at 100 rpm, 25°C for 30 min, the supernatant liquid was discarded after centrifugation. 2.0 ml of freshly prepared 80 mM 2-(2-pyridinyldithio)-ethaneamine hydrochloride (PDEA) in 50 mM sodium borate buffer at pH 8.5 was added to the MPS. This is to introduce the reactive disulfide groups onto the MPS after incubated on the shaker at 100

rpm, 25°C for 1 h. These MPS were then reacted with 1.5 ml of 0.18 mM of BSA in 0.1 M formate buffer at pH 4.3 for another 1 h. The supernatant (BSA) was collected after centrifugation and analyzed for the protein concentration via Bradford Reagent assay ($OD_{595\ nm}$). The MPS were added with 1.5 ml of deionized water and mixed well to rid of any left over reagent and this process was repeated for three times. The unreacted disulfide groups were deactivated with 2.0 ml of 50 mM L-cysteine/1 M NaCl in 0.1 M sodium acetate buffer at pH 4.0. The MPS were then washed with deionized water and stored in 4°C for later use. The *in vitro* delivery studies were conducted as mentioned in the previous section.

3. RESULTS AND DISCUSSION

3.1. Formation of Mesoporous Silica Spheres

MPS were formed in water by agglomerations of silica colloids via destabilization of electrolyte. The electrolyte dissolved in the water interferes with the surface charge of the colloids and this resulted in a charge imbalance that disrupts the stability of the colloids (Allen, L. H. and Matijevi.E, 1969). In order to retrieve these spherical agglomerates from the destabilized colloids, a highly crosslinked polyacrylamide hydrogel (Wang, H. et al., 2000) was used to prevent their further agglomeration during drying and calcination. High temperature treatment is adopted to improve the bonding strength of the starting silica nanoparticles, and therefore the resulting MPS are mechanically strong. Meanwhile, the polymer hydrogel was converted to carbon which acted as the barrier. Individual mesoporous silica spheres were obtained after the removal of the carbon barrier by calcination. As expected, large mesoporous silica particles were formed without using polyacrylamide hydrogel and MPS with a narrow particle size distribution were obtained when using polyacrylamide hydrogel as shown in Figure 1a and Figure 1b respectively.

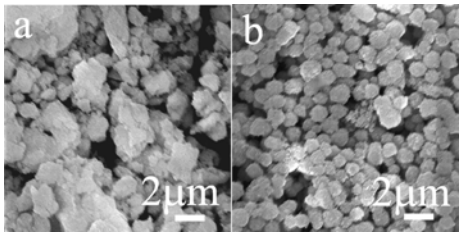

Figure 1 SEM images of MPS prepared from SNOWTEX ST-20L (40-50 nm) and NaCl (0.5 mol L^{-1}). (a)Without polyacrylamide hydrogel, calcined at 500°C and (b) with polyacrylamide hydrogel, calcined at 500°C. Large agglomerates were formed when polyacrylamide hydrogel was not used. This can be compared with uniform particles being obtained in the present of polymer network.

When ammonia nitrate (NH_4NO_3) was used as a destabilizer, the MPS with well-dispersed morphology was obtained. The MPS diameters ranged from 0.5 to 0.8 μm for the SNOWTEX® ST-50 (20-30 nm), 0.6 to 1.3 μm for the SNOWTEX® ST-20L (40-50 nm) and 0.8 to 1.6 μm for the SNOWTEX® ST-ZL (70-100 nm) (Ho, J. et al., 2007). The hysteresis loops noticed in nitrogen sorption isotherms of MPS clearly indicated a mesoporous structure was formed in the silica spheres. It can be seen that the pore size of silica spheres increased as the precursor particle diameter increased since the pore structure is the interstice of the packed precursor particles. Therefore, it is clear that the pore size of the MPS can be readily adjusted by changing the precursor particle diameter (Ho, J. et al., 2007). Several concentrations of NH_4NO_3 solution (0.13 to 0.35 mol L^{-1}) were used to destabilize the silica colloids. Bulky and irregular silica agglomerates were formed when the concentration of electrolyte was lower than the critical concentration. However, regular agglomerates with a narrow pore size distribution were obtained when the concentration approached the critical level. Therefore, the concentration of electrolyte is a crucial factor in determining the agglomeration of the silica precursor into mesoporous particles. Sodium chloride (NaCl) was also used as the destabilizer to synthesize MPS. However, coalescence of precursor nanoparticles occurred in the resultant spherical mesoporous silica particles as shown in Figure 2. The BET surface areas were small and have wide pore size distributions. The precursor silicas were sintered in the presence of sodium chloride since the sodium silicate might form when silica reacts with sodium chloride at high temperatures (Clews, F. H. and Thompson, H. V., 1922). In contrast, NH_4NO_3 decomposed at a low temperature (approximately 210°C), and could be completely removed from the mesoporous spheres (Ho, J. et al., 2007). The characteristics of the MPS synthesized via using both electrolytes are compared in Table 1.

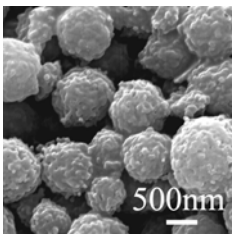

Figure 2 SEM image of spherical MPS prepared using SNOWTEX ST-20L (40-50 nm) and NaCl as electrolyte, calcined at 500°C. Coalescence of silica nanoparticles was noticed in MPS due to the formation of sodium silicate.

Table 1. Nitrogen sorption results for MPS prepared using NH_4NO_3 or NaCl as electrolyte and calcined at 500°C

Electrolyte	Silica colloids	BET surface area (m^2g^{-1})	Mean pore size (nm)
NH_3NO_3	SNOWTEX ST-50	123.0	14.1
	SNOWTEX ST-20L	54.7	17.5
	SNOWTEX ST-ZL	31.2	28.8
NaCl	SNOWTEX ST-50	26.1	25.9
	SNOWTEX ST-20L	47.6	22.1
	SNOWTEX ST-ZL	23.6	30.2

In this experiment, the heat treatment is to allow strained siloxane bonds to form between precursor silica nanoparticles and hence improve the mechanical strength of each individual MPS. Mesoporous silica particles with well-defined pore size distribution were obtained by calcination at 500°C. However, high temperature treatment (700°C) leads to the coalescence of precursor silica nanoparticles (Figure 3). Thus, decrease of BET surface area, wider pore size distribution and increase of average pore size were noticed due to the intensive sintering. The same trends were observed in the synthesis of mesoporous spheres by using NaCl.

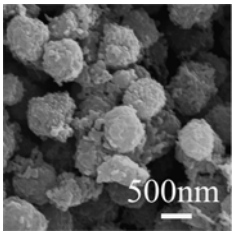

Figure 3 SEM image of spherical MPS prepared using SNOWTEX ST-20L (40-50 nm) and 0.25 mol L^{-1} NH_4NO_3 as electrolyte. Sample was obtained by calcination at 700°C and coalescences were noticed within the MPS.

3.2. Adsorption of Protein and *In vitro* Delivery Studies

In the present work, the pore size of MPS was tailored for protein. With an in depth understanding of the physio-chemical characteristics of the protein and MPS, current work has yielded a more effective binding capacity and delivery profile. The hydrodynamic diameter of BSA ranges from 2.23 nm at pH 7.03 up to 7.80 nm at pH 4.74, hence BSA is sufficiently small at all pH levels that were examined to diffuse into the pores of MPS which are ~ 17.5 nm and this was confirmed by the BJH method. The adsorption isotherm of BSA onto MPS at ~ pH 4 fitted the Langmuir model and displayed the highest adsorption capacity (71.4 mg ml^{-1} MPS). The dissociation constant (K_D) obtained from the Langmuir correlation is 9.88×10^{-5} M. pH values play a crucial role in these adsorption studies, since the surface charge will change and affect the stability of the system. Expansion and contraction of hydrodynamic diameter of the BSA at different pH values are a result of the cohesive attractive and repulsive forces associated with the BSA molecule. Furthermore, the delivery rates of BSA from the mesoporous silica spheres under physiological condition were shown to be dependent on the concentration of protein loaded. The results of the initial burst period (first 250 min) are displayed in Figure 4, which shows that each concentration has a similar delivery profile. However, higher concentrations show greater variation in burst rates. This was probably due to the dissolution of BSA near the MPS surface, which is not uncommon in *in vitro* delivery studies. In general, the delivery profiles plateau after 250 mins.

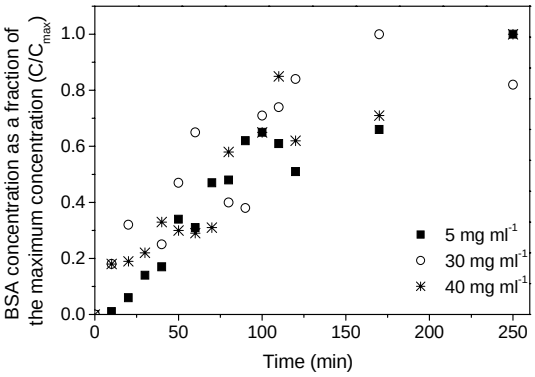

Figure 4 Delivery of BSA *in vitro* under physiological condition (PBS buffer, 37°C, 100 rpm) from MPS that are loaded with different concentrations of BSA (31.27mg ml^{-1}, 58.84 mg ml^{-1} and 61.55 mg ml^{-1}). Protein concentration was determined via a Bradford Reagent assay. The average from three runs are shown (n=3).

3.3. Thiol Coupling of Protein and *In vitro* Delivery Studies

The incorporation of protein into the mesoporous silica spheres can protect them against degradation. This conjugation also enables controlled release of protein via the *in vivo* enzymatic hydrolysis of the sulphur-sulphur bridge between the silica surface and the protein. Direct linking of protein molecules to particle surfaces is possible via the thiol group, but this may lead to a decreased biological activity if the thiol group is present within an active site or region. Thus, a thiol group that is not involved for biological activity should be used to attach protein covalently to the particle surface. BSA contains 35 cysteine residues with a thiol group out of its 607 residues (Brown, J. R., 1975), hence there are numerous sites for immobilization of the BSA molecule. None of the disulphide bonds are accessible to reducing agents in the range of pH 5-7, but they became progressively available as the pH increased or decreased (Katchalski, E. et al., 1957). This shows that the disulphides in albumin are protected from reducing agents at neutral pH. The chemistry of the thiol-disulphide exchange to immobilize the BSA molecules to the functionalized MPS surface is outlined in Figure 5. Biacore's surface plasmon resonance (SPR) technology was used to analyse the multiple aspects of BSA and hydroxyl interactions via BIAcore®X instrument. Figure 6 shows overlay plots of the sensorgrams obtained from the BSA binding to the sensor chip surface. The concentrations of BSA ranged from 0.2 to 2000 μg ml^{-1}. Most of the concentrations being used bind rapidly and a steady state binding level is reached during injection. However, the dissociation is almost plateau which shows relatively strong covalent binding. The K_D value was calculated from plot of binding response against concentration, using BIAevaluation software. The K_D value obtained from this evaluation is 3.04 x 10^{-12} M which indicates strong covalent binding form via the sulphur-sulphur bridge. The immobilization via thiol coupling is stable and protein can be delivered under physiological condition by enzymatic hydrolysis. The controlled release profile of the BSA under physiological condition for the first 24 h is displayed in Figure 7. The profile shows a lesser fluctuation due to the steady hydrolysis reaction of the covalent binding. It has slower release kinetic compared to the physical adsorption being discussed in the previous section. The release profile agreed closely with that expected from the K_D value.

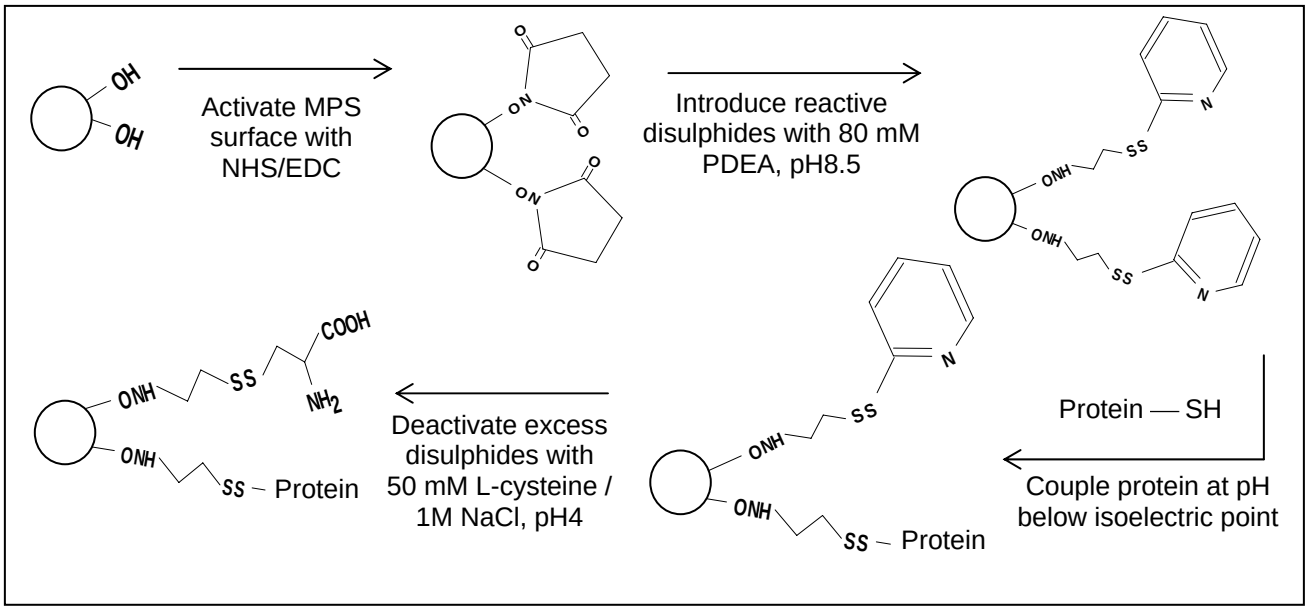

Figure 5 Schematic illustration for chemistry of thiol-disulphide exchange coupling to immobilize the protein onto MPS.

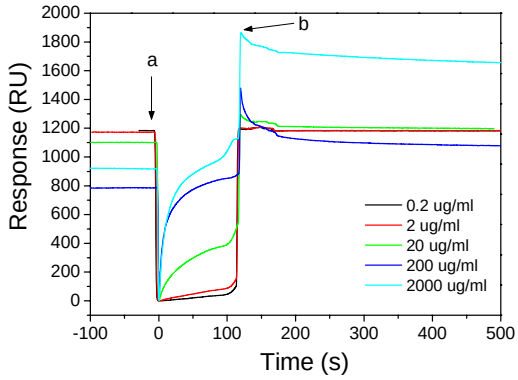

Figure 6 Overlay plots of BSA binding sensorgrams. The sensorgrams show the real-time SPR response over time for each binding reaction. The start and end points of the sample injections, which define the association (a) and dissociation (b) phases respectively, are indicated by the arrows.

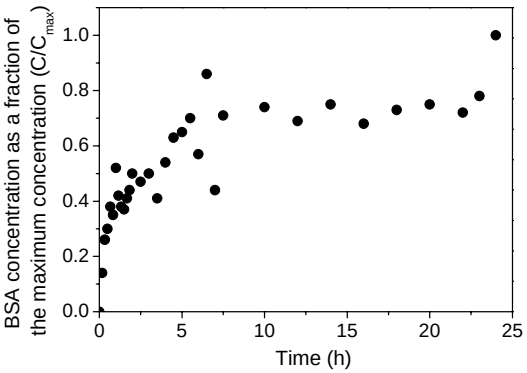

Figure 7 Delivery of BSA *in vitro* under physiological condition (PBS buffer, 37°C, 100 rpm) from MPS immobilized with BSA via thiol coupling. Protein concentration was determined via a Bradford Reagent assay. The average from three runs are shown (n=3).

4. CONCLUSION

Presented in this paper was a strategy to synthesize MPS from silica colloids. The immobilizations of BSA onto this mesoporous material were also discussed. The pore size of the MPS (14.1 to 28.8 nm) can be tailored to suit the potential biopharmaceuticals. The maximum binding capacity (q_{max}) of 71.4 mg ml^{-1} was higher than previous reported studies. The initial burst rate of biopharmaceuticals varied from 4 h to 10 h, depending on the interactions involved. Economics and scale-up considerations of this mesoporous material, which synthesized via destabilization of colloids, indicated the flexible scaleability and commercial viability of this technology to serve a delivery platform for biopharmaceuticals. MPS has great potential to become an attractive biomaterial because of its biocompatibility and excellent ability for functionalization through a broad range of physical and chemical methods. Thus, enabling a tailored interaction with the biomolecule of interest and enabling a tuned controlled release profile of biopharmaceuticals.

5. ACKNOWLEDGEMENTS

This work was supported by the Monash University. G.M.F thanks the Victorian Endowment for Science, Knowledge and Innovation (VESKI) for the Innovation Fellowship and support of this research. H.W. thanks the Australian Research Council for the QEII Fellowship. J.H gratefully acknowledges the financial support from Monash Research Graduate Scholarship. We thank SNOWTEX®, Nissan Chemical Industries, Tokyo, Japan for providing the silica colloids.

6. REFERENCES

Allen, L. H. & Matijevi.E (1969), *Stability Of Colloidal Silica .I. Effect Of Simple Electrolytes*, Journal Of Colloid And Interface Science, 31(3)**,** 287-&.

Baccile, N., Grosso, D. & Sanchez, C. (2003), *Aerosol generated mesoporous silica particles*, Journal of Materials Chemistry, 13(12)**,** 3011-3016.

Beck, J. S., Vartuli, J. C., Roth, W. J., Leonowicz, M. E., Kresge, C. T., Schmitt, K. D., Chu, C. T. W., Olson, D. H., Sheppard, E. W., McCullen, S. B., Higgins, J. B. & Schlenker, J. L. (1992), *A New Family of Mesoporous Molecular-Sieves Prepared with Liquid-Crystal Templates*, Journal of the American Chemical Society, 114(27)**,** 10834-10843.

Brown, J. R. (1975), *Structure of Bovine Serum-Albumin*, Federation Proceedings, 34(3)**,** 591-591.

Clews, F. H. & Thompson, H. V. (1922), *The interaction of sodium chloride and silica*, Journal of the Chemical Society, 1211442-1448.

Davis, S. S. (2001), *Nasal vaccines*, Advanced Drug Delivery Reviews, 51(1-3)**,** 21-42.

Frost & Sullivan (2005) Strategic Analysis of the World Biogenerics Market.

Fujiwara, M., Yamamoto, F., Okamoto, K., Shiokawa, K. & Nomura, R. (2005), *Adsorption of duplex DNA on mesoporous silicas: Possibility of inclusion of DNA into their mesopores*, Analytical Chemistry, 77(24)**,** 8138-8145.

Hartmann, M. (2005), *Ordered mesoporous materials for bioadsorption and biocatalysis*, Chemistry Of Materials, 17(18)**,** 4577-4593.

Ho, J., Zhu, W., Wang, H. & Forde, G. M. (2007), *Mesoporous silica spheres from colloids*, Journal of Colloid and Interface Science, 308(2)**,** 374-380.

Katchalski, E., Benjamin, G. S. & Gross, V. (1957), *The Availability of the Disulfide Bonds of Human and Bovine Serum Albumin and of Bovine Gamma-Globulin to Reduction by Thioglycolic Acid*, Journal of the American Chemical Society, 79(15)**,** 4096-4099.

Kneuer, C., Sameti, M., Bakowsky, U., Schiestel, T., Schirra, H., Schmidt, H. & Lehr, C. M. (2000a), *A nonviral DNA delivery system based on surface modified silica-nanoparticles can efficiently transfect cells in vitro*, Bioconjugate Chemistry, 11(6)**,** 926-932.

Kneuer, C., Sameti, M., Haltner, E. G., Schiestel, T., Schirra, H., Schmidt, H. & Lehr, C. M. (2000b), *Silica nanoparticles modified with aminosilanes as carriers for plasmid DNA*, International Journal of Pharmaceutics, 196(2)**,** 257-261.

Wang, H., Wang, Z. & Yan, Y. (2000), *Colloidal suspensions of template-removed zeolite nanocrystals*, Chemical communications 2333-2334.

Wang, Y. J. & Caruso, F. (2005), *Mesoporous silica spheres as supports for enzyme immobilization and encapsulation*, Chemistry of Materials, 17(5)**,** 953-961.

Yu, A. M., Wang, Y. J., Barlow, E. & Caruso, F. (2005), *Mesoporous silica particles as templates for preparing enzyme-loaded biocompatible microcapsules*, Advanced Materials, 17(14)**,** 1737-1741.

Zhao, D. Y., Feng, J. L., Huo, Q. S., Melosh, N., Fredrickson, G. H., Chmelka, B. F. & Stucky, G. D. (1998), *Triblock copolymer syntheses of mesoporous silica with periodic 50 to 300 angstrom pores*, Science, 279(5350)**,** 548-552.

APPENDIX 2

Inorganic-organic composite particle as a staged delivery platform for plasmid DNA-based biopharmaceuticals

Jenny Ho, Gareth M. Forde and Huanting Wang

AIChE Annual Meeting 2007 Proceeding

P84273

Inorganic-Organic Composite Particle as a Staged Delivery Platform for Plasmid DNA-Based Biopharmaceuticals

Jenny Ho, Gareth M. Forde, Huanting Wang

Monash University, Melbourne, VIC, Australia.

Introduction

Infectious diseases such as influenza may spread exponentially throughout communities. In fact, most infectious diseases remain as major health risks due to the lack of vaccine or the lack of facilities to deliver the vaccines. Conventional vaccinations are based on damaged pathogens, live attenuated viruses and viral vectors. If the damage was not complete, the vaccination itself may cause adverse effects. Therefore, researchers have been prompted to prepare viable replacements for the attenuated vaccines that would be more effective and safer to use.

DNA vaccines are generally composed of a double stranded plasmid that includes a gene encoding the target antigen under the transcriptional directory and control of a promoter region which is active in cells. Plasmid DNA (pDNA) vaccines allow the foreign genes to be expressed transiently in cells, mimicking intracellular pathogenic infection and inducing both humoral and cellular immune responses. Currently, because of their highly evolved and specialized components, viral systems are the most effective means for DNA delivery, and they achieve high efficiencies (generally >90%), for both DNA delivery and expression. As yet, viral-mediated deliveries have several limitations, including toxicity, limited DNA carrying capacity, restricted target to specific cell types, production and packing problems, and high cost. Thus, nonviral systems, particularly a synthetic DNA delivery system, are highly desirable in both research and clinical applications [1].

At present, DNA immunization can be achieved using intramuscular or intradermal injection, gene gun administration, and etc. The direct injection of naked plasmid DNA is possible, but relatively few cells take up the DNA (1-3%) due to the high molecular weight and polyanionic nature of the nucleic acids, leading to reduced expression of the encoded protein. Moreover, free pDNA deliveries are also hindered by their instability in biological fluids due to the degradation by the endonucleases. Efficiency issues surrounding the delivery of DNA vaccines can be overcome by administering larger doses, but this can cause the unwanted side effects of toxicity and multi-drug resistance, as well as increased cost per dose [2].

One of the problems with vaccinations affecting global health is the unsafe injection practices. The World Health Organization (WHO) estimates that over 12 billion injections are administered annually and up to 30% of these injections are unsafe [3]. The transmission of bloodborne pathogens from patient to patient with unsterilized needles has been recorded for over half a century. These unsafe injection practices are associated with substantial morbidity and mortality, particularly from hepatitis B, hepatitis C and HIV infections, especially in poorer and developing countries [4]. Currently, oral administration is another popular route for drug/vaccine delivery. However, oral drug delivery is hampered by the low mucosal permeability of drugs, and lack of stability in the gastrointestinal (GI) environment, results in degradation of the drugs compound prior to its absorption.

As a result, there are an increasing number of drugs/vaccines being administered to humans via the nasal route. The nasal route is an important arm of the mucosal immune system since it is often the first point of contact for inhaled antigens. After intranasal immunisation, both humoral and cellular immune responses can occur. Intranasal administration will greatly assist progress of health programs around the world since nasal vaccines offer non-invasive administration, are easily accessible for a larger population, and do not require trained persons for administration. Easier and safer administration in addition to a decreased total cost of treatment would represent a major breakthrough for global vaccination programs, especially for developing countries. The use of particulate delivery systems for administration of DNA through the nasal route is not a strategy that has attracted a large volume of research as the advent of DNA vaccination is relatively new.

Another problem associated with DNA vaccines is there is an urgent need to develop their potent and efficient before they can be used effectively in humans, since the failure to elicit antibodies against antigens when used in human has been reported recently. The development of an effective carrier system may be the key element in improving and homogenizing the overall immune response to DNA vaccines. One of the today's trends is to associate DNA-based immunization with other immunization approaches, such as vectors or antigens, as part of prime-boost (mixed) immunization regimes. DNA prime-protein boost immunization involves priming with DNA vaccines and boosting with protein or recombinant protein. These strategies aim to augment immune responses to pathogens. Thus, there needs to be a particulate delivery system that enables staged delivery of DNA prime-protein boost in the nasal tract. Improved staged delivery of vaccine can be achieved by employing a composite of inorganic mesoporous silica and biodegradable polymer-based particulate delivery system. These particulates are able to maintain sustained vaccine release over a period of time to specific sites for prime-boost vaccination.

Inorganic host materials, mesoporous silica is a relatively benign material in terms of biocompatibility and versatile in terms of the variety of chemical and physical modifications that are available. It possesses high specific surface areas,

high specific pore volumes, and well-ordered pore structures adjustable within the range of 2 - 50 nm. Great progress has recently been made in the utilization of mesoporous silica spheres as a nonviral gene delivery vector [5], as well as its good immobilization capacity for various biomaterials [6]. Mesoporous silica exhibits its diversity and potential applications in many facets of biological science. Methods such as solution growth and aerosol self assembly have been developed to synthesize mesoporous silica spheres. Organosilicates such as tetraethylorthosilicate (TEOS) are used in these syntheses, and particularly organic templates are essential for generating the mesoporous structures of silica spheres. However, organosilicates are expensive. This drawback has hindered the usage of these alkoxide precursors in large-scale application. Economic considerations have aroused the usage of inexpensive inorganic silica as a starting material for mesoporous silica and further increase its realistic applications. Moreover, larger pore is demanded for advanced application of the mesoporous materials in biotechnology due to the encapsulation of biomolecules in these materials.

Research Methods and Results

In this current study, a novel synthesis of mesoporous silica spheres has been developed by using a simple electrolyte and inexpensive commercial inorganic silica colloids. This new method will offer a great flexibility in tuning or tailoring the pore size of the mesoporous silica spheres to match specific molecules or applications, and to produce large quantities of mesoporous silica spheres for potential use in bio-nanotechnology, drug delivery and inorganic adsorbent applications. Mesoporous silica spheres at the sub-micrometer and micrometer scale (0.5 to 1.6 μm) with a tailored pore size (14.1 to 28.8 nm) has been obtained. The influences of synthesis conditions including solution composition and calcination temperature on the formation of the mesoporous silica spheres were systematically investigated. Crosslinked polyacrylamide hydrogel was used as a temporary barrier to obtain dispersible spherical mesoporous silica spheres. Adsorption of protein onto these particles and the *in vitro* release profile will be presented. The adsorption isotherm fitted the Langmuir model; a very high adsorption capacity (71.4 mg/ml adsorbent) has been obtained. The mesoporous silica spheres released ~21 % of protein loaded in the initial burst period and starts to plateau subsequently. Results obtained from the automated electrophoresis gel revealed that the conformation and size (in kDa) of protein were the same before and after the adsorption studies. This indicates that biopharmaceuticals can retain intact upon desorption from a mesoporous silica spheres delivery platform.

The embedding of biopharmaceutical compounds into biodegradable polymer microspheres has gained considerable interest over the last decade [7, 8]. Vaccines can be released from such microparticles in a sustained and controlled fashion, while non-release biopharmaceuticals are protected from rapid *in vivo* degradation. Adhesive properties of biodegradable polymer make them suitable

for transmucosal delivery applications and prolong the contact time of biopharmaceuticals with the nasal surface. Moreover, these biodegradable polymers can degrade to toxicologically harmless products. In the present work, several candidates (*i.e.* PLGA and etc.) will be studied for their suitability in the encapsulation of pDNA, which mainly based on their degradation mechanism and profile, porosity, and network structure. Furthermore, the selection of a suitable microencapsulation technique for biopharmaceuticals is crucial due to sensitivity of these biopharmaceuticals towards processing conditions. As a result, several characteristics can be used to evaluate the suitability of a chosen method, include molecular interaction properties between biopharmaceutical and polymer, stability during processing and etc. Therefore, a new and improved process, shielding the antigen from deleterious conditions has to be developed. In this study, a microencapsulation method using ultrasonic atomization to synthesize biodegradable polymer microspheres that encapsulate both the pDNA and the mesoporous silica spheres loaded with protein for nasal delivery application will be presented. The *in vitro* staged delivery profile for pDNA and protein from the resulting composite particle will also be presented. The use of ultrasonic atomization for the production of biopharmaceuticals containing biodegradable polymer particles is a comparatively new application. The advantages of this atomization are the possibility of particle size control, and the fact that it does not require elevated temperature and phase separation inducing agents. This novel technology appears to have the potential for aseptic manufacturing and easy up-scaling for industrial applications. Several parameters were systematically investigated for their effects onto the size distribution and morphology of the final microparticles. Particle yields of above 80% were obtained and pDNA encapsulation efficiencies were in the region of 90%. Mean particle sizes ranged from 8 to 12 μm, depending on the polymer concentration, flowrate and solid contents, with excellent reproducibility. The *in vitro* profiles revealed that average 96 $\pm$ 2.5 % of the pDNA were released within 30 days and the delivery rate is considerable constant.

Conclusion

Despite the fact that researches have been conducted for the DNA vaccines delivery system over a decade, there is still much work to be done in the area of DNA delivery for the vaccination and gene therapy applications. The efficiency and specificity of DNA delivery by nonviral methods are, surprisingly, still quite poor compared with viral-mediated methods. There needs to be a system that can control release the DNA vaccines and their booster (protein) with inhaled application, as both systemic and mucosal immune responses can be induced through the nasal tract. The novel method being discussed in this paper is easily scalable to produce a large number of particles for realistic applications in vaccines delivery. Optimisation of all the parameters (*i.e.* types of polymers, encapsulation methods, and ultrasonic atomization conditions) will further ensure the production of high quality composite particles for vaccine delivery. The adopted scalable and cheap production method for these particles represents a

good start towards the ultimate goal of commercially viable production of a staged delivery system for DNA vaccines.

References

1 Donnelly JJ, Ulmer JB, Shiver JW, and Liu MA (1997), "DNA vaccines", *Annu. Rev. Immunol.* **15**: pp. 617-648.

2 Donnelly JJ, Wahren B, and Liu MA (2005), "DNA vaccines: Progress and challenges", *J. Immunol.* **175**: pp. 633-639.

3 Hutin YJF and Chen RT (1999), "Injection safety: a global challenge", *Bull. World Health Organ.* **77**: pp. 787-788.

4 Kane A, Lloyd J, Zaffran M, Simonsen L, and Kane M (1999), "Transmission of hepatitis B, hepatitis C and human immunodeficiency viruses through unsafe injections in the developing world: model-based regional estimates", *Bull. World Health Organ.* **77**: pp. 801-807.

5 Luo D and Saltzman WM (2006), "Nonviral gene delivery - Thinking of silica", *Gene Ther.* **13**: pp. 585-586.

6 Wang YJ and Caruso F (2005), "Mesoporous silica spheres as supports for enzyme immobilization and encapsulation", *Chem. Mat.* **17**: pp. 953-961.

7 Ugwoke MI, Agu RU, Verbeke N, and Kinget R (2005), "Nasal mucoadhesive drug delivery: Background, applications, trends and future perspectives", *Adv. Drug Deliv. Rev.* **57**: pp. 1640-1665.

8 Tamber H, Johansen P, Merkle HP, and Gander B (2005), "Formulation aspects of biodegradable polymeric microspheres for antigen delivery", *Adv. Drug Deliv. Rev.* **57**: pp. 357-376.

APPENDIX 3

Production of nano and micro particles via ultrasonication for biopharmaceutical delivery

Gareth M. Forde, **Jenny Ho**, Wen Li,

Judin Sahayanathan, Nyomi Uduman, Chamithri Wimalajeewa

CHEMECA 2007 Proceeding

pp. 11 – 21

Production of Nano and Micro Particles via Ultrasonication for Biopharmaceutical Delivery

G. M. Forde*, J. Ho, W. Li, J. Sahayanathan, N. Uduman, C. Wimalajeewa.
Bio Engineering Laboratory (BEL),
Department of Chemical Engineering, Monash University,
Clayton, Melbourne, 3800. AUSTRALIA
*E-mail: gareth.forde@eng.monash.edu.au

Abstract

Biopharmaceuticals have been shown to have low delivery and transformation efficiencies. To over come this, larger doses are administered in order to obtain the desired response which may lead to toxicity and drug resistance. This paper reports upon approaches for the development of scalable particle production methods utilizing ultrasonication or surface acoustic wave atomization to reliably produce micro and nanoparticles with physical characteristics to facilitate the cellular uptake of biopharmaceuticals. By producing particles of an optimal size for cellular uptake, the efficacy and specificity of drug loaded nano and micro particles will be increased. Better delivery methods are an important technological development for pandemic preparedness, as reducing the amount of antigen (biomolecule) required to produce immunity will enable more people to be vaccinated in the case of vaccine shortages. Better delivery reduces the amount required per dose (hence cost per dose), reduces toxicity, and reduces problems associated with multi-drug resistance due to over dosing. The approaches presented also harness encapsulation and biodegradable polymers or lipids in order to enhance the delivery and stability of the biomolecule. The first approach is the encapsulation of protein in a biodegradable polymer for delivery via the nasal mucosa whilst the second approach is the encapsulation of plasmid DNA (pDNA) into lysosomes to improve cellular transformation efficiencies.

1. INTRODUCTION

There exists a need for scalable, continuous and commercially viable methods to encapsulate biomolecules in formulations that enhance the delivery of the biomolecule and to protect the biomolecule during storage and delivery. There are a number of disadvantages with current processing technology includes: spray-drying cannot be used for highly temperature-sensitive compounds (Johansen et al., 2000) whilst oil-in-water emulsion and solvent extraction may result in the presence of residual solvents and have scale-up limitations (Thomasin et al., 1996). Ultrasonication can be performed at almost any temperature, uses no phase separation, and usually results in higher encapsulation efficiency than emulsion methods (Putney, 1998). The mechanism by which the biomolecule (protein or DNA) is encapsulated into the polymer network or liposome (reagent) is based on the sonication of the biomolecule/reagent mixture. Sonication of the mixture transfers energy to the molecules which enables the biomolecule to mix with or enter the reagent and become encapsulated.

Reported are results for the production of two types of particles via : microparticles suitable for inhalation leading to payload delivery via the nasal mucosa and nanoparticles for enhanced cellular endocytosis with specific application to gene therapy.

The microparticles presented in this work have applications in the rapid delivery of protein to the blood stream via the nasal mucosa. Particles for the delivery of drugs via the nasal route should have a mass median diameter between 10 and 20 μm in order to increase nasal deposition and minimize deposition in the lungs and gastro-intestinal tract (Kippax and Fracassi, 2003).

The nanoparticles presented in this work have application in the area of gene therapy and DNA vaccine delivery. DNA is soon to be a new generation of block buster, reverse engineered biopharmaceuticals

(Danquah and Forde, 2006). The rapidly rising demand for therapeutic grade DNA requires associated improvements in the biochemical and bioprocessing technology. This includes is the formulation of the DNA into nanoparticles for enhanced cellular transformation efficiencies, in particular for gene therapy applications. Gene therapy involves the deliberate transfer of DNA into the body's cells for therapeutic purposes. There have been many techniques developed that involve the efficient delivery of genes into cells such as the exposure of cells to naked plasmid DNA and the incorporation of DNA into viruses. Safety concerns associated with using viruses in human therapeutics has resulted in a growing interest in DNA based delivery systems due to simplicity of use, ease of large scale production and lack of specific immune response (Li and Huang, 2000). Due to the size and charge of naked DNA and the enzymatic and membrane barriers imposed by the cell, the entry of whole DNA into cells and subsequent expression is a very inefficient process (Felgner *et al.*, 1987). Hence the demand for improved delivery systems as explored in this paper.

Internalization of DNA molecules into cells is enhanced by encapsulating the DNA into liposomes or complexing the DNA with cationic liposomes (Lasic, D, 1997). Cationic liposomes (also known as cationic lipoplexes) are made of positively charged lipids and enhance the electrostatic interaction of the otherwise negatively charged DNA and cell membranes. Cationic liposome-mediated transfection allows efficient delivery of DNA into a wide variety of eukaryotic cell types with relatively high levels of expression of the exogenous DNA (Gershon *et al.*, 1993) and exhibit low toxicity, are non-immunogenicity and can be produced via scalable methods (Joachum, *et al.*, 1997). A cationic polymer, polyethylenimine (PEI), was used to further enhance the transport of DNA into the cell and facilitate encapsulation into lysosomes. Even through PEI can operate as a condensing agents for DNA.(Bloomfield, V.A, 1998), the aim of the cationic polymer in this body of work was to mask the negative DNA charges. High molecular weight polymers tend to form small, stable particles relative to lower molecular weight polymers, yet low molecular weight polymers can enhance transfection efficiencies, most likely due to a decreased cytotoxicity and the increased ability of the plasmid to dissociate from the cationic polymer (De Laporte *et al.*, 2006).

2. MATERIALS AND METHODS

2.1. Ultrasonicator

The ultrasonicator was a 40 kHz system (VCX134 AT, Sonics, USA) with a 6 mm full wave ultrasonic atomization probe. Feed stocks were fed to the ultrasonic atomizer via a peristaltic pump at a constant flow rate of 0.01 ml/s except for the study to determine the effect of flow rate on the particle size distribution. The atomizer tip was fixed at 150 mm above the hardening agent liquid, contained in a collection flask. This height enabled sufficient time for the volatile acetone solvent to evaporate from the particles before collection in the hardening agent. The feed was pumped through the atomization tip before the tip was energized at an amplitude of 100%. For the nanoparticle work, the very small volumes in use (< 5 ml) required the use of a blunt ended sonicating probe.

2.2. Preparation of Microspheres

All solutions were prepared using analytical grade reagents. Deionised water was prepared with a Milli-Q Gradient A10 system and filtered through a 0.22 μm sterile filter. The polymeric solution (Stock A) was prepared by dissolving pellets of poly-1-caprolactone (PCL, MW 65 000, Sigma-Aldrich) in acetone (99.5%, LabScan) to create solutions varying in PCL concentration from 0.5 to 4.0% w/v, in 0.5% w/v increments. Dissolution was assisted by incubating the PCL/acetone solution at 378C, 100 rpm. The protein solution (Stock B) was prepared by dissolving bovine serum albumin (BSA, MW ~66 kDa, Sigma-Aldrich) in deionized water along with poly(vinyl alcohol) (PVA, MW 30 000–70 000, Sigma-Aldrich) at a ratio of 1.5 g PVA for every 10 g of BSA. Two concentrations of Stock B were prepared: 100 mg ml21 BSA with 15 mg/ml PVA (Stock B1) and 200 mg/ml BSA with 30 mg/ml PVA (Stock B2). The PVA acts as an emulsion stabilizer (Cohen et al., 1991; Baras et al., 2000). A range of protein encapsulation feed stocks were prepared by mixing 100 parts of Stock A (15.0 ml) with one (0.15 ml), two 2 (0.30 ml), five (0.75 ml) or 10 parts

(1.50 ml) of Stock B until a homogenous emulsification was obtained. Particle size characteristics of the microparticles were determined using a Malvern Mastersizer/E (Malvern Instruments Ltd, UK) or a Mastersizer 2000 (Malvern Instuments Ltd, UK).

2.3. Preparation of Naoparticles

The plasmid DNA used in this study was pEGFP-N1 (4733 bp, CLONTECH Laboratories, Inc., CA, USA). This plasmid confers resistance to kanamycin (30 mg/ml) in *E. coli* hosts, resistance to neomycin in mammalian cells and encodes for an enhanced green fluorescence proteins (EGFP). Plasmid DNA was prepared using Promega SV DNA Maxipreps according to the manufacturer's instructions. The form and concentration of the pDNA was confirmed by ethidium bromide electrophoresis gels and spectrophotometric assays (data not shown).

DNA loaded nanoparticles were prepared by ultrasonicating the components of pDNA, and liposome reagent. The required nitrogen to phosphate ratios (N:P) were created by adding PEI (diluted in PBS buffer where required) to DNA, inverting to mix then incubating at room temperature for 15 mins to allow electrostatic binding between the DNA and PEI. Liposomes were prepared by dissolving 5 mg of lyophilised liposome powder (liposome kit: cholesterol 6.1% w/w, l-α-Phosphatidylcholine 85.3 % w/w and stearylamine 8.6% w/w, Sigma-Aldrich Co., USA) into 5 ml of PBS buffer. Due to the small volumes of solution used for the production of the liposomes (< 10 ml), ultrasonication was performed in batch mode using a blunt ended stainless steel probe. For larger volumes, it is expected that the nanoparticles could be produced in a continuous mode by recycling the feed continuously through the atomization probe for several passes. Liposomes were added to the DNA/PEI solutions in 50 ml centrifuge tubes at appropriate ratios then the whole solution was sonicated for 20 secs with the centrifuge tube immersed in an ice bath to keep prevent the solution increasing in temperature due to the heat evolved from soncication. After 20 secs, sonications were repeated until the nanoparticle size was constant. Particle size distributions and zeta potentials of the nanoparticles were determined using a Zetasizer Nano NS (Malvern Instuments Ltd, UK).

2.4. Cellular Transformation Studies

The cells used for the transformation studies were EaHy 926 cells kindly supplied by the Baker Heart Research Institute (Melbourne, Australia). The cells are immortalised human umbilical cord vein endothelial cells fused with the permanent (immortalised) human cell line A549. Endothelial cells predominantly cover the internal and external body surfaces (i.e. blood vessels and skin). Experiments were conducted using 24 well plates (Falcon) and were incubated at 37 ^{0}C, 5% CO_2, and 100% humidity for 4 hours. After 4 hrs, the cells were washed with PBS buffer and maintained using fresh DMEM medium (Invitrogen) in order to facilitate cell growth (cells were washed with PBS and new medium added every 2 days). After 4 days, cells were examined for the expression of green fluorescent protein (GFP) by use of fluorescent microscopy (cells were exited with blue light and emissions detected in the green spectrum using a green light filter).

2.4.1 Transformation with naked DNA

For the base-line (naked DNA) transformation studies, 10 μl, 50 μl and 100 μl of pDNA in PBS buffer at a concentration of 5μg/μl was added to 500 μl of bathing EaHy 926 cells. Experiments were performed in triplicate (n = 3).

2.4.2 Transformation via electroporation

Electroporation is the process where brief electrical pulses are employed to facilitate the entry of pDNA into the cell. P100 plates of 70% confluent cell cultures were washed with 6 ml of PBS. After 1 min the washing solution was aspirated and 1 ml of trypsin (serine protease) was added to the solution-less cell culture plate in order to detach the EaHy 926 from the well plate. Cell-trypsin solutions were transferred into 9 ml of fresh cell culture medium and mixed gently together. This mixture was then centrifuged at 1500 x g for 8 min. The

supernatant was removed and the cells were resuspended in 1.5 ml of PBS solution. 400µl aliquot of this mixture was delivered into each of the 3 x 1.5 ml tubes and mixed with 5 µl of pDNA (5 µg/µl). Electroporation was then carried out at 960 µF and 200 V, 300 V and 400 V (Bio-Rad Laboratories, US). Following electroporation the cells were transferred into 7 ml of culture medium in a 10 ml container. 1ml aliquots of this solution was pipetted into well plates containing 1 ml of fresh DMEM medium. Experiments were performed in triplicate (n = 3).

2.4.1 Transformation with liposomes

For the liposome transformation studies, 5 µl, 10 µl, 20 µl, 50 µl, 100 µl, 200 µl and 250 µl of the liposomes in PBS buffer at a concentration of 1mg/ml were added to 500 µl of bathing EaHy 926 cells. Experiments were performed in triplicate (n = 3).

3. RESULTS AND DISCUSSION

3.1. Microparticles for the delivery of biomolecules via the nasal mucosa

Parameters reported to affect particle size distributions were varied to determine the process conditions required for producing a particle suitable for nasal inhalation (10 - 20 µm). These were solids percent, feed flow rate, volumetric ratio of the polymer stock to the protein stock, and protein concentration in the protein stock. It was found that over the first several seconds of operation, atomization was unstable resulting in a wide particle size distribution (Figures 1a – 1d). Hence, particles were collected for analysis after the system had reached stable operating conditions (determined via visual inspection). This instability is due to the time period required for the probe to increase in frequency from 0 to 40 kHz.

It was shown that feed stocks containing 100 parts of 0.5 or 1.0% PCL in acetone with one part 100 mg/ml BSA and 15 mg/ml PVA were the most suitable feed stocks of those examined for the delivery of PCL encapsulated protein via the nasal route, as these feed conditions yielded particles samples with mass median diameters (13.17 µm and 9.10 µm, respectively) in the approximate target range of 10 – 20 µm. High protein encapsulation efficiencies were also displayed (93% and 95%, respectively). Protein delivery studies showed that biodegradable microparticles made from a stock containing 100 parts of 0.5% PCL in acetone with one part 100 mg/ml BSA and 15 mg/ml PVA delivered the protein payload *in vitro* under physiological conditions between 40 – 110 mins (n = 3).

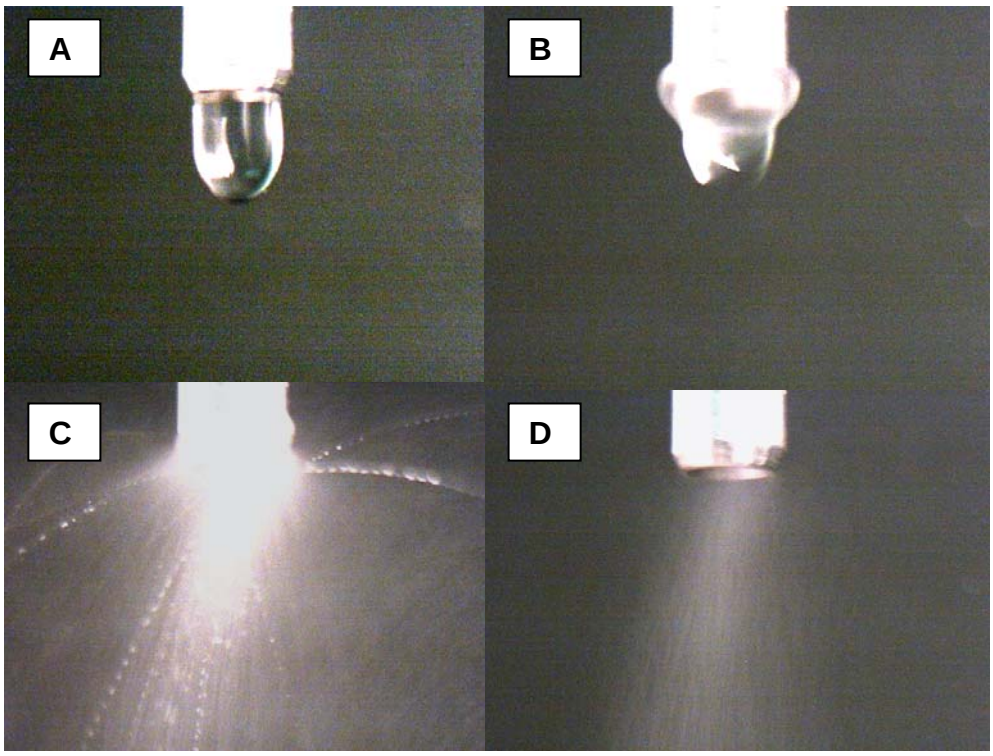

Fig. 1: Continuous atomization using a 40 kHz, 6 mm full wave atomization probe (VCX134 AT, Sonics, USA). Sequence of images displays particle size distribution instability at start up. A: Time = 0.000 sec. B: Time = 0.033 sec. C: Time = 0.100 sec. D: Time = 0.627 sec, approximate frame at which a constant particle size distribution is obtained.

3.2. Nanoparticles for enhanced cellular delivery

3.2.1. Physical characterization of pDNA

The zeta potential and particle size distribution were determined for pEGFP-N1. A range of concentrations (8.7 – 430 μg/ml) were considered to perform the zeta potential and size studies as it was found that the median particle size varied greatly as a function of concentration (Fig. 2). For the higher concentrations (26.16 μg/ml and above) this may be attributed to emulsions of naked pDNA being unstable as indicated by the zeta potentials being predominantly less than -19 mV (an absolute zeta potential value of greater than 30 mV indicates a stable emulsion) leading to the formation of large agglomerates of pDNA (> 4 μm). Interestingly, at low concentrations (13 μg/ml and below) the particle size increased again which may be attributed to the supercoiled pDNA becoming relaxed due to higher ion to phosphate group ratios and reduced molecule-molecule interactions at these dilute concentrations. All experiments were performed in triplicate. The zeta potential results confirm that pEGFP-N1 has a strong negative charge which reduces the electrostatic interaction of the naked pDNA with cell membranes. A sample of the results for zeta potential (Fig. 3) and particle size distribution (Fig. 4) at 19.35 μg/ml appear below.

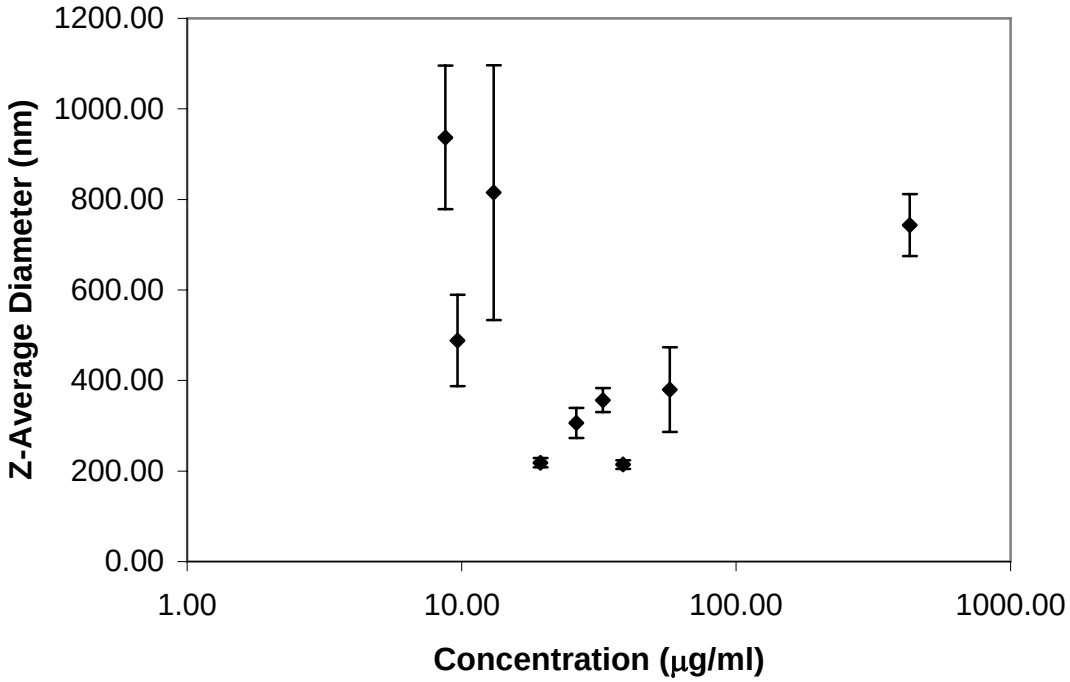

Fig. 2: Particle diameter (Z-Average diameter) results for different concentrations of pEGFP-N1 plasmid DNA in PBS buffer.

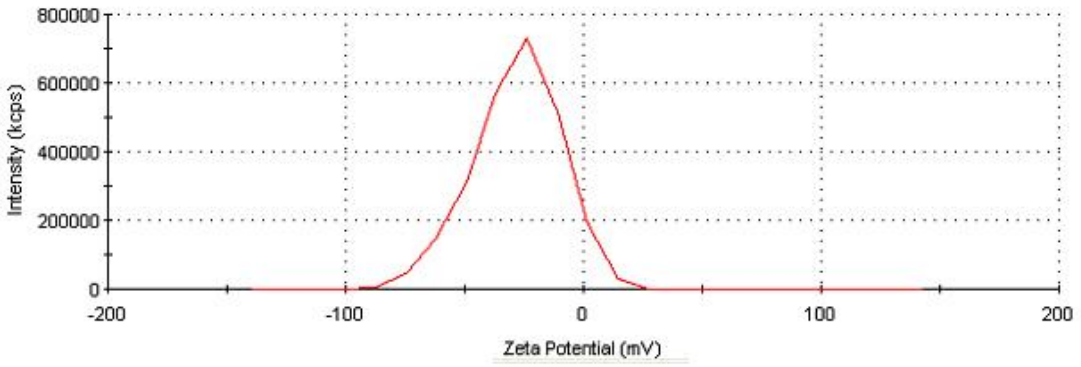

Fig. 3: Zeta potential graph for the plasmid DNA pEGFP-N1 obtained from the Malvern Zetasiser (pDNA concentration of 19.35 μg/ml).

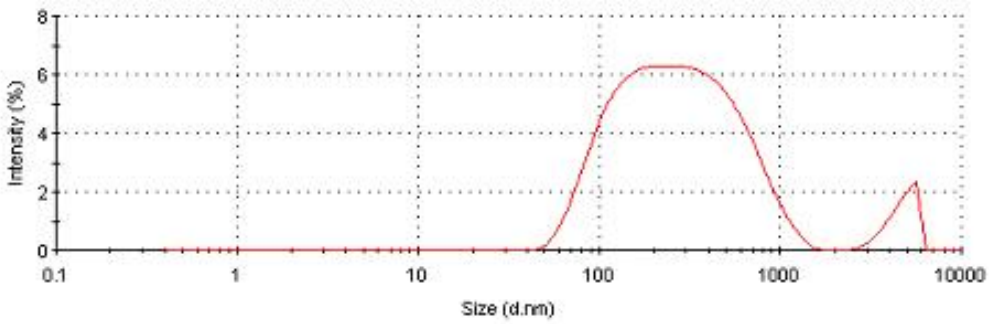

Fig. 4: Particle size distribution for the plasmid DNA pEGFP-N1 obtained from the Malvern Zetasiser.

3.2.2. Naked pDNA as a non-viral vector

The use of naked pDNA to transfect EaHy cells produced no detectable level of GFP expression (t = 96 hrs), even at concentrations of up to 500 µg pDNA per well, as shown below in Table 1. The lack of transfection efficiency by naked pDNA can be explained by the fact that, *in vitro,* EaHy cells lack an efficient DNA uptake mechanism or pathway. In order for the pDNA to access the non-specific cellular uptake mechanism such as endocytosis, the pDNA must briefly come into contact with the cell plasma membrane. The electrostatic repulsion between the polyanionic pDNA and the negatively charged cell membrane makes contact difficult. This essentially means that the frequency and duration of pDNA contacts with the cell membrane are low thus resulting in the complete absence of transfection by naked pDNA in the experiments outlined in Table 1. Additionally, naked pDNA are prone to cleavage by both extracellular and intracellular nucleases, which may contribute to the lack of transfection efficiency.

Table 1: Results for percentage transformation of initial viable cell number and the percentage cell death rate using naked pDNA at various concentration. Negligible levels are less than 0.1%.

Concentration of pDNA solution used (µg)	Total no. of viable cells prior to transfection (t = 0)	Total no. of viable cells 4 days post-transfection (t = 96 hrs)	Cell Death Rate (%)	no. of GFP Expressing Cells	Transformation of Initial Cell Number (%)	Repetitions (n)
50	240	NA	Negligible	0	0	3
250	251	NA	Negligible	0	0	3
500	253	NA	Negligible	0	0	3

3.2.3. Electroporation

The electroporation method resulted in a transfection efficiency of 1.92 - 3.26 % with a cell death rate being directly proportional to the magnitude of voltage used. From Figure 3.1 it can be observed that electroporation produces high cell death rates: 35%, 40 % and 50% for voltages of 200, 300 and 400 V respectively. These electrical pulses cause major disruption to cell structures where some pores become too large or fail to close consequently resulting in cell rupture and death. The high death rate of this particular transfection method is directly related to the magnitude of the voltage applied. Transfection efficiencies of 1.92%, 2.36% and 3.26% were achieved at voltages of 200, 300 and 400 V respectively. These results confirm that increased applied voltages enhance the opening of transient pores allowing easier uptake of the foreign DNA thus resulting in a higher transfection efficiency.

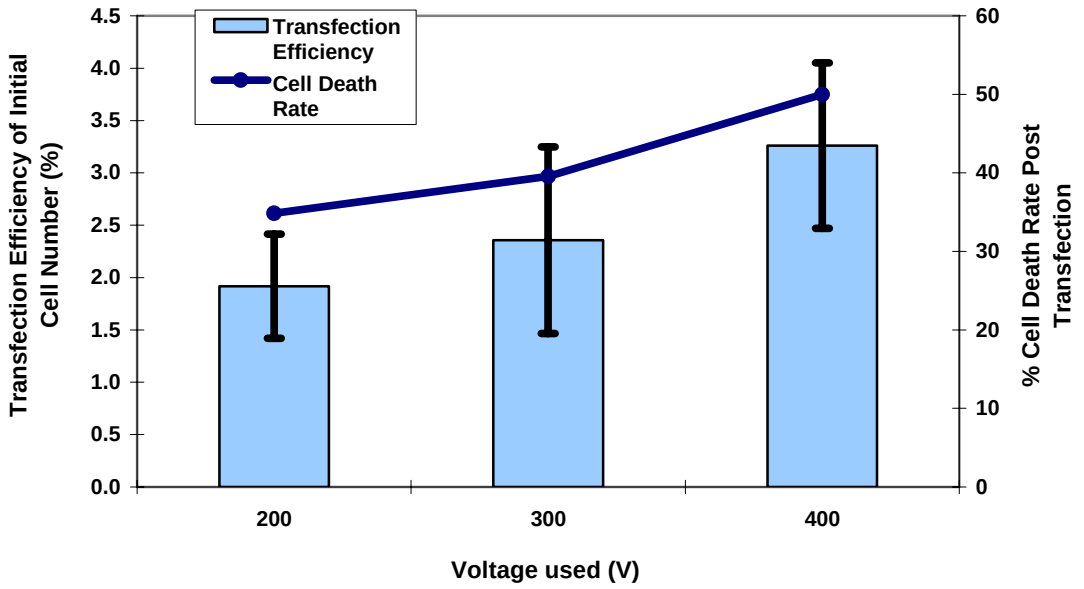

Fig. 5: The graph represents the data for transfection efficiency of initial cell number and the percentage cell death rate using electroporation at voltages. Error bars indicated 1 standard deviation.

3.2.4. Creation and characterization of pDNA loaded liposomes

The decrease in liposome particle size versus ultrasonication is shown in Fig. 6 below. A stable liposome particle size is obtained after 3 bursts of 20 secs (~ 190 nm) so that further ultrasonication does not further decrease the particle size. Ultrsonication has no effect on the zeta potential (~ 15 mV) which indicates that the liposome emulsifications are unstable yet the DNA loaded nanoparticles now have a charge to enhance the electrostatic interactions with the cells.

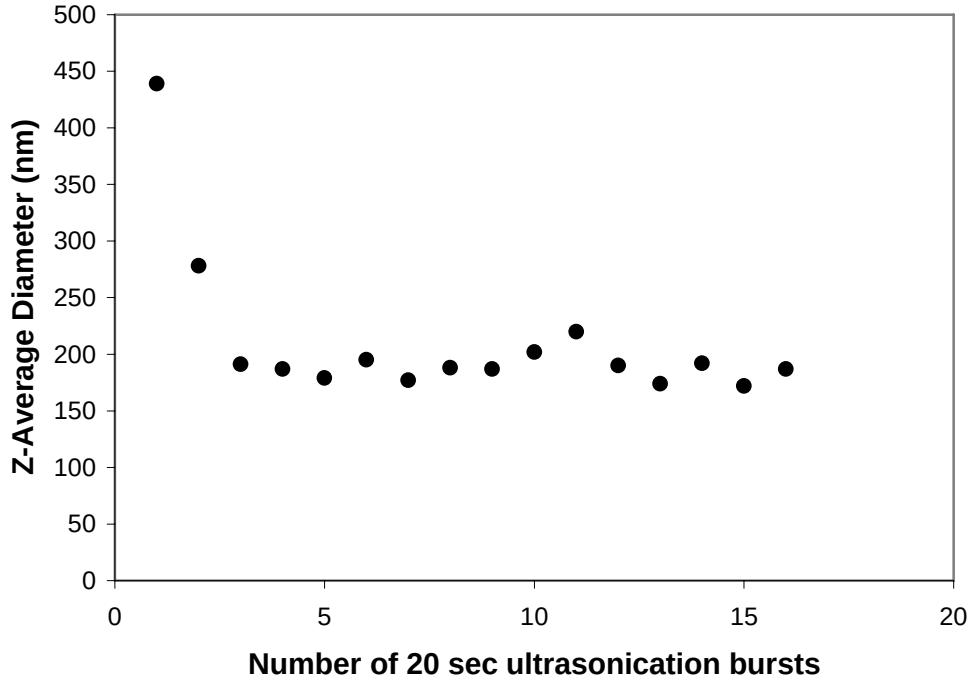

Fig. 6: Z-Average liposome particle diameter versus number of 20 sec ultrasonication bursts on solutions of 1mg/ml liposome in PBS buffer.

To improve the stability of the pDNA, pEGFP-N1 was incubated with a condensing agent (PEI) where the negative phosphate groups of the DNA electrostatically interact with the positive nitrogen groups of PEI. A nitrogen to phosphate ratio (N:P) of 2:1 was found to be the most suitable for the creation of stable nanoparticles with a Z-average diameter of 569 nm (n = 3). The transfection efficiencies of the pDNA:PEI nanoparticles were determined and the results are shown below in Fig. 7.

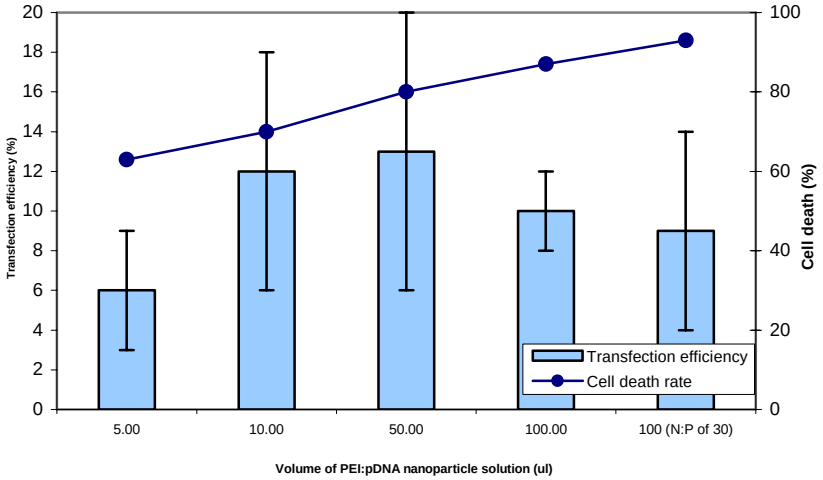

Fig. 7: Transfection efficiency of initial cell number and cell death rate for pDNA:PEI nanoparticles prepared in PBS buffer. Error bars indicated 1 standard deviation.

The pDNA:PEI polyplexes induced a higher transfection efficiency compared to naked DNA and electroporation as can be seen in Fig. 7. However, the pDNA:PEI polyplexes also resulted in the highest percentage of cell death. The 25 kDa branched PEI produces high cell death rates due to the membrane disrupting ability of PEI as the cellular damage caused by the polyplexes induces a cellular death pathway. This membrane disrupting ability of PEI also allows the polyplexes to have higher transfection efficiencies. The positive surface charge (indicated by the zeta potential) of the polyplexes allows effective cellular surface binding which facilitates endocytosis of the nanoparticle. The PEI in the polyplexes then disrupts the endosomal membrane through the 'proton sponge' mechanism, allowing the polyplexes to then escape into the cellular cytoplasm. Polyplexes do not dissociate in the cytoplasm, but instead are transported into the nucleus in the nanoparticle form. However, the high toxicity of the higher molecular weight PEI, especially the branched form, makes it unsuitable for direct *in vivo* applications. Lower molecular weight PEI and especially the linear form of PEI are less cytotoxic and are expected to have a decreased ability to disrupt the cellular membrane. However, this also means the transfection efficiency of polyplexes produced from these types of PEI may be lower. Hence, a compromise exists between the cytotoxicity and transfection efficiency of polyplexes.

The death rate was sown to be directly proportional to the volume of polyplex mixture added to the cell culture (Fig. 7). The N:P ratio also affects the cell toxicity of the polyplexes (an example of which is shown in Fig. 7 for a N:P ratio of 30 resulting in death rates of 93%). These results confirm the trade off between transfection efficiency and cell death. Fig. 7 indicates that of the combinations analysed, a nanoparticle volume of 50 µl displayed the optimum balance between transfection and cytotoxicity.

The pDNA:PEI:liposome complexes (lipopolyplexes) were formulated using a range of liposome:DNA mass ratios (50, 100 and 200 w/w). The zeta potentials for all ratios were relatively consistent (18.9 – 24 mV) and indicates that the DNA loaded liposomes have a charge suitable for interaction with cellular membranes. For the high liposome:DNA mass ratio, a small peak with a particle diameter less than 200 nm became more prominent which may be attributed to the presence of liposomes which did not contain or was not complexed with pDNA:PEI polyplexes (569 nm). The transfection efficiencies of the pDNA:PEI nanoparticles were determined and the results are shown below in Fig. 8. Data for the lipopolyplexes was repeated once only due to the limited volume of lipopolyplex feedstock.

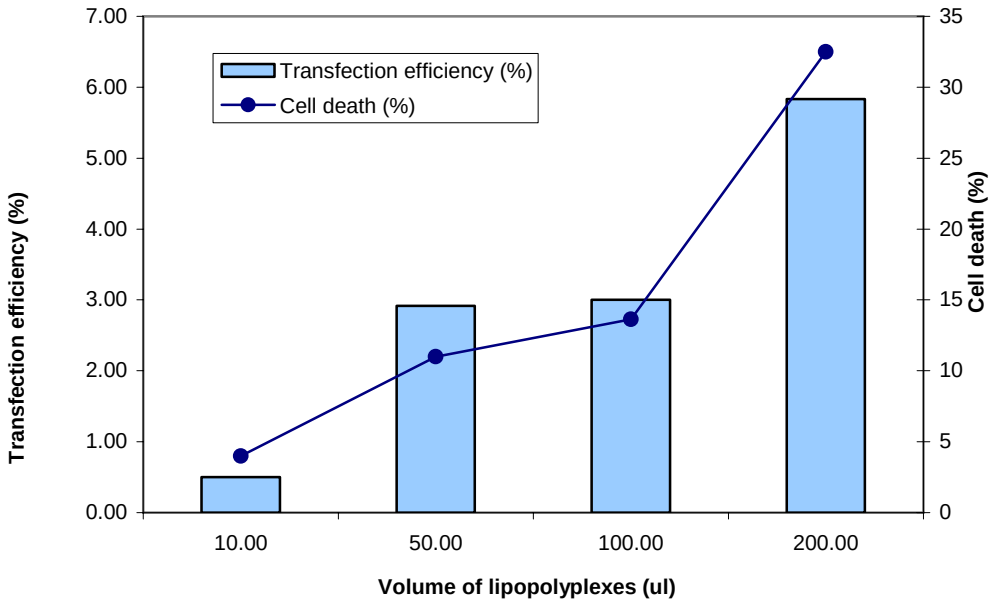

Fig. 8: Transfection efficiency of initial cell number and cell death rate for pDNA:PEI:Lipid nanoparticles (lipopolyplexes) prepared in PBS buffer.

For the lipopolyplexes, the transfection efficiency increased when the liposome ratio increased in the presence of PEI condensing agent. This suggests that increased lipid concentrations enhances uptake of the nanoparticle via endocytosis leading to higher transformation efficiencies yet higher cell deaths as well, as

displayed by Fig. 8. Previous research with cationic liposomes shows that the cholesterol moiety helps to disrupt the endosomal membrane (Congiu *et al*., 2004). Large cell death was only observed at high liposome volume of above 100 µl, for smaller concentrations the liposome and pDNA mixture should be considered safe (i.e. not cytotoxic). Comparisons with the pDNA:PEI complexes indicated that for commensurate transformation efficiencies (~ 6%), the lipopolyplexes are less cytotoxic (~32.5 % cell death) than the polyplexes (compared to 63 %).

4. CONCLUSIONS

Ultrasonic atomization was found to be a suitable method for the production of microparticles and nanoparticles. By controlling the feedstock properties, BSA loaded biodegradable particles suitable for nasal delivery were produced using a continuous unit operation of ultrasonic atomization. Particles in the approximate target range of 10 – 20 µm were produced with high encapsulation efficiencies (up to 95%) with the protein payload delivered *in vitro* under physiological conditions between 40 – 110 mins (n = 3).

Nanoparticles were also produced and showed that by using condensing agents (PEI) or lipid particles that transformation can be increased from 0 % for naked DNA to 13 and 5.8% respectively. PEI was shown to have a very strong cytotoxic effect. The formulation of the pDNA:PEI particles into lipopolyplexes appear to reduce the toxic effect of the PEI. Further work should explore how lower molecular weight PEI and linearized forms of PEI may have a reduced cytotoxic effect and the reproducibility of this production and transformation technology.

5. ACKNOWLEDGMENTS

G.M. Forde wishes to acknowledge the support of the Victorian Endowment for Science, Knowledge and Innovation (VESKI) in funding this research. The authors kindly acknowledge the support of Dr Zhiyong Yang and Prof David Kaye in completing this research project.

6. REFERENCES

Bloomfield, V.A. (1998) *DNA Condensation by Multivalent Cations,* Biopolymers/Nucleic Acid Sci.Vol. 44, pp 269-282.

Congiu, A., Pozzi, D., Esposito, C., Castellano, C., and Mossa, G., (2004) *Correlation between structure and transfection efficiency: a study of DC-Chol-DOPE/DNA complexes*. Colloids and Surfaces B: Biointerfaces, Vol 36, pp 43-48.

Danquah, M.K. and Forde, G.M. (2006), *Rapid therapeutic plasmid DNA isolation: Addressing the looming vaccine crisis*, BIOFORUM EUROPE, ISSN 1611-597X, Vol. 10, pp 24 – 27.

Felgner, P.L., Gadek, T.R., Holm, M., Roman, R., Chan, H.W. (1987), *Lipofection: A highly efficient, lipid-mediated DNA-transfection procedure*', Biochemistry, Vol. 84, pp 7413-7417.

Gershon, H. Ghirlando, R., Guttman, S.B., Minsky, A. (1993), *Mode of formation and structural features of DNA-Cationic Liposome complexes used for transfection*, Biochemistry, Vol. 1193, pp 7143-7151.

Johansen, P., Merkle, H.P. and Gander, B. (2000), *Technological considerations related to the up-scaling of protein microencapsulation by spray-drying*, Eur J Pharm Biopharm, Vol. 50, pp 413–417.

Kippax, P. and Fracassi, J. (2003), *Particle size characterisation in nasal sprays and aerosols*, LabPlus Int, February/March edition.

Lasic, D.D. (1997) *Liposomes in Gene Delivery*. CRC Press, Boca Raton, Florida, US

Li, S. and Huang, L. (2000), Nonviral gene therapy: promises and challenges, Gene therapy, Vol. 7, pp 31-34.

Putney, S.D. (1998), *Encapsulation of proteins for improved delivery*, Current Opinion in Chemical Biology, Vol. 2, pp 548–552.

Rädler J., Koltover, I., Salditt, T. and Safinya, C.R. (1997) *Structure of DNA-Cationic Liposome Complexes: DNA Intercalation in Multilamellar Membranes in Distinct Interhelical Packing Regimes, Science Vol* **275,** pp. 810 – 814.

Thomasin, C., Johanson, P., Alder, R., Bemsel, R., Hottinger, G., Altorfer, H., Wright, A.D., Wehrli, E., Merkle, H.P. and Gander, B. (1996), *A contribution to overcoming the problem of residual solvents in biodegradable microspheres prepared by coacervation*, Eur J Pharm Biopharm, Vol. 42, pp 16–24.

APPENDIX 4

Spotlight featured article

Delivering a new generation of potential biopharmaceutical blockbusters: ultrasonic process engineering of plasmid DNA

Jenny Ho, Huanting Wang, Gareth M. Forde

Biotechnology and Bioengineering

101(1), September 1 (2008)

SPOTLIGHT

BIOTECHNOLOGY and BIOENGINEERING

All for One: Intimate Coupling of Photocatalytic Oxidation With Biofilm Biodegradation

Unconventional synergies can reshape the way we think about degrading recalcitrant organic wastewater pollutants. Marsolek and co-workers describe a novel system—intimately coupled photo-biocatalysis—which combines into a single stage the unlikely partners of photocatalytic advanced oxidation and biofilm biodegradation. Conventionally, photocatalysis has the advantage of wide-ranging applicability for attacking recalcitrant organic contaminants, but is not practical for full mineralization. Biodegradation is efficient for removing readily biodegradable organics, but is thwarted by recalcitrant or inhibitory pollutants. Combining these two approaches into a single-stage maximizes the benefits of each, while minimizing their drawbacks.

Success with this unconventional pairing comes from growing the microorganisms inside macroporous biofilm carriers, immediately exposing the microbes to biodegradable compounds produced by photocatalysis in the bulk solution while keeping them well protected from the harsh conditions of advanced oxidation and UV light. Electron micrograph, confocal laser scanning microscopy and photographic evidence, coupled with biomass and substrate concentration effects, highlight the synergistic relationship between these seemingly incompatible partners. *Page 83*

DOI: 10.1002/bit.22052

Biofilm Growth Influences the Electrochemistry of Microbial Fuel Cells

Microbial fuel cells (MFCs) present a technology with the potential to revolutionize wastewater treatment, contribute to bioenergy production, generate power for remote devices, and advance our fundamental understanding of extracellular electron transfer capabilities of microorganisms. The past decade of research on MFCs has promoted more than five orders of magnitude increase in power density retrieved from these systems, but they are still electrochemically constrained. Ramasamy and coworkers used electrochemical impedance spectroscopy to characterize the sources and magnitude of these constraints in a two-chamber, acetate-fed MFC with ferricyanide as an electron acceptor and an undefined mixed culture as the biocatalyst. They found that over 95% of the total cell impedance was due to ohmic losses in the solution and membrane in this design. Following the initial development of the anode biofilm, the charge transfer resistance at the anode decreased dramatically as the biofilm developed, yet dominating the kinetic constraints relative to the reaction at the cathode. *Page 101*

DOI: 10.1002/bit.22053
Published online in Wiley InterScience (www.interscience.wiley.com).

Deploying Commensal Bacteria to Signal a Stop to Enteric Disease

One of the biggest challenges to combating enteric disease in the developing world is lowering the cost and raising the efficacy of preventative treatments. While vaccines and small molecules can be effective, they can also be prohibitively expensive. Duan and March reveal a potential solution to this problem by engineering enteric commensal bacteria to express a signal that prevents *Vibrio cholerae*, the causative agent of the enteric disease cholera, from colonizing the GI tract. By emitting the *V. cholerae* quorum signals CAI-1 and AI-2 the commensal strain significantly reduced *V. cholerae* virulence in a human epithelial cell co-culture model. The work was carried out with the "probiotic" strain *E. coli* Nissle 1917 which has been sold over-the-counter in Europe for almost 100 years. This novel approach could be expanded to include other enteric diseases and even diseases that revolve around human rather than bacterial signaling. *Page 128*

DOI: 10.1002/bit.22054

Delivering a New Generation of Potential Biopharmaceutical Blockbusters: Ultrasonic Process Engineering of Plasmid DNA

Plasmid DNA therapeutics have the potential to revolutionize the pharmaceutical industry. Two major areas for improvement from a bioprocess engineering perspective are production and delivery. Plasmid DNA (pDNA) has been recognized since the 1990s as a potential non-viral vector for vaccination, however low transfection efficiencies have led to the need for innovative delivery methods. The encapsulation of large biomolecules into polymeric delivery systems presents a challenge due to the delicacy (including shear sensitivity) of the biomolecules. The current article by Ho et al. explores the potential of ultrasonic atomization for encapsulating pDNA with biodegradable polymers. The process shows potential as a continuous, large scale production method for the preparation of therapeutic particles for the controlled release of pDNA while circumventing key obstacles in synthesizing polymeric carriers. The scalability inherent in their approach brings us closer to the commercially viable manufacture of genetic-based prophylactic vaccines. *Page 172*

DOI: 10.1002/bit.22055

ADDENDUM

In response to the comments made by the examiners of this thesis, a number of amendments have been made to the content by the author. These are outlined below.

(1) The following addition is to be made to **Chapter 4**, *page 48, line 32*

"The increase in the content of nitrogen from PEI has rendered the effective surface charge of the complexes – causing it to become positive. When the complexes have large positive zeta potential ($\geq$ 30 mV), they tend to repel each other; thereby, having no tendency to flocculate."

(2) The following amendment is to be made to **Chapter 5**

Page 66 line 23:

delete "In this study" and read "The focus in this study is on the hydrodynamic diameter of microspheres in suspensions for nasal inhalation. As a result,..."

Page 69: Add to line 10:

"From our previously reported study, volumetric ratio and feed flowrate of feedstocks have significant effects on the mean particle size (D[4,3]). Nevertheless, due to more uniform atomization, the effect of feed flowrate was less significant for feedstock with less solid contents. As a result, in this novel ultrasonic atomization through the dual-concentric-feeding needles, the effect of feed flowrate can be further reduced by only controlling the internal content flowrate."

Page 70: Add at the end of paragraph 2:

"*Span* is the measurement of the width of the size distribution. The narrower the distribution, the smaller the *span* becomes. The *span* is calculated as:

$$\frac{d(0.9)-d(0.1)}{d(0.5)}$$

where d(0.1), d(0.5) and d(0.9) are the sizes of particle below which 10 %, 50 % and 90 % respectively of the sample lies."

Page 83: Add to line 9:

"Standard deviation of D[4,3] and *span* are the deviation values respectively from triplicate microspheres batches"

Page 84 line 2 should read

"...a linear line of best fit to the overall 40 days release profiles..."

Page 86

Comment: The composite microspheres were synthesised at a volumetric ratio of 5 pDNA/MPS to 100 PLGA (5 %v/v). The composite microspheres do not have distinct shell and core structure. The effects of varying the flowrates of PLGA and pDNA/MPS on the configuration of composite microspheres are discussed in page 72 paragraph 1 and page 83 Table I.

Page 86: Add at the end of caption of Fig.2

"The composite microspheres within the size range being obtained (6 – 16 μm) could possibly be used for nasal cavity delivery of biomolecules."

(3) The following amendment is to be made to **Chapter 6 - Conclusions**

Page 99: Add at the end of line 4

"This high-throughput method has comparatively higher encapsulation efficiencies and yield than previously reported technology [80 - 82]."

Page 99: Add at the end of line 6

"This new method has potential in addressing major problems associated with pDNA vaccines encapsulation and release from polymer microspheres. Comparing to previous

study results [83], the smaller microsphere sizes obtained make the microspheres favourable for intranasal delivery while maintained the supercoil structure of pDNA."

(4) The following amendment is to be made to **Appendix 3**

Page A-23: Add at the end of caption of Fig. 2

"The Z-average diameter is the intensity weighted mean hydrodynamic size of the ensemble collection of particles, and this is measured by dynamic light scattering (DLS). The z-average is derived from a Cumulants analysis of the measured correlation curve, wherein a single particle size is assumed and a single exponential fit is applied to the autocorrelation function."

(5) The following references are to be added to **References**

[80] C. Berkland, M. King, A. Cox, K. Kim, D.W. Pack, Precise control of PLG microsphere size provides enhanced control of drug release rate, J. Control. Release 82 (2002) 137 – 147.

[81] C. Berkland, K. Kim, D.W. Pack, PLG microsphere size controls drug release rate through several competing factors, Pharm. Res. 20(7) (2003) 1055 – 1062.

[82] C. Berkland, A.Cox, K. Kim, D.W. Pack, Three-month, zero-order piroxicam release from monodispersed double-walled microspheres of controlled shell thickness, J. Biomed. Mater. Res. A 70 (2004) 576 – 584.

[83] N.K. Varde and D.W. Pack, Influence of particle size and antacid on release and stability of plasmid DNA from uniform PLGA microspheres, J. Control. Release 124(3) (2007) 172 – 180.